

University of Alberta

**METABOLIC ADAPTATION IN SKELETAL MUSCLE:
IMPLICATIONS OF AMPK ACTIVITY *IN VITRO***

by

Marcia Leigh Reinhart

A thesis submitted to the Faculty of Graduate Studies and Research in partial fulfillment of the requirements for the degree of Master of Science

Neuroscience

The Centre for Neuroscience

Edmonton, Alberta

Fall 2004



Library and
Archives Canada

Bibliothèque et
Archives Canada

Published Heritage
Branch

Direction du
Patrimoine de l'édition

395 Wellington Street
Ottawa ON K1A 0N4
Canada

395, rue Wellington
Ottawa ON K1A 0N4
Canada

Your file *Votre référence*
ISBN: 0-612-95840-X
Our file *Notre référence*
ISBN: 0-612-95840-X

The author has granted a non-exclusive license allowing the Library and Archives Canada to reproduce, loan, distribute or sell copies of this thesis in microform, paper or electronic formats.

L'auteur a accordé une licence non exclusive permettant à la Bibliothèque et Archives Canada de reproduire, prêter, distribuer ou vendre des copies de cette thèse sous la forme de microfiche/film, de reproduction sur papier ou sur format électronique.

The author retains ownership of the copyright in this thesis. Neither the thesis nor substantial extracts from it may be printed or otherwise reproduced without the author's permission.

L'auteur conserve la propriété du droit d'auteur qui protège cette thèse. Ni la thèse ni des extraits substantiels de celle-ci ne doivent être imprimés ou autrement reproduits sans son autorisation.

In compliance with the Canadian Privacy Act some supporting forms may have been removed from this thesis.

Conformément à la loi canadienne sur la protection de la vie privée, quelques formulaires secondaires ont été enlevés de cette thèse.

While these forms may be included in the document page count, their removal does not represent any loss of content from the thesis.

Bien que ces formulaires aient inclus dans la pagination, il n'y aura aucun contenu manquant.

Canada

ACKNOWLEDGEMENTS

I would like to genuinely thank my supervisor, Dr. Ted Putman, for his knowledge, enthusiasm, guidance and patience. In addition, Drs Jason Dyck and Moira Glerum provided me with much expertise and support both during and following my time spent working in their laboratories, as well as through service on my supervisory committee. My final committee member, Dr. John Greer, has also been very helpful in numerous respects during the various trials and tribulations I experienced during my M.Sc.

I would also like to express my gratitude for numerous others who assisted me throughout the course of my study. Firstly, a special thank you to Ian MacLean for all his technical assistance with the set up and partial data collection of real-time RT-PCR as well as his positive attitude. In addition, undergraduate summer student Winnie Wong provided invaluable cell culture and western blotting assistance when it was most required. Another thank you to Gord and Brenda Murdoch for their generosity and advice with respect to real-time RT-PCR, as well as to Carrie Soltys, Suzanne Kovacic and Amy Barr for their assistance with adenoviral infection and western blotting techniques. Others deserving recognition for their assistance include Dr. Gary Lopaschuk, Joan Turchinsky and Jean Pearcey. I am also grateful to NSERC for their support over the duration of my degree with a Postgraduate Scholarship.

Furthermore, I would like to express my appreciation to my fellow graduate students who made my entire laboratory experience an enjoyable one. And finally, a big thank you to my family and friends who have been and will always be supportive throughout my various endeavours.

TABLE OF CONTENTS

| | |
|---|----|
| <u>CHAPTER I: INTRODUCTION AND LITERATURE REVIEW</u> | 1 |
| <u>1.1 Overview of Study</u> | 1 |
| <u>1.2 Review of AMPK</u> | 2 |
| 1.2.1 <i>AMPK Structure and Tissue Distribution</i> | 2 |
| 1.2.2 <i>Function of AMPK</i> | 3 |
| 1.2.3 <i>Role of AMPK in Skeletal Muscle</i> | 6 |
| 1.2.3.1 <i>Fatty Acid Metabolism</i> | 6 |
| 1.2.3.2 <i>Carbohydrate Metabolism</i> | 8 |
| 1.2.3.3 <i>Exercise</i> | 9 |
| 1.2.3.4 <i>Protein Synthesis</i> | 10 |
| 1.2.3.5 <i>Oxidative Stress</i> | 11 |
| <u>1.3 Review of Mitochondrial Biogenesis</u> | 11 |
| 1.3.1 <i>Skeletal Muscle Plasticity</i> | 11 |
| 1.3.2 <i>Transcriptional Regulation</i> | 13 |
| 1.3.3 <i>Role of AMPK</i> | 15 |
| <u>1.4 Development of a Novel In Vitro Experimental Model</u> | 17 |
| 1.4.1 <i>Skeletal Muscle In Vitro</i> | 17 |
| 1.4.2 <i>Adenovirus Constructs</i> | 19 |
| 1.4.3 <i>Pharmacological Activation</i> | 21 |
| 1.4.3.1 <i>Metformin</i> | 21 |
| 1.4.3.2 <i>AICAR</i> | 22 |
| <u>1.5 Activation and Inhibition of AMPK In Vitro</u> | 23 |
| 1.5.1 <i>Experimental Conditions</i> | 23 |
| 1.5.2 <i>Protein Expression</i> | 23 |
| 1.5.3 <i>Real-Time RT-PCR</i> | 24 |
| 1.5.4 <i>Research Hypothesis</i> | 26 |
| 1.5.5 <i>Limitations of Study</i> | 27 |
| <u>1.6 References</u> | 28 |
| | |
| <u>CHAPTER II: MATERIALS AND METHODS</u> | 43 |
| <u>2.1 Experimental Model</u> | 43 |
| 2.1.1 <i>In Vitro System</i> | 43 |
| 2.1.2 <i>Testing of Differentiation State</i> | 43 |
| 2.1.3 <i>Pharmacological Treatment</i> | 44 |
| 2.1.4 <i>Viral Infection</i> | 44 |
| 2.1.4.1 <i>Retroviral Infection and CAR Overexpression</i> | 44 |

| | |
|--|----|
| 2.1.4.2 Poycationic Lipid Infection Aid..... | 45 |
| <u>2.2 Protein Expression Analysis.....</u> | 46 |
| 2.2.1 <i>Harvesting: Whole-Cell Lysate.....</i> | 46 |
| 2.2.2 <i>Harvesting: Nuclear Extract Enhancement.....</i> | 47 |
| 2.2.3 <i>SDS-PAGE and Western Blotting.....</i> | 47 |
| <u>2.3 Real-Time RT-PCR.....</u> | 49 |
| 2.3.1 <i>RNA Isolation and Preparation.....</i> | 49 |
| 2.3.2 <i>Reverse Transcription of RNA to cDNA.....</i> | 50 |
| 2.3.3 <i>Synthesis of Primers and Probes.....</i> | 50 |
| 2.3.4 <i>Real-Time Polymerase Chain Reaction.....</i> | 51 |
| <u>2.4 Statistical Analysis.....</u> | 52 |
| <u>2.5 References.....</u> | 53 |
| | |
| <u>CHAPTER III: RESULTS.....</u> | 54 |
| <u>3.1 Model Efficiency.....</u> | 54 |
| 3.1.1 <i>In Vitro System.....</i> | 54 |
| 3.1.2 <i>Pharmacological Treatment.....</i> | 55 |
| 3.1.3 <i>Virus Treatment.....</i> | 56 |
| 3.1.3.1 <i>Infection Enhancement.....</i> | 56 |
| 3.1.3.2 <i>Infection Efficiency.....</i> | 57 |
| 3.1.3.3 <i>Activation and Inhibition of AMPK.....</i> | 57 |
| <u>3.2 Experimental Results: Protein Expression.....</u> | 58 |
| 3.2.1 <i>Metabolic Enzymes.....</i> | 58 |
| 3.2.2 <i>Transcription Factors.....</i> | 59 |
| <u>3.3 Experimental Results: mRNA Expression.....</u> | 59 |
| 3.3.1 <i>Mitochondrial mRNA.....</i> | 59 |
| 3.3.2 <i>Transcription Factor mRNA.....</i> | 60 |
| <u>3.4 References.....</u> | 88 |
| | |
| <u>CHAPTER IV: DISCUSSION.....</u> | 89 |
| <u>4.1 Evaluation of Experimental Model.....</u> | 89 |
| 4.1.1 <i>Differentiation of Cells.....</i> | 89 |
| 4.1.2 <i>Efficiency of AMPK Activation and Inhibition.....</i> | 91 |
| 4.1.3 <i>Limitations of the Experimental Model.....</i> | 93 |
| <u>4.2 Evaluation of Mitochondrial Biogenesis.....</u> | 95 |

| | |
|--|-----|
| <u>4.3 Evaluation of Transcription Factor Expression</u> | 97 |
| <u>4.4 Implications of Altering AMPK Activity</u> | 99 |
| <u>4.5 Future Directions for Research</u> | 100 |
| <u>4.6 References</u> | 102 |

LIST OF TABLES

| | | |
|------------|--|----|
| Table 2.1: | Western blotting conditions for various antibodies. | 48 |
| Table 2.2: | DNA sequences for real-time RT-PCR primers and probes. | 51 |

LIST OF FIGURES

| | | |
|--------------|--|----|
| Figure 1.1: | Subunit structure of AMPK (adapted from Kemp et al., 1999). | 2 |
| Figure 1.2: | The adenylate kinase reaction. | 4 |
| Figure 1.3: | Schematic diagram of AMPK subunit association and activation as a result of AMP binding. | 5 |
| Figure 1.4: | Schematic diagram of AMPK activation by AMPKK phosphorylation and AMP binding to both the $\alpha\gamma$ interface of AMPK and the upstream kinase AMPKK.. | 6 |
| Figure 1.5: | Downstream effects of AMPK activation on fatty acid metabolism. | 7 |
| Figure 1.6: | Proposed transcriptional regulation during mitochondrial biogenesis. | 15 |
| Figure 1.7: | Differentiation-induced changes in myoD and myogenin mRNA expression in the C2C12 cell line as previously reported in Shimokawa et al. (1998). | 18 |
| Figure 1.8: | Polycationic lipid and virus complexes, as viewed through an electron microscope. | 19 |
| Figure 1.9: | Structural comparison of AMP and ZMP. | 22 |
| Figure 1.10: | Real-time RT-PCR primer/probe annealing and DNA synthesis. | 24 |
| Figure 1.11: | Representative plot of real-time RT-PCR fluorescence. | 26 |
| Figure 3.1: | Myoblast differentiation and myotube formation on (A) day 0, (B) day 1, (C) day 4, and (D) day 6 following serum withdrawal. | 61 |
| Figure 3.2: | Pharmacological treatment does not affect myoD protein expression, as indicated in samples harvested on day 4 post-treatment (n=4). | 62 |
| Figure 3.3: | AICAR treatment, but not metformin, results in an elevation in myogenin protein expression, as indicated in samples harvested on day 4 post-treatment (n=4). | 63 |
| Figure 3.4: | Adenovirus treatment does not affect myoD protein expression, as indicated in cells harvested 5 days following infection (n=4). | 64 |
| Figure 3.5: | α 2DN adenovirus and AICAR, but not AICAR and the control adenovirus, result in an elevation in myogenin protein expression, as indicated in samples harvested on day 5 post-infection (n=4). | 65 |
| Figure 3.6: | Treatment effects on cell morphology: appearance of cells following pharmacological treatment on (a) day 1 and (b) day 3 post-treatment. | 66 |
| Figure 3.7: | Variable cell death at different doses of AICAR. | 66 |
| Figure 3.8: | Both AICAR and metformin result in increases in ACC phosphorylation, providing evidence of increased AMPK activity in cells harvested on day 4 post-treatment (n=5). | 67 |

| | | |
|--------------|---|----|
| Figure 3.9: | Metformin, but not AICAR, results in increases in AMPK phosphorylation, providing evidence of increased AMPK activity on day 4 post-treatment (n=5). | 68 |
| Figure 3.10: | CAR protein expression in various retrovirally-infected C2C12 clones. | 69 |
| Figure 3.11: | Lipofectamine treatment produces a more efficient infection than the CAR-overexpressing clones, as assessed by GFP expression. | 69 |
| Figure 3.12: | The presence of an extracellular matrix gel <i>in vitro</i> does not appear to affect infection efficiency. | 70 |
| Figure 3.13: | Expression of (A) GFP-encoding and (B) AMPK-encoding adenoviral constructs in cells fixed and treated with a TRITC-labelled myc-tag antibody and visualized for GFP fluorescence. | 70 |
| Figure 3.14: | ACC phosphorylation following AICAR treatment is not inhibited in the presence of a control adenovirus, however phosphorylation with or without AICAR treatment is inhibited by the presence of an $\alpha 2$ -dominant negative AMPK construct in cells harvested day 5 post-infection (n=5). | 71 |
| Figure 3.15: | AMPK phosphorylation following AICAR treatment is not inhibited in the presence of a control adenovirus, however phosphorylation with or without AICAR treatment is inhibited by the presence of an $\alpha 2$ -dominant negative AMPK construct in cells harvested day 5 post-infection (n=5). | 72 |
| Figure 3.16: | Both AICAR and metformin treatment result in increases in citrate synthase expression, providing evidence of mitochondrial biogenesis on day 4 post-treatment (n=8). | 73 |
| Figure 3.17: | No changes in citrate synthase expression visible for any adenovirus-treated condition, providing no evidence of mitochondrial biogenesis on day 5 post-infection (n=8). | 74 |
| Figure 3.18: | Both AICAR and metformin treatment result in increases in GAPDH expression, providing evidence of increased glycolytic flux on day 4 post-treatment (n=8). | 75 |
| Figure 3.19: | $\alpha 2$ DN + AICAR results in a small but significant increase in GAPDH expression, indicating an increase in glycolytic flux on day 5 post-infection (n=8). | 76 |
| Figure 3.20: | Whole-cell (W) and nuclear extracts (N) treated with various pharmacological conditions, blotted for PGC-1 α . | 77 |
| Figure 3.21: | Metformin treatment, but not AICAR, results in nearly a 3-fold increase in PGC-1 α expression, providing evidence of PGC-1 α signalling during mitochondrial biogenesis on day 4 post-treatment (n=8). | 78 |
| Figure 3.22: | No changes in PGC-1 α expression visible for any adenovirus-treated condition, providing no evidence of PGC-1 α signalling during mitochondrial biogenesis on day 5 post-infection (n=8). | 79 |

| | | |
|--------------|--|----|
| Figure 3.23: | Citrate synthase mRNA expression at various time points following pharmacological treatment (n=6). Early increase in citrate synthase transcription following metformin treatment provides evidence of mitochondrial biogenesis. | 80 |
| Figure 3.24: | Citrate synthase mRNA expression at various time points following adenovirus infection (n=6). No evidence of changes in citrate synthase mRNA expression was apparent. | 81 |
| Figure 3.25: | ALA synthase mRNA expression at various time points following pharmacological treatment (n=6). Early increase in ALA synthase transcription following metformin treatment provides evidence of mitochondrial biogenesis. | 82 |
| Figure 3.26: | ALA synthase mRNA expression at various time points following adenovirus infection (n=6). Early increase in ALA synthase transcription following α 2DN adenovirus treatment provides evidence of mitochondrial biogenesis. | 83 |
| Figure 3.27: | PGC-1 α mRNA expression at various time points following pharmacological treatment (n=6). Decreases in PGC-1 α transcription 48 hours following metformin treatment fails to explain the large increase in protein expression visible on day 4. | 84 |
| Figure 3.28: | PGC-1 α mRNA expression at various time points following adenovirus infection (n=6). Increases in PGC-1 α transcription following α 2DN adenovirus treatment at 6 hours, 48 hours and 5 days post-treatment refute the hypothesis of PGC-1 α downregulation in response to AMPK inhibition. The increase in PGC-1 α mRNA following 5d of AICAR treatment does support the hypothesis of PGC-1 α upregulation in response to AMPK activation. | 85 |
| Figure 3.29: | p300 mRNA expression at various time points following pharmacological treatment (n=6). Increase in p300 transcription 5 days following metformin indicates potential long-term transcriptional regulation of p300 expression by AMPK. | 86 |
| Figure 3.30: | p300 mRNA expression at various time points following adenovirus infection (n=6). No evidence of changes in p300 mRNA expression. | 87 |

LIST OF ABBREVIATIONS

ACC = acetyl-CoA carboxylase
ADP = adenosine diphosphate
AICAR = 5-aminoimidazole-4-carboxamide ribofuranoside
Akt = protein kinase B
ALAS = δ -aminolevulinic synthase
AMPK = AMP-activated protein kinase
AMPKK = AMP-activated protein kinase kinase
AMP = adenosine monophosphate
ANOVA = analysis of variance
Asp = aspartate
ATCC = American Type Culture Collection
ATP = adenosine triphosphate
 β -GPA = β -guanidinopropionic acid
bp = base pair
BSA = bovine serum albumin
CAMKIV = calcium/calmodulin kinase IV
CAR = Coxsackie and adenovirus receptor
CBS = cystathionine β synthase
cDNA = complimentary DNA
CHO = Chinese hamster ovary
CK1 = casein kinase 1
CMV = cytomegalovirus
CoA = coenzyme A
CPT1 = carnitine-palmitoyl transferase 1
CREB = cAMP responsive element-binding protein
CS = citrate synthase
 C_T = threshold cycle
DEPC = diethyl pyrocarbonate
DMEM = Dulbecco's modified Eagle's media
DMSO = dimethyl sulfoxide
DN = dominant negative
DNA = deoxyribonucleic acid
dNTP = deoxy nucleotide-5'-triphosphate
DTT = dithiothreitol
dUTP = deoxyuridine-5'-triphosphate
ECM = extracellular matrix
EDTA = ethylenediaminetetraacetic acid
eEF2 = eukaryotic elongation factor 2
g = acceleration due to gravity (9.81 m/s^2)
GAPDH = glyceraldehyde-3-phosphate dehydrogenase
GFP = green fluorescent protein
 H_2O_2 = hydrogen peroxide
HCl = hydrochloric acid
HK = hexokinase

HMG-CoA = 3-hydroxy-3-methylglutaryl-CoA
HSL = hormone-sensitive lipase
kDa = kilodalton
KOH = potassium hydroxide
mA = milliamp
MAPK = mitogen-activated protein kinase
MCD = malonyl-CoA decarboxylase
MCK = muscle creatine kinase
MEF2 = myocyte-specific enhancer factor
MO25 = mouse protein 25
MOI = multiplicity of infection
mRNA = messenger RNA
mTFA = mitochondrial transcription factor A
mTOR = mammalian target of rapamycin
 μg = microgram
 μl = microlitre
NADH = nicotinamide adenine dinucleotide (reduced form)
nm = nanometer
NRF = nuclear respiratory factor
PAGE = polyacrylamide gel electrophoresis
PBS = phosphate-buffered saline
PEI = polyethylimine
PFK = phosphofructokinase
PFU = plaque-forming units
PGC-1 α = PPAR- γ coactivator 1 α
PI3 kinase = phosphatidylinositol 3 kinase
PKA = protein kinase A
PP2C = protein phosphatase 2C
PPAR = peroxisome proliferator-activated receptor
RNA = ribonucleic acid
RPCL = retrovirus-packaging cell line
RPM = rotations per minute
RT-PCR = reverse transcriptase polymerase chain reaction
SDS = sodium dodecyl sulfate
Ser = serine
STRAD = STe20 Related Adaptor Protein
TBS = Tris-buffered saline
Thr = threonine
TNF = tumour necrosis factor
TRITC = tetramethylrhodamine isothiocyanate
V = volts
ZMP = 5-aminoimidazole-4-carboxamide ribofuranotide

CHAPTER I: INTRODUCTION AND LITERATURE REVIEW

1.1 Overview of Study

AMP-activated protein kinase (AMPK) is a serine/threonine protein kinase second messenger that has been localized in a variety of mammalian tissues. As the name suggests, it is activated when the cellular energy potential, defined by the intracellular ATP/AMP ratio, is low (Stapleton *et al.*, 1996). Upon activation, the kinase acutely inhibits numerous energy-consuming biosynthetic pathways while promoting energy-producing reactions via phosphorylation of various metabolic enzymes (Stapleton *et al.*, 1996). Other experiments have indicated AMPK may also exert nuclear effects on gene transcription, suggesting it may have a long-term influence on cellular energy balance when activated chronically (Bamford *et al.*, 2003; Holmes *et al.*, 1999; Putman *et al.*, 2003).

Skeletal muscle is a highly adaptable tissue that can change both structurally and metabolically as a result of the demands placed upon it. The ATP/AMP ratio is largely influenced by these demands, making AMPK a logical candidate to mediate such long-term adaptations. Certain studies in which AMPK was either directly or indirectly activated through pharmacological means produced an increase in the activity of certain mitochondrial enzymes (Ojuka *et al.*, 2000; Shoubridge *et al.*, 1985; Winder *et al.*, 2000), indicating the biogenesis of new mitochondria may be one enduring effect of AMPK activation.

While numerous studies have provided evidence of AMPK's various effects on gene transcription in skeletal muscle, many have used pharmacological treatment *in vivo* as an experimental model. Unfortunately, potential untoward effects treatments such as AICAR may produce, described in further detail below, may be unknowingly influencing experimental results and limiting the approach. This study sought to develop a novel model to examine possible nuclear actions of AMPK and subsequent downstream effects in skeletal muscle.

1.2 Review of AMPK

1.2.1 AMPK Structure and Tissue Distribution

AMP-activated protein kinase was originally identified in 1988 (Sim & Hardie, 1988), and was purified in 1994 (Davies *et al.*, 1994b). It consists of a heterotrimer that shares sequence homology with the yeast SNF1 protein kinase (Celenza & Carlson, 1986). Structurally, AMPK is composed of a 63-kDa catalytic α subunit, a 38-kDa regulatory β subunit, and a 35-kDa γ subunit (Davies *et al.*, 1994a) (Figure 1.1). Two different isoforms of both α and β exist, while 3 γ isoforms have been identified in mammalian tissue (Kemp *et al.*, 1999). The α subunit contains the catalytic core at the N-terminal region, while its C-terminus consists of a tail targeting α to the other subunits (Kemp *et al.*, 1999). The regulatory β subunit is myristoylated on its N-terminus, which is partially responsible for the ability of AMPK to bind membranes (Mitchelhill *et al.*, 1997). In addition, its C-terminal domain allows formation of the $\alpha\beta\gamma$ complex, while its central domain binds to glycogen (Hudson *et al.*, 2003; Polekhina *et al.*, 2003). The regulatory γ subunit, meanwhile, is almost entirely composed of four sequence motifs referred to as cystathionine β synthase (CBS) domains (Bateman,

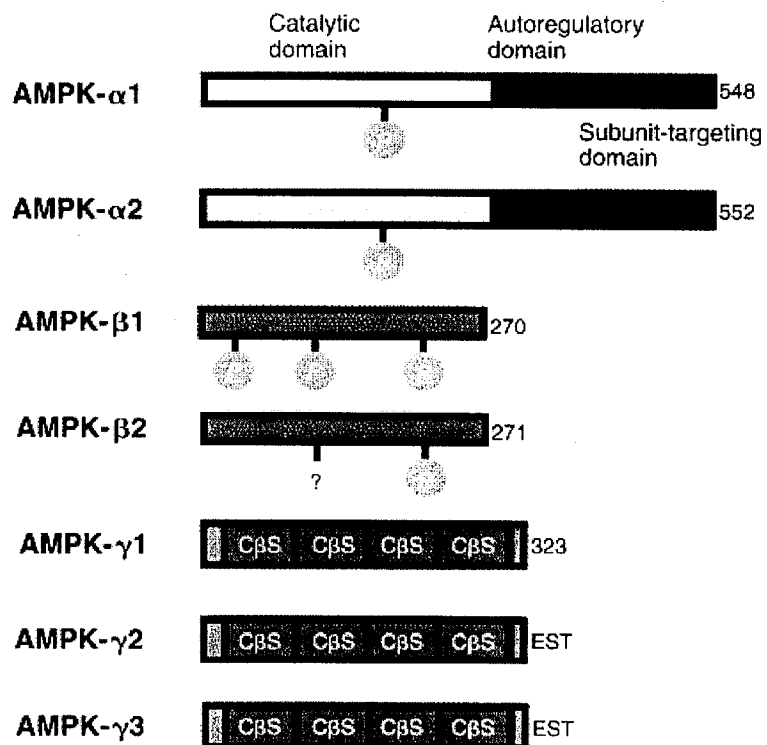


Figure 1.1: Subunit structure of AMPK (adapted from Kemp *et al.*, 1999).

1997). These are thought to be involved in AMP binding (Cheung *et al.*, 2000).

All potential subunit isoform combinations appear capable of heterotrimeric association, with $\alpha_1\beta_1\gamma_1$ being the most common variety (Hardie, 2004). α_2 , β_2 , γ_2 and γ_3 , however, are the most common isoforms present in cardiac and skeletal muscle (Hardie, 2004), while the $\alpha_2\beta_2\gamma_1$ heterotrimer has been identified in rat muscle (Stapleton *et al.*, 1997). α_2 has also been located in the nucleus (Salt *et al.*, 1998), and studies have indicated it translocates from the cytosol to this region following exercise (McGee *et al.*, 2003), providing further evidence that AMPK may be involved in long-term transcriptional regulation.

1.2.2 Function of AMPK

AMPK is activated allosterically by adenosine monophosphate (AMP) (Figures 1.3 and 1.4), which is thought to bind in a pocket created by the α and γ subunit interface (Kemp *et al.*, 1999). Purified α_1 was stimulated 2- to 3-fold while α_2 was activated 3- to 4-fold above basal levels following AMP exposure (Salt *et al.*, 1998; Stapleton *et al.*, 1996). Levels of intracellular free AMP rise as a result of the adenylate kinase reaction, which transfers a phosphate group from one molecule of ADP to another in an attempt to regenerate ATP when stores begin to decline (Figure 1.2). Inversely, high concentrations of ATP can antagonize AMPK activation by AMP, as ATP appears to compete with AMP for binding on the allosteric site (Hardie, 2004).

In addition to AMP binding, AMPK is also activated by phosphorylation of Thr¹⁷² on the activation loop of the α subunit (Kemp *et al.*, 1999) (Figures 1.3 and 1.4). The upstream kinase responsible for this phosphorylation was described for many years as AMPK

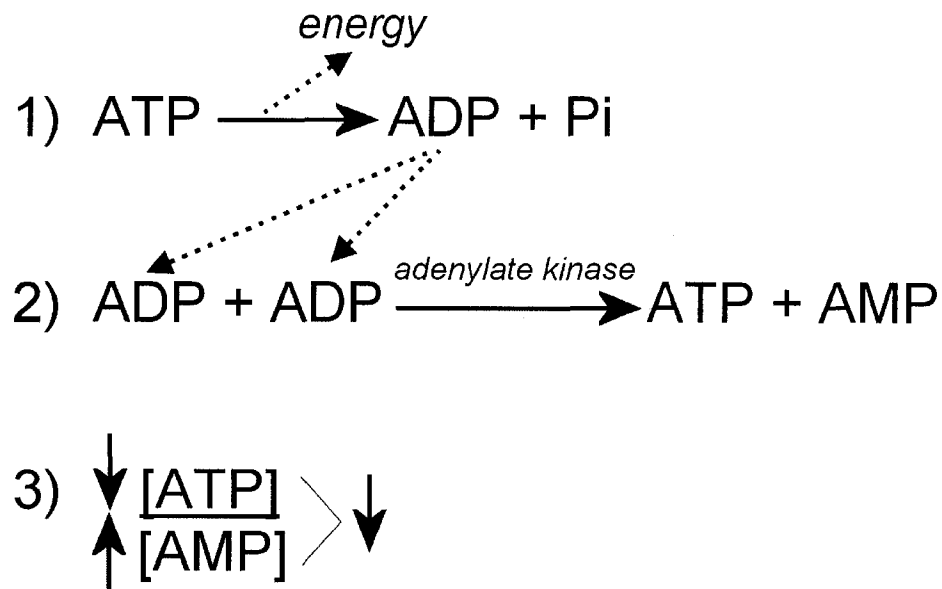


Figure 1.2: The adenylate kinase reaction. 1) ATP is broken down to ADP and inorganic phosphate to provide energy for intracellular processes, 2) to replete ATP stores, the adenylate kinase reaction takes place producing one AMP molecule for each regenerated ATP molecule, 3) while the ATP concentration begins to decrease, the relative concentration of AMP increases, decreasing the ATP/AMP ratio.

kinase, or AMPKK. Recently, however, LKB1, a 50-kDa serine/threonine protein kinase, has also been discovered to possess kinase activity specific to AMPK (Hawley *et al.*, 2003). LKB1 is known primarily for its tumour suppressing actions, and many human tumour cell lines such as HeLa and G361 fail to express it (Hawley *et al.*, 2003). LKB1, the product of the gene mutated in Peutz-Jeghers syndrome (Jenne *et al.*, 1998), also associates with two accessory proteins known as STRAD α/β and MO25 α/β (Hawley *et al.*, 2003). Meanwhile, dephosphorylation and inactivation of AMPK is accomplished by protein phosphatase 2C (PP2C) (Figure 1.4).

AMP binding and Thr¹⁷² phosphorylation have additive effects on AMPK activity, as shown in Figure 1.4. Furthermore, AMP is capable of binding upstream kinases to further promote phosphorylation of AMPK (Figure 1.3). Findings from Hawley *et al.* (2003) indicate LKB1 can be activated in this manner, as AMPK

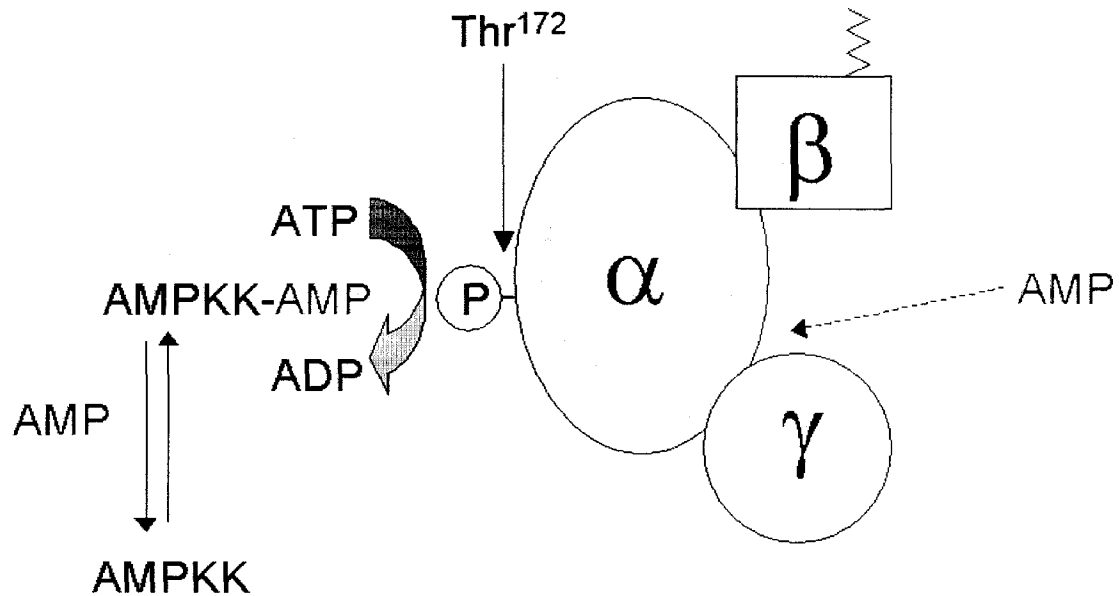


Figure 1.3: Schematic diagram of AMPK subunit association and activation as a result of AMP binding to both the $\alpha\gamma$ interface of AMPK and the upstream kinase AMPKK.

activation was restored when LKB1 was expressed in HeLa cells treated with an AMP analogue.

Recent experiments have also indicated that AMPK can be activated independent of changes in AMP concentrations. Metformin, a diabetes treatment discussed in further detail below, appears capable of activating AMPK without causing any changes in nucleotide levels (Fryer *et al.*, 2002b). In addition, hyperosmotic stress was found to have a similar effect (Fryer *et al.*, 2002b). These conditions, however, still caused Thr¹⁷² phosphorylation, providing evidence that some upstream kinases are also activated by means independent of AMP. As LKB1 expression in HeLa cells also restored AMPK activation in cells treated with phenformin, a relative of metformin, it appears LKB1 may also be activated independent of AMP concentration (Hawley *et al.*, 2003).

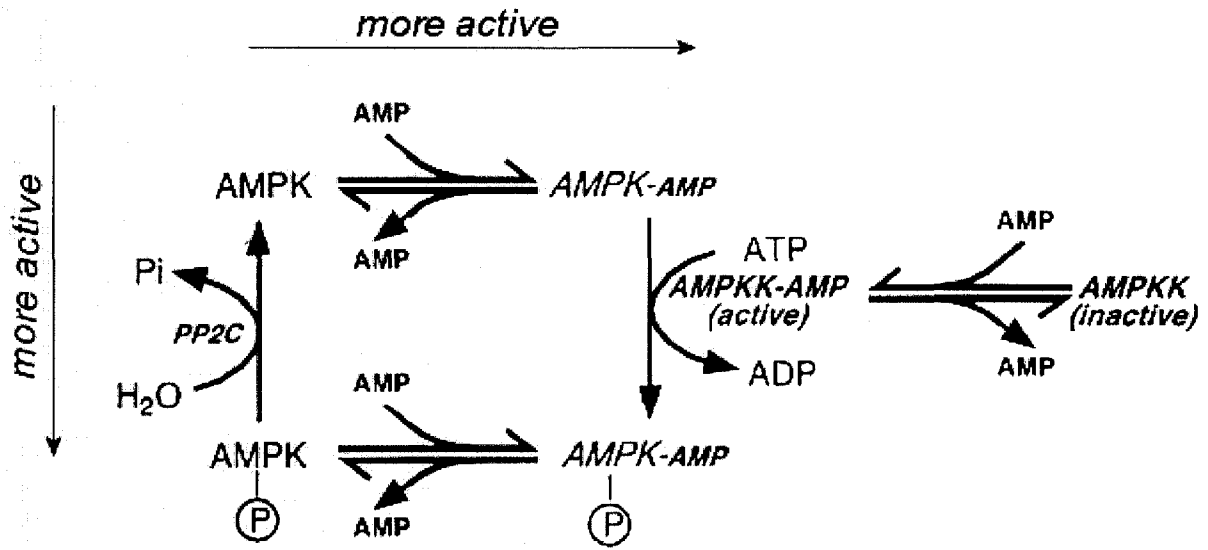


Figure 1.4: Schematic diagram of the different stages of AMPK activation due to both AMPKK phosphorylation and AMP binding (adapted from Hardie and Carling, 1997).

1.2.3 Role of AMPK Activity in Skeletal Muscle

1.2.3.1 Fatty Acid Metabolism

AMPK phosphorylates and inactivates both acetyl-CoA carboxylase (ACC) and 3-hydroxy-3-methylglutaryl-CoA (HMG-CoA) reductase, the rate-limiting enzymes in fatty acid and cholesterol synthesis, respectively (Henin *et al.*, 1996). Phosphorylation of ACC leads to a decrease in malonyl CoA synthesis, which in turn lowers inhibition of carnitine palmitoyltransferase 1 (CPT1) in oxidative tissues allowing increased transfer of cytosolic long-chain fatty acids into the mitochondria for β -oxidation (Ruderman *et al.*, 2003b) (Figure 1.5). As a result, ATP-consuming biosynthetic pathways are inhibited, while ATP-producing reactions are promoted. Recent evidence indicates AMPK can directly enhance activity of malonyl CoA decarboxylase (MCD), promoting decarboxylation of malonyl CoA to acetyl CoA and consequently adding another level of regulation for malonyl CoA concentration (Ruderman *et al.*, 2003b). Furthermore,

AMPK phosphorylates hormone-sensitive lipase (HSL) at Ser⁵⁶⁵ (Donsmark *et al.*, 2004). HSL is normally activated by epinephrine via cAMP-dependent protein kinase (PKA) (Langfort *et al.*, 1999), and mobilizes the energy stored in the intramyocellular triglyceride (IMTG) depot when muscle is contracting. The interplay between AMPK, HSL and PKA remains unclear, however it appears intuitive that AMPK would promote triglyceride mobilization to supply further energy as muscle ATP becomes depleted. Further evidence of this interaction comes from α_2 knockout mice, in which the level of free fatty acids is chronically increased, indicative of HSL inhibition (Viollet *et al.*, 2003).

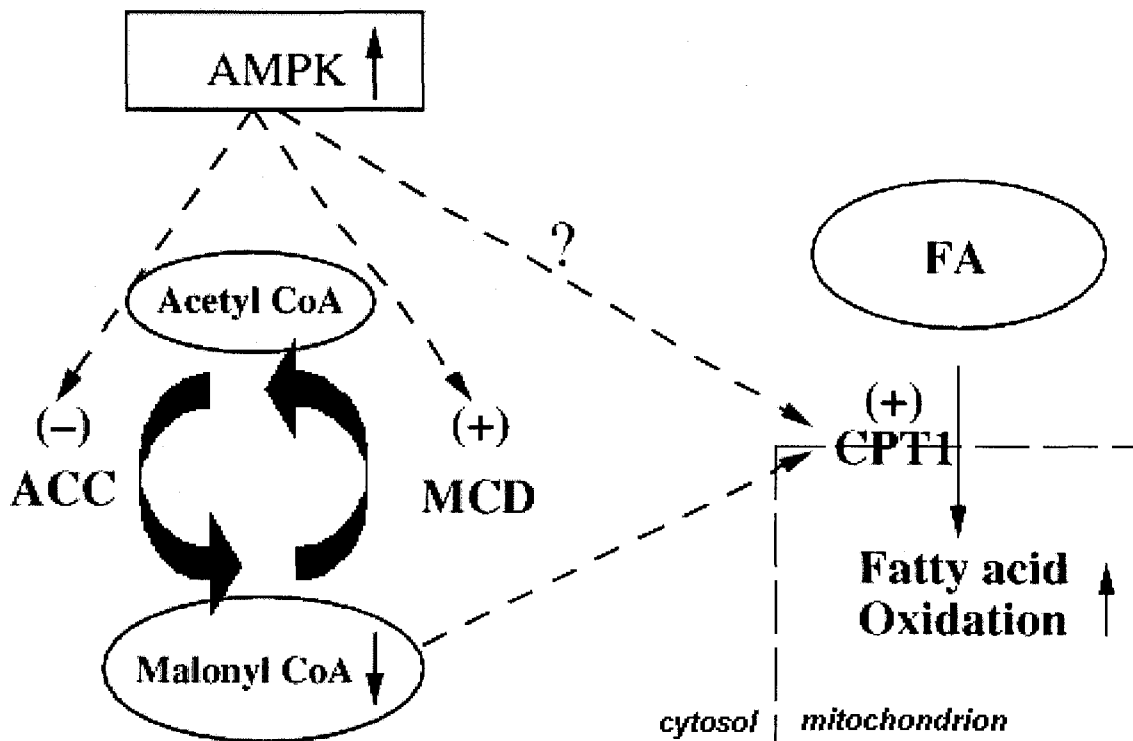


Figure 1.5: Downstream effects of AMPK activation on fatty acid metabolism. ACC is inhibited and MCD is stimulated leading to a decrease in malonyl CoA levels and increased translocation of fatty acids into the mitochondria for β -oxidation (adapted from Ruderman *et al.*, 2003)

1.2.3.2 Carbohydrate Metabolism

Early experiments that used rats treated with AICAR, another AMPK activator further described below, indicated stimulation of glucose uptake in skeletal muscle was one downstream effect of AMPK activation (Merrill *et al.*, 1997). This was later shown to occur due to increased translocation of glucose transporters, such as GLUT4, to the cell membrane (Hayashi *et al.*, 1998; Kurth-Kraczek *et al.*, 1999), although further studies using transgenic mice indicated AMPK was only partly responsible for enhanced muscle glucose uptake as a result of contraction (Mu *et al.*, 2001). Notably, α_1 -knockout mice display no obvious metabolic deficiencies, whereas α_2 knockouts exhibit high plasma glucose and insulin sensitivity in skeletal muscle (Viollet *et al.*, 2003), along with decreased uptake of 2-deoxyglucose (Jorgensen *et al.*, 2003). These results indicate that α_2 , which is more specific to skeletal muscle than α_1 , is the predominant isoform in regards to downstream effects on glucose metabolism. Furthermore, AICAR-injected rats also exhibit increased activity and expression of the glycolytic enzyme hexokinase (Bamford *et al.*, 2003). While this may indicate increased flux through the glycolytic pathway, the possibility also exists that glucose-6-phosphate, produced by hexokinase, is converted to glycogen. As glycogen synthesis is a biosynthetic, energy-requiring process, it makes little sense that AMPK would promote such an action. It has been previously shown, however, that glycogen synthase is phosphorylated by AMPK at Ser⁷ in cell-free assays (Carling & Hardie, 1989), making the nearby Ser¹⁰ a better substrate for casein kinase 1 (CK1). Phosphorylation of Ser¹⁰ inactivates glycogen synthase, demonstrating how AMPK exerts consistent actions on cellular energy balance throughout various metabolic pathways (Flotow & Roach, 1989). Interestingly, however, a naturally-occurring mutation of the AMPK γ_3 subunit leads to both increased basal AMPK activity along with a substantial elevation in both muscle glycogen stores and glycogen synthesis post-exercise (Barnes *et al.*, 2004). These findings may imply that while during exercise glycogen synthesis is likely inhibited by AMPK activity, the enhanced glucose transport and hexokinase activity resulting from kinase activation allow more glucose-6-phosphate to be made available for glycogen synthesis post-exercise.

1.2.3.3 Exercise

AMPK activation due to exercise was first reported in 1996 (Winder & Hardie, 1996). The extent of kinase activation appears to be proportional to exercise intensity (Rasmussen & Winder, 1997), and kinase activity also remains elevated for 15-90 minutes post-exercise (Rasmussen *et al.*, 1998; Ruderman *et al.*, 2003a). This indicates that while the preliminary decrease in the ATP/AMP ratio following the onset of exercise may be responsible for initial AMPK activation, activity levels remain high long after the nucleotide balance is restored, further supporting the proposal that AMPK is involved in long-term intracellular changes. Interestingly, the extent to which highly trained subjects rely on AMPK during exercise has produced some conflicting results. For example, human subjects that underwent a three-week endurance-training program in one leg displayed a 30-40% upregulation of mitochondrial enzymes in the trained skeletal muscle (Frosig *et al.*, 2004). In addition, the activity of α_1 -AMPK and α_2 -AMPK increased 94% and 49% respectively, while phosphorylation of α -AMPK was elevated 74%. Results such as these that examine α_1 and α_2 activities separately following immunoprecipitation must be interpreted cautiously, however, as the different antibodies may have different affinities for their respective antigenic sites and may therefore reduce catalytic activities to different degrees.

In a separate study, the physiological responses of endurance athletes were compared to untrained control subjects following an acute bout of cycling exercise (Nielsen *et al.*, 2003). In general, the activity of skeletal muscle α_2 -AMPK was elevated post-exercise in both groups, but the increase in phosphorylation of both AMPK and acetyl-CoA carboxylase (ACC), a direct target of AMPK, was significantly blunted in the trained subjects. The authors of this study concluded that the diminished AMPK response of already-trained subjects provided further evidence that AMPK plays a role in exercise-induced gene expression. Such results support the possibility that AMPK is involved in initial adaptations to chronic energy deprivation, but the signalling pathway is downregulated as the cell adapts to its new energy demands. Opposing results, however, were discovered in a separate study examining well-trained athletes who underwent 3

weeks of intense exercise training rather than a single bout (Clark *et al.*, 2003). In this instance, there was no decline in the AMPK response to exercise when pre- and post-training results were compared. The authors of that study proposed that muscle glycogen stores might influence the degree of AMPK activation, as AMPK activity appears to be inversely proportional to glycogen content. Interestingly, chronic aerobic training results in overall elevation of glycogen storage within skeletal muscle (Ness *et al.*, 1975), even though AMPK is proposed to acutely inactivate glycogen synthesis when intracellular energy levels decline. This represents somewhat of a paradox within the muscle cell, and serves to illustrate the complexity of various long-term metabolic adaptations. One explanation could be that in earlier studies, trained and untrained subjects exercised at the same intensity relative to their maximum. While this is an understandable control, many training-induced cellular adaptations appear to require progressive increases in volume and intensity, therefore the highly-trained subjects should exercise at a greater intensity relative to their maximum to achieve a similar physiological response as untrained subjects (Booth & Watson, 1985; Hawley, 2002). Another noteworthy finding by Clark and colleagues (2003) was that activation of the α_1 -AMPK isoform was seen at submaximal, albeit intense, exertion levels. Previous reports have suggested that α_1 is only activated in maximal sprint-type activities (Chen *et al.*, 2000), while α_2 activation is associated with prolonged low- and moderate-intensity exercise (Wojtaszewski *et al.*, 2000). Interestingly, recent findings regarding AMPK isoform distribution in various muscle fibres do not support the proposal of α_1 activation solely during maximal sprint activity (Saranchuk, 2004). More specifically, α_1 -AMPK was expressed predominantly in slower-twitching Type I skeletal muscle fibres in rats, while α_2 prevailed in the faster-twitching Type II fibres which are preferentially recruited during sprint-type exercise. Overall, AMPK appears to play a significant role in skeletal muscle during the onset and continuation of exercise, as well as during the post-exercise adaptive period.

1.2.3.4 Protein Synthesis

AMPK has been shown to phosphorylate eukaryotic elongation factor 2 (eEF2) kinase (Horman *et al.*, 2002). eEF2 is a key factor for protein translation initiation and

elongation, but is inhibited when the upstream eEF2 kinase is phosphorylated (Horman *et al.*, 2002). AMPK has also been shown to associate with and possibly inhibit mammalian target of rapamycin (mTOR) (Tokunaga *et al.*, 2004), which in turn may lead to phosphorylation of eEF2 kinase via decreased activation of p70S6 kinase (Chan *et al.*, 2004). Through these and potentially other mechanisms, AMPK is able to inhibit protein synthesis.

1.2.3.5 Oxidative Stress

AMPK is also activated by elevations in intracellular reactive oxygen species, and as with metformin this occurs independent of changes in the ATP/AMP ratio or concentration of free AMP (Toyoda *et al.*, 2004). As higher-intensity exercise causes free radical production and oxidative damage (Hood, 2001), this represents another mechanism by which exercise may elicit AMPK activation. It should be noted, however, that AMPK activation in this manner may be mediated solely through the α_1 isoform, as incubation of rat epitrochlearis muscle in H₂O₂ failed to alter α_2 activity (Toyoda *et al.*, 2004).

1.3 Review of Mitochondrial Biogenesis

1.3.1 Skeletal Muscle Plasticity

As mentioned above, skeletal muscle is a plastic tissue with the ability to adapt both structurally and metabolically to chronic changes in energy demand. For example, chronic electrical stimulation and endurance exercise both result in an increase in mitochondrial volume and enzyme activity (Booth & Thomason, 1991; Holloszy & Coyle, 1984) along with fast-to-slow myosin heavy chain-based fibre type transitions (Pette & Staron, 2000). Endurance training can result in a 50%-100% increase in mitochondrial content within ~6 weeks (Hood, 2001). Obviously, the biogenesis of new mitochondria allows tissue to increase its oxidative metabolic capacity, promoting efficient ATP generation and thus resulting in a greater energy supply for skeletal muscle

contraction. In addition, the decreased reliance on glycolysis as a means of ATP production translates into lower lactic acid production, while biogenesis of further mitochondria may actually decrease the levels of reactive oxygen species and oxidative damage as they are able to spread the ATP requirements over a larger volume of mitochondrial machinery (Davies *et al.*, 1981). While all of these modifications are obviously favourable adaptations during situations of increased metabolic demand, the mechanisms by which such changes occur remain to be fully elucidated.

Initially, many believed that mitochondrial biogenesis simply involved an increase in both mitochondrial size and number (Gollnick & King, 1969), yet further structural studies have indicated perhaps a reticulum or network of mitochondria exist within skeletal muscle (Bakeeva *et al.*, 1978; Kirkwood *et al.*, 1986; Kirkwood *et al.*, 1987). While this finding makes point counting of individual mitochondria an obsolete measure, mitochondrial volume (Hood, 2001), maximal activity of certain marker enzymes such as citrate synthase (Reichmann *et al.*, 1985), or content of certain proteins such as cytochrome *c* (Terjung, 1979), are all suitable markers to measure changes within the organelle. Alterations in mitochondrial protein content and enzyme activity, however, occur much earlier than the 6 week time period for complete adaptation. Mitochondrial proteins have a half-life of ~1 week, while phospholipids have a much shorter ~4 day half-life in comparison (Hood, 2001). As a result, changes indicative of biogenesis can be observed and measured relatively early during the adaptive process.

The causes of mitochondrial biogenesis appear primarily to be local contractile activity rather than neural or humoral factors, as isolated muscle systems can still undergo similar changes (Williams, 1986; Williams *et al.*, 1986). In addition, this process is more likely to occur in tissue with the least initial oxidative capacity, such as the fast-twitching type IIB muscle fibres (Hood, 2001). Indeed, a study by Bamford *et al.* (2003), indicated that increases in mitochondrial enzyme activities as markers of mitochondrial biogenesis were proportional to the fastest-twitch IIB content of rat muscles, and changes were absent in the slow-twitch soleus muscle (Bamford *et al.*, 2003). Muscle contraction itself causes numerous alterations within the muscle including

membrane depolarization, calcium mobilization and mechanical force transduction (Connor *et al.*, 2001). In addition, other local influential factors may include oxygen tension, free radical production, growth factors and cytokines (Pilegaard *et al.*, 2003). Many of these products and processes may act together to induce second-messenger signalling cascades, likely bringing about change through many redundant intracellular mechanisms. While acute contraction has shown to stimulate many different kinases, including MAP kinase, c-Jun, p38 (Connor *et al.*, 2001) and CAMKIV (Wu *et al.*, 2002), AMPK has emerged as one of the prime candidates involved in mitochondrial biogenesis signalling.

1.3.2 Transcriptional Regulation

The majority of mitochondrial proteins are encoded by nuclear DNA within each cell, however a small proportion of these proteins, including select subunits of major respiratory chain complexes, are encoded by the small circular DNA found within the mitochondria itself (Hood, 2001). As a result, a well-controlled coordination of both genomes is required for effective mitochondrial biogenesis. Such control is obtained through coordinated activation of numerous transcription factors, which are known to stimulate transcription of various mitochondrial genes as well as trans-activate other transcription factors.

Nuclear respiratory factor-1 (NRF-1) is a known trans-activator of many mitochondrial genes *in vitro* (Andersson & Scarpulla, 2001). Binding sites for this factor have been identified on promoters for δ -aminolevulinate (ALA) synthase, a mitochondrial matrix enzyme that catalyzes the rate-limiting step of heme biosynthesis, and cytochrome *c*, an electron carrier in the electron transport chain (Braidotti *et al.*, 1993; Evans & Scarpulla, 1989). Cellular energy depletion and subsequent AMPK activation can be achieved by feeding rats the creatine analogue β -guanidinopropionic acid (β -GPA), which competes with endogenous creatine transport and effectively decreases high-energy phospho-creatine stores (Bergeron *et al.*, 2001). β -GPA treatment increased binding of NRF-1 to the ALA synthase promoter, elevated cytochrome *c*

translation, and increased mitochondrial density (Bergeron *et al.*, 2001). This provides strong evidence of AMPK's involvement in the genesis of new mitochondria.

In concert with NRF-1, PPAR- γ coactivator-1 α (PGC-1 α) is also involved in mitochondrial biogenesis. PGC-1 α was first identified as a factor upregulated during thermogenesis following cold exposure, however it has more recently been induced *in vivo* by low-intensity physical activity (Terada *et al.*, 2002). More specifically, a 30% increase in citrate synthase activity followed PGC-1 α mRNA upregulation in rat epitrochlearis muscle after seven days of swimming, indicating PGC-1 α transcription may regulate mitochondrial enzyme expression. PGC-1 α has been expressed at physiological levels under the control of a muscle creatine kinase (MCK) promoter in transgenic mice, causing mRNA levels of both nuclear- and mitochondrial-encoded electron transport enzyme subunits to increase significantly (Lin *et al.*, 2002). Furthermore, expression of PGC-1 α in mouse C2C12 skeletal muscle cells via retroviral infection produced similar results (Wu *et al.*, 1999). Additionally, PGC-1 α appears to be reciprocally induced by NRF, as ectopically expressed PGC-1 α stimulates both NRF-1 and -2 in skeletal muscle cell culture, while transient adenoviral expression of a dominant-negative NRF-1 isoform prevented both PGC-1 α translation and further mitochondrial biogenesis (Wu *et al.*, 1999). Indeed, PGC-1 α appears capable of binding the NRF-1 promoter, while the two factors also appear to interact physically after they are transcribed (Wu *et al.*, 1999). It is believed these two transcription factors act in conjunction to regulate transcription of mitochondrial DNA by inducing transcription of the nuclear-coded mitochondrial transcription factor A (mTFA or Tfam) (Figure 1.6) (Virbasius & Scarpulla, 1994; Wu *et al.*, 1999). Not surprisingly, muscle contraction elevates the levels of mTFA mRNA while increasing the rate of mTFA import into the mitochondria (Hood, 2001). This is one plausible explanation for the reliable coordination between the nuclear mitochondrial genomes during biogenesis.

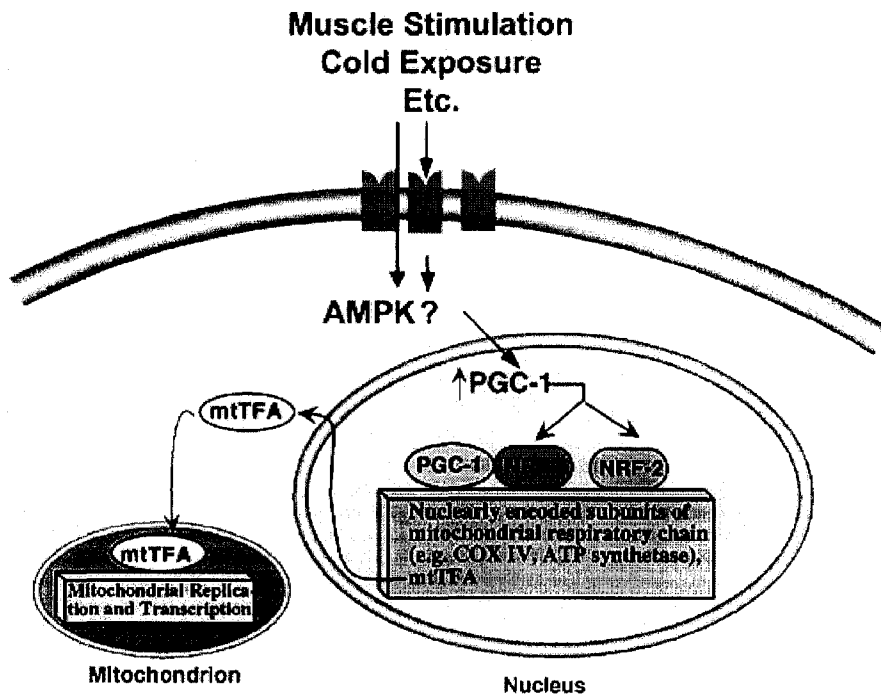


Figure 1.6: Proposed transcriptional regulation during mitochondrial biogenesis (adapted from Wu *et al.*, 1999).

NRF-1 promoter/protein (Andersson & Scarpulla, 2001), PPAR- α and - γ , c-Jun, c-Fos, and Sp1 (Lenka *et al.*, 1998; Nelson *et al.*, 1995).

1.3.3 Role of AMPK

Extensive experimental evidence has implicated AMPK in the process of mitochondrial biogenesis. The most direct example was evident in various studies involving rodents administered the AMPK-activator 5-aminoimidazole-4-carboxamide ribofuranoside (AICAR), in which activity of certain mitochondrial enzymes increased significantly over those of control animals (Bamford *et al.*, 2003; Ojuka *et al.*, 2000; Putman *et al.*, 2003; Winder *et al.*, 2000). This can be combined with the β -GPA evidence mentioned above, as β -GPA indirectly activates AMPK by lowering the cellular energy potential (Bergeron *et al.*, 2001). As mentioned earlier, AMPK can also be

In addition to the major candidates described above, there are numerous other transcription factors implicated in the process and coordination of mitochondrial biogenesis. These include PGC-1 α related cofactor (PRC), which shares some sequence homology with PGC-1 α and also appears capable of binding the

activated by oxidative stress, which can result from exercise and therefore lead to adaptive mitochondrial changes independent of the ATP/AMP ratio. Interestingly, as mitochondrial volume increases, the potential to generate reactive oxygen species will likely decline as the energy requirements can be more spread out (Hood, 2001). This provides another explanation for the lower AMPK activation in pre-trained subjects exercised at the same relative intensity as untrained individuals, mentioned above (Nielsen *et al.*, 2003). Because of the possibility of nuclear transcriptional activity by AMPK, other studies have examined the actions of this kinase on transcription factors implicated in mitochondrial biogenesis. For example, when rat muscle was incubated in a 0.5 mM AICAR medium, PGC-1 α mRNA expression doubled as compared to control muscles (Terada *et al.*, 2002). The limitations of AICAR *in vivo* notwithstanding, these results implicate PGC-1 α as a downstream target of AMPK activity within the nucleus, although the exact mechanisms of activation remain to be elucidated.

Another transcription factor, p300, is a known downstream target of AMPK, and phosphorylation impairs the factor's affinity for nuclear receptors (Yang *et al.*, 2001). p300 influences numerous downstream pathways, and in particular it coactivates various PPAR isoforms, which have further downstream implications in both lipid metabolism (Gilde & Van Bilsen, 2003; Leff, 2003) and mitochondrial biogenesis (Hood, 2001).

Besides acting through an isolated pathway, AMPK may also work in conjunction with other well-known signal transduction pathways to exert long-term changes in mRNA and protein expression. Potential candidate pathways include calcium signalling via calcium-calmodulin kinase IV (CaMKIV) (Freyssenet *et al.*, 2004; Irrcher *et al.*, 2003) and mitogen-activated protein kinase (MAPK) pathways (Yu *et al.*, 2003). Where such pathways may converge and diverge with that of AMPK has not yet been clarified, but nevertheless the underlying message remains that mitochondrial biogenesis is likely a product of numerous redundant interactions within the cell.

1.4 Development of a Novel *In Vitro* Experimental Model

1.4.1 Skeletal Muscle In Vitro

The C2C12 cell line, chosen for the current experimental model, was originally cloned from mouse primary skeletal muscle cells (Yaffe & Saxel, 1977). These cells have an approximate doubling time of 16 hours (Durante *et al.*, 2002), and grow preferentially on an extracellular matrix layer.

In culture as well as *in vivo*, myoblasts proliferate in an environment enriched with growth factors. When conditions become less desirable for growth, the cells will align and fuse, exit the cell cycle and form multinucleated myotubes (Holtzer & Abbott, 1958; Kalderon & Gilula, 1979). Myotubes continue to further differentiate and eventually become striated adult tissue *in vivo*, producing distinct isoforms of muscle proteins such as myosin at each stage of development (Blau *et al.*, 1985).

Differentiation itself is a complex process, governed by the coordinated expression of muscle specific transcription factors that initially establish myogenic lineage of mesodermal cells and then proceed to activate different genes required at the appropriate stages of development. The primary transcription factors involved come from a family of basic helix-loop-helix (bHLH) proteins that includes myoD, Myf5, myogenin and MRF4 (Arnold & Winter, 1998; McKinsey *et al.*, 2001). These proteins form heterodimers with other ubiquitous bHLH proteins known as E proteins, and together the proteins bind E box sequences in regulatory regions of various muscle-specific genes (McKinsey *et al.*, 2001). Targeted disruptions of these proteins indicate they all play a key role in myogenesis (Arnold & Braun, 1996; Molkentin & Olson, 1996; Yun & Wold, 1996), although some functional overlap appears to exist between myoD and Myf5. The simplest model of myogenic determination and differentiation consists of two steps: initially myoD and Myf5 establish mesodermal cells as myoblasts, while myogenin later mediates muscle cell differentiation (Arnold & Winter, 1998). Indeed, many studies have indicated that in C2C12 mouse skeletal muscle cells, myoD mRNA

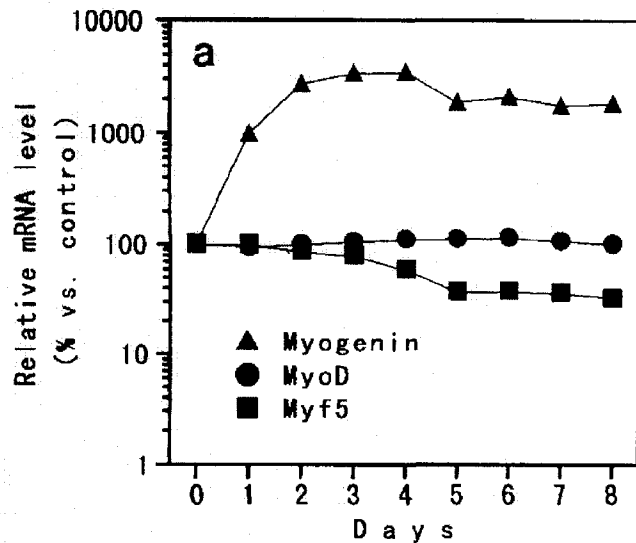


Figure 1.7: Differentiation-induced changes in myoD and myogenin mRNA expression in the C2C12 cell line as previously reported in Shimokawa et al. (1998).

and protein levels remain constant during differentiation (Dedieu *et al.*, 2002; Shen *et al.*, 2003; Shimokawa *et al.*, 1998). In contrast, myogenin is virtually absent in myoblasts, while peaks in mRNA and protein expression occur roughly 3 and 4 days, respectively, following induction of differentiation (Dedieu *et al.*, 2002; Shen *et al.*, 2003; Shimokawa *et al.*, 1998). (Figure 1.7)

C2C12 myoblasts are primarily glycolytic and express low levels of aerobic enzymes, whereas differentiated myotubes are predominantly oxidative (Leary *et al.*, 1998; Moyes *et al.*, 1997). In addition, inhibition of mitochondrial protein synthesis prevents differentiation of C2C12 myoblasts (Hamai *et al.*, 1997), therefore any experimental conditions that affect AMPK may be preventing differentiation through this and potentially other mechanisms. As a result, cells were permitted to differentiate quite extensively, and analysis of both myoD and myogenin protein expression helped to establish the extent of differentiation prior to treatment. As other studies involving C2C12 cells or other skeletal muscle cell lines often involve transfection, infection, or other forms of treatment immediately following differentiation (Fryer *et al.*, 2002a; Michael *et al.*, 2001), this model is rather unique and may be able to produce results that other models could not.

1.4.2 Adenovirus Constructs

Adenovirus-mediated gene delivery was used to inhibit AMPK in this study independent of pharmacological means. Viruses are submicroscopic particles, often referred to as virions, which lack the genetic information to produce the necessary machinery for protein synthesis or energy production (Blake & Stacy, 1999). They are relatively simple in structure, with an outer capsid composed of redundant subunits responsible for recognition and attachment to the host cell as well as protecting the genome within (Cann & Irving, 1999). Native adenoviruses contain a linear, double-stranded DNA genome consisting of 30-38 kb containing 30-40 genes (Minor, 1999). Replication of this genome requires the exploitation of host cell machinery, which is achieved by binding and penetration, primarily via endocytosis, of the virion into such a cell (Gray, 1999). Once inside, the particle uncoats to expose the genetic material, and replication or expression of the genome proceeds. For adenoviruses in particular, initial recognition and binding requires the Coxsackie and adenovirus receptor (CAR), a 46-kDa transmembrane protein with high affinity for types 2 and 5 adenoviruses as well as the Coxsackie B virus (Bergelson *et al.*, 1997; Tomko *et al.*, 1997). Following the initial binding step, an interaction between the viral penton base and the cell's $\alpha_v\beta_3$ or $\alpha_v\beta_5$ integrins takes place, facilitating endocytosis into endosomes and eventual access to the cytoplasm (Wang *et al.*, 2000; Wickham *et al.*, 1993).

Unfortunately, many tissues such as alveolar macrophages (Kaner *et al.*, 1999) and skeletal muscle (Nalbantoglu *et al.*, 1999), express low levels of CAR making them poor targets for adenovirus-mediated gene delivery. Indeed, in

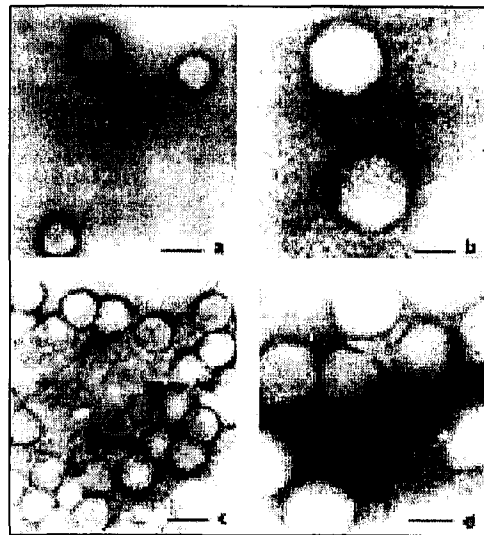


Figure 1.8: Polycationic lipid and virus complexes, as viewed through an electron microscope. Pictures (a) and (b) are uncomplexed, while (c) and (d) show particles that have been complexed with lipofectamine (adapted from Dodds *et al.*, 1999).

preliminary experiments of this study, infection efficiency was quite low and increasing the virus dose up to 500 plaque-forming units (PFU) per cell did not appear to resolve the problem. Resolution of the underlying predicament was attempted by retroviral overexpression of the CAR receptor followed by cloning selection, and also via the use of polycationic lipid. Retroviral infection resulted in great success in other studies (Kimura *et al.*, 2001; Nalbantoglu *et al.*, 1999; Orlicky *et al.*, 2001), including a 80-fold increase in adenovirus transduction following such a procedure (Nalbantoglu *et al.*, 1999). In addition, the creation of virus and polycationic lipid complexes has overcome a complete lack of CAR in some tissues (Dodds *et al.*, 1999). Polycationic lipids, such as Lipofectamine and polyethylimine (PEI), are thought to promote aggregation of virus particles, which may protect them from neutralizing antibodies, and/or increase their contact with the cell monolayer (Figure 1.8) (Dodds *et al.*, 1999). Others believe the lipid may allow virions to bypass CAR completely and enter the cell through another pathway (Fasbender *et al.*, 1997; Qiu *et al.*, 1998). Although its mechanism remains somewhat unclear, this infection aid is nonetheless an effective means to improve adenovirus-mediated gene delivery *in vitro*.

Adenovirus constructs for this study included an adenovirus containing the green fluorescent protein (GFP) gene alone, and another encoding a myc-tagged dominant-negative form of the α_2 AMPK subunit (α_2 DN) as well as GFP. The dominant negative construct was created by mutating Asp¹⁵⁷, which lies in the DFG motif essential for ATP binding, to alanine (Johnson *et al.*, 1996). The construct therefore remains capable of binding to the β and γ subunits, but it lacks kinase activity. As a result, its overexpression within the cell causes competition between the α_2 DN subunit and endogenous α -AMPK for $\beta\gamma$ binding, thus the majority of α bound to $\beta\gamma$ is the mutated form and AMPK activity is largely “knocked out”. GFP expression was used to assess infection efficiency in live cells, thus the virus encoding GFP alone served as a control condition for infection.

1.4.3 Pharmacological Activation

1.4.3.1 Metformin

Metformin, also known as dimethylbiguanide, is a derivative of guanidine often used to treat hyperglycemia and Type II diabetes (El-mir *et al.*, 2000). It promotes insulin-stimulated glucose uptake in skeletal muscle (Galuska *et al.*, 1991) while causing much less of a metabolic acidosis than related compounds such as phenformin and buformin (Mehnert, 2001). Metformin is also a known activator of AMPK, as primary rat hepatocytes treated with 0.5 mM or higher concentrations exhibited significant increases in AMPK activity and significant decreases in ACC activity both 1h and 7h following exposure (Zhou *et al.*, 2001). Another study using Chinese hamster ovary (CHO) fibroblasts indicated that only 0.25 mM metformin was required to cause significant increases in ACC phosphorylation 18 hours following treatment, while 0.1 mM metformin produced similar results in rat hepatoma H4IIE cells (Hawley *et al.*, 2002).

The mechanism of action for metformin has not been fully elucidated, although there has been some recent progress in this area. Earlier experiments using isolated mitochondria and permeabilized hepatocytes were able to pinpoint its effect to complex I (NADH quinone oxidoreductase) of the electron transport chain (El-mir *et al.*, 2000). As a result, it was proposed that metformin inhibited electron transport through complex I, thus preventing aerobic ATP production and leading to a decline in the cellular energy potential (El-mir *et al.*, 2000). This claim, however, was debated by Hawley *et al.* (2002), after measuring no detectable change in the ADP/ATP ratio during AMPK activation by metformin. Recently published data proposed that metformin activation was accomplished via the actions of reactive oxygen species such as peroxynitrite (Zou *et al.*, 2004). More specifically, inhibition of complex I by metformin was proposed to lead to superoxide radical production, which can react with nitric oxide in a reaction catalyzed by endothelial nitric oxide synthase (eNOS) to produce peroxynitrite (Zou *et al.*, 2004). This leads to subsequent activation of the PI-3 kinase signalling pathway, resulting in

Thr¹⁷² phosphorylation due to activation of LKB1 and/or other upstream kinases of AMPK (Zou *et al.*, 2004). This mechanism is consistent with earlier findings indicating metformin is not a direct allosteric activator of AMPK (Zhou *et al.*, 2001), nor was it capable of affecting AMPK inactivation via protein phosphatase 2C (Hawley *et al.*, 2002).

1.4.3.2 AICAR

5-aminoimidazole-4-carboxamide ribofuranoside, or AICA riboside, is metabolized intracellularly to AICA ribotide, also known as ZMP, and proceeds to act as an AMP analogue thus activating AMPK (Henin *et al.*, 1996) (Figure 1.9). Indeed, AMP and ZMP shared the same maximum stimulatory effect on rat liver AMPK, and the affinity of AMPK for both molecules increased to the same extent as the ATP concentration was lowered, indicating they bind allosterically at the same site (Henin *et al.*, 1996). AICAR has also proven to be an effective AMPK activator in skeletal muscle, causing a large increase in intracellular ZMP concentration and ACC phosphorylation following chronic injections in rats (Bamford *et al.*, 2003).

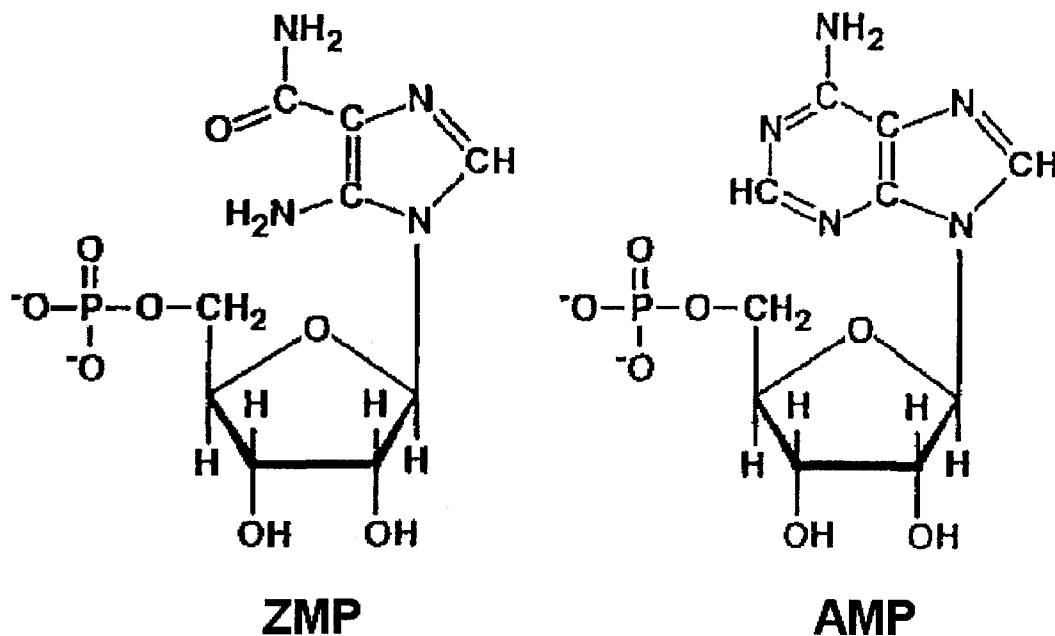


Figure 1.9: Structural comparison of AMP and ZMP (adapted from Henin *et al.*, 1996).

AMPK, however, is not AICAR's sole target as ZMP also inhibits fructose-1,6-bisphosphatase leading to suppression of gluconeogenesis (Vincent *et al.*, 1991). In addition, AICAR appears to suppress lipopolysaccharide-induced TNF- α production in macrophages independent of AMPK activity, possibly by inhibiting the PI3 kinase/Akt pathway (Jhun *et al.*, 2004). *In vitro*, AICAR has been used at doses of 0.5 mM in primary rat hepatocytes (Zhou *et al.*, 2001) and H-2K^b cells (Fryer *et al.*, 2002b).

1.5 Activation and Inhibition of AMPK *In Vitro*

1.5.1 Experimental Conditions

AMPK activation was achieved using the well-established pharmacological activators described above on C2C12 cells, and results were compared to an untreated control. In a separate set of experiments, both activation and inhibition was achieved using AICAR and the α_2 DN adenovirus treatment. By treating the cells with the dominant negative adenovirus, followed by AICAR 24 hours later, it was shown that AICAR was acting, at least in part, via the AMPK pathway in our system. In addition, as two variables were manipulated in the second set of experiments, three controls were required: α_2 DN alone, AICAR + control GFP-containing virus, and a control GFP-containing virus alone

1.5.2 Protein Expression

Protein expression was assessed by Western blotting, a technique in which proteins from both whole-cell lysates and nuclear extracts were solubilized with detergent, separated electrophoretically on a polyacrylamide gel, blotted onto a nitrocellulose membrane and probed with antibodies of interest to examine relative differences in protein expression between various samples. Specifically, this study examined both markers of glycolysis (glyceraldehyde-3-phosphate dehydrogenase or GAPDH) and mitochondrial biogenesis (citrate synthase), as well as the transcription factor PGC-1 α . β -actin, a commonly-used loading control (Rondinelli *et al.*, 1997;

Tamiya *et al.*, 2003) was used to normalize blotting results in most instances. Initial time-course experiments, as well as background knowledge regarding mitochondrial biogenesis, allowed determination of the proper harvesting day post-treatment.

1.5.3 Real Time RT-PCR

Expression of mRNA at various time points was assayed in real-time using the method of reverse transcriptase polymerase chain reaction (RT-PCR). This PCR method is advantageous as it is capable of precisely quantifying the amount of RNA over a wide range of concentrations (Wilhelm & Pingoud, 2003). In addition to regular primers,

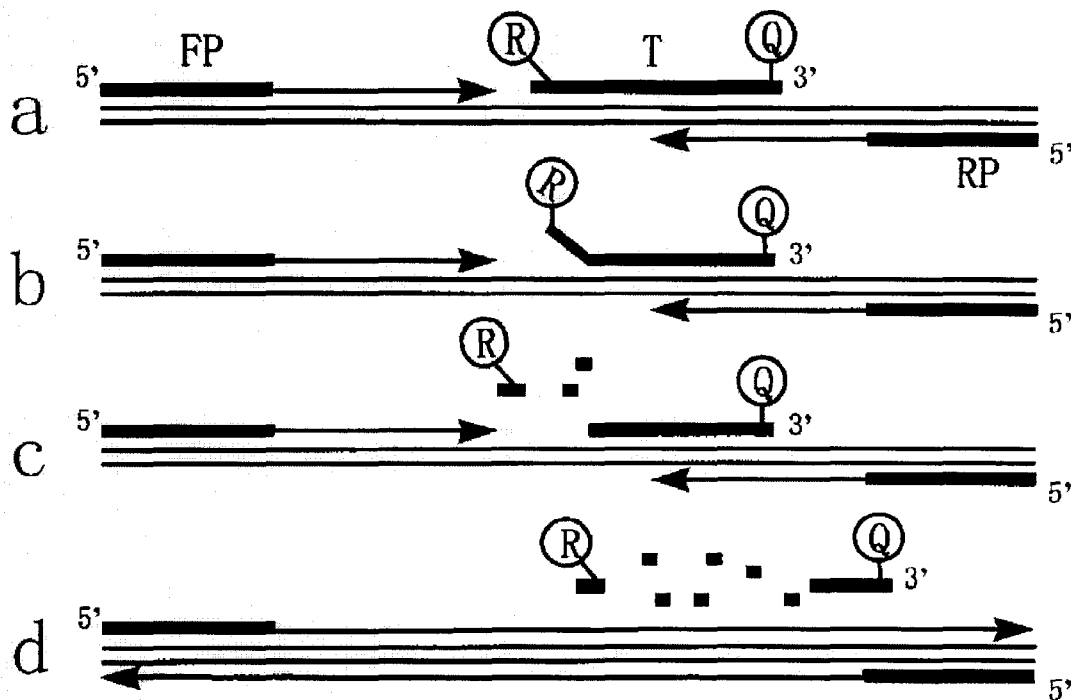


Figure 1.10: Real-time RT-PCR primer/probe annealing and DNA synthesis: a) after DNA strands are separated by high temperature, forward primers (FP) and reverse primers (RP) bind to the appropriate 5' end, while the probe (T) binds along the length of the DNA, b) as DNA polymerase synthesizes DNA from the primers, it moves along the DNA strand until it reaches the probe, c) DNA polymerase cleaves the probe to remove it and continues with DNA synthesis, d) once cleaved, the 3'-quencher dye (Q) is not longer in close proximity with the 5'-fluorescent dye, resulting in fluorescence emission (adapted from Shimokawa *et al.*, 1998).

sequence-specific probes with a fluorescent tag on their 5' ends and a fluorescence quencher on their 3' ends are also added to the reaction mixture. When the probe is free in solution, the 3' quencher activity prevents fluorescence emission. As complementary DNA strands dissociate during the PCR process, the probe binds to a specific sequence in the middle of the DNA strand for the appropriate gene, and again the 5' and 3' ends of the probe remain in close proximity preventing fluorescence emission. As the DNA polymerase moves along the single strand synthesizing complementary DNA, it cleaves the probe, separating the fluorescent tag from its quencher and allowing fluorescence emission (Figure 1.10) (Wilhelm & Pingoud, 2003). In general, the reaction produces fluorescence signals proportional to the amount of PCR product during each cycle of amplification, which is detected and plotted over time to produce a sigmoidal curve.

At any point on the linear portion of the curve, which represents the exponential phase of amplification, an arbitrary threshold can be set to determine the threshold cycle (C_T) where the threshold intersects the curve. The C_T values are then expressed relative to a reference gene to determine the initial relative amount of mRNA present in each sample. This ΔC_T value is obtained by subtracting the housekeeping gene C_T from the C_T for the gene of interest. Following this, the control sample at each time point is chosen as the baseline ΔC_T , and the comparative $\Delta\Delta C_T$ value is determined by subtracting the ΔC_T of experimental conditions from this baseline or control ΔC_T . As a result, mRNA expression is expressed relative to the control condition.

$$\Delta C_T = C_T (\text{gene of interest}) - C_T (\text{housekeeping gene}) \quad (1)$$

$$\Delta\Delta C_T = \Delta C_T (\text{control condition}) - \Delta C_T (\text{experimental condition}) \quad (2)$$

Finally, the $\Delta\Delta C_T$ values are converted into absolute values, the comparative expression level, based on the principle that DNA doubles during each cycle (Livak & Schmittgen, 2001). The formula for this is as follows:

$$\text{comparative expression level} = 2^{(-\Delta\Delta C_T)} \quad (3)$$

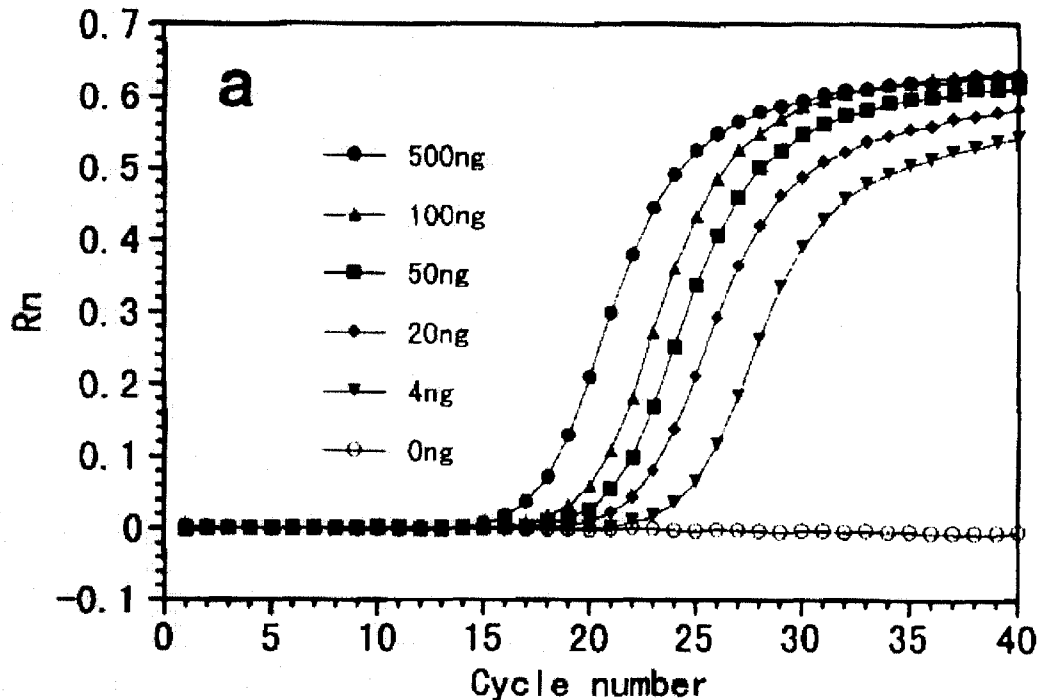


Figure 1.11: Representative plot of real-time RT-PCR fluorescence. Normalized reporter (Rn) represents fluorescence signal from probe 5'-reporter dye divided by a passive reference. Samples with a higher quantity of initial DNA reach the linear phase of the curve after fewer cycles than those with less initial DNA (adapted from Shimokawa et al., 1998).

This study examined mRNA expression at various time points post-treatment for markers of mitochondrial biogenesis and transcription factors. Citrate synthase mRNA expression was examined alongside ALA synthase to assess potential biogenesis of mitochondrial proteins. The transcription factor PGC-1 α was also examined at the mRNA level, as was p300. Cyclophilin, a cytosolic peptidyl-prolyl cis-trans isomerase involved in protein folding, was used as a housekeeping gene. Both cyclophilin and β -actin have been shown to be stable housekeeping genes for real-time RT-PCR studies involving high-intensity exercise in skeletal muscle (Murphy *et al.*, 2003).

1.5.4 Research Hypothesis

Based on reported findings in earlier literature, AMPK activation should cause an upregulation in mRNA encoding mitochondrial proteins and their subsequent expression

following an appropriate lag time, thus citrate synthase and ALA synthase expression will become elevated. Prior to and possibly in conjunction with mitochondrial biogenesis, PGC-1 α mRNA and protein expression will increase as well. GAPDH expression should not change, as GAPDH is not a flux-generating enzyme of glycolysis. p300 expression will also likely remain unchanged, as p300 is a downstream target of AMPK and decreases its nuclear receptor affinity as a result of phosphorylation. Thus, while its binding affinity for DNA may decrease, there is no indication that changes in p300 expression will result from changes in AMPK activity. Opposite results are expected when AMPK is inhibited, therefore decreases in protein and/or mRNA expression levels for citrate synthase, ALA synthase and PGC-1 α should take place. The null hypothesis is that no change will occur in either protein or mRNA expression levels of citrate synthase, ALA synthase, and PGC-1 α , while significant changes will be apparent in both GAPDH protein and p300 mRNA expression.

1.5.5 Limitations of the Study

As this study focuses on changes in mRNA and protein expression, any alterations in DNA binding of transcription factors as a result of AMPK activation or inhibition will be not be detected. In addition, the short-term nature of the experiments due to limitations of the model, as described below, may limit the accuracy of our results. Furthermore, while *in vitro* systems often permit more experimental manipulation than an *in vivo* system could support, they may not always reflect the responses of an *in vivo* system, which is more complex and possesses considerably more redundancy. Skeletal muscle *in vitro*, for example, receives signals from both the nervous and endocrine systems, both of which are absent in our model.

1.6 References

- Andersson, U. & Scarpulla, R. C. (2001). Pgc-1-related coactivator, a novel, serum-inducible coactivator of nuclear respiratory factor 1-dependent transcription in mammalian cells. *Mol. Cell Biol.* 21, 3738-3749.
- Arnold, H. H. & Braun, T. (1996). Targeted inactivation of myogenic factor genes reveals their role during mouse myogenesis: a review. *Int. J. Dev. Biol.* 40, 345-353.
- Arnold, H. H. & Winter, B. (1998). Muscle differentiation: more complexity to the network of myogenic regulators. *Curr. Opin. Genet. Dev.* 8, 539-544.
- Bakeeva, L. E., Chentsov, Y., & Skulachev, V. P. (1978). Mitochondrial framework (reticulum mitochondriale) in rat diaphragm muscle. *Biochim. Biophys. Acta* 501, 349-369.
- Bamford, J. A., Lopaschuk, G. D., MacLean, I. M., Reinhart, M. L., Dixon, W. T., & Putman, C. T. (2003). Effects of chronic AICAR administration on the metabolic and contractile phenotypes of rat slow- and fast-twitch skeletal muscles. *Can. J. Physiol. Pharmacol.* 81, 1072-1082.
- Barnes, B.R., Marklund, S., Steiler, T.L., Walter, M., Hjalms, G., Amarger, V., Mahlapuu, M., Leng, Y., Johansson, C., Galuska, D., Lindgren, K., Abrink, M., Stapleton, D., Zierath, J.R., Andersson, L. (2004). The 5'-AMP-activated protein kinase {gamma}3 isoform has a key role in carbohydrate and lipid metabolism in glycolytic skeletal muscle. *J. Biol. Chem.*, 279, 38441-38447.
- Bateman, A. (1997). The structure of a domain common to archaebacteria and the homocystinuria disease protein. *Trends Biochem. Sci.* 22, 12-13.
- Bergelson, J. M., Cunningham, J. A., Droguett, G., Kurt-Jones, E. A., Krithivas, A., Hong, J. S., Horwitz, M. S., Crowell, R. L., & Finberg, R. W. (1997). Isolation of a common receptor for Coxsackie B viruses and adenoviruses 2 and 5. *Science* 275, 1320-1323.
- Bergeron, R., Ren, J. M., Cadman, K. S., Moore, I. K., Perret, P., Pypaert, M., Young, L. H., Semenkovich, C. F., & Shulman, G. I. (2001). Chronic activation of AMP kinase results in NRF-1 activation and mitochondrial biogenesis. *Am. J. Physiol. Endocrinol. Metab.* 281, E1340-E1346.

- Blake, K. & Stacy, A. (1999). Cell Culture. In *Virus Culture: A Practical Approach*, ed. Cann, A. J., pp. 1-31. Oxford University Press, New York.
- Blau, H. M., Pavlath, G. K., Hardeman, E. C., Chiu, C. P., Silberstein, L., Webster, S. G., Miller, S. C., & Webster, C. (1985). Plasticity of the differentiated state. *Science* 230, 758-766.
- Booth, F. W. & Thomason, D. B. (1991). Molecular and cellular adaptation of muscle in response to exercise: perspectives of various models. *Physiol. Rev.* 71, 541-585.
- Booth, F. W. & Watson, P. A. (1985). Control of adaptations in protein levels in response to exercise. *Fed. Proc.* 44, 2293-2300.
- Braidotti, G., Borthwick, I. A., & May, B. K. (1993). Identification of regulatory sequences in the gene for 5-aminolevulinate synthase from rat. *J. Biol. Chem.* 268, 1109-1117.
- Cann, A. J. & Irving, W. (1999). Virus Isolation. In *Virus Culture: A Practical Approach*, ed. Cann, A. J., pp. 33-60. Oxford University Press, New York.
- Carling, D. & Hardie, D. G. (1989). The substrate and sequence specificity of the AMP-activated protein kinase. Phosphorylation of glycogen synthase and phosphorylase kinase. *Biochim. Biophys. Acta* 1012, 81-86.
- Celenza, J. L. & Carlson, M. (1986). A yeast gene that is essential for release from glucose repression encodes a protein kinase. *Science* 233, 1175-1180.
- Chan, A. Y., Soltys, C. L., Young, M. E., Proud, C. G., & Dyck, J. R. (2004). Activation of AMP-activated protein kinase inhibits protein synthesis associated with hypertrophy in the cardiac myocyte. *J. Biol. Chem.* 279, 32771-32779.
- Chen, Z. P., McConell, G. K., Michell, B. J., Snow, R. J., Canny, B. J., & Kemp, B. E. (2000). AMPK signaling in contracting human skeletal muscle: acetyl-CoA carboxylase and NO synthase phosphorylation. *Am. J. Physiol. Endocrinol. Metab.* 279, E1202-E1206.
- Cheung, P. C., Salt, I. P., Davies, S. P., Hardie, D. G., & Carling, D. (2000). Characterization of AMP-activated protein kinase gamma-subunit isoforms and their role in AMP binding. *Biochem. J.* 346 Pt 3, 659-669.

- Clark, S. A., Chen, Z. P., Murphy, K. T., Aughey, R. J., McKenna, M. J., Kemp, B. E., & Hawley, J. A. (2003). Intensified exercise training does not alter AMPK signalling in human skeletal muscle. *Am. J. Physiol. Endocrinol. Metab.* 286, E737-E743.
- Connor, M. K., Irrcher, I., & Hood, D. A. (2001). Contractile activity-induced transcriptional activation of cytochrome C involves Sp1 and is proportional to mitochondrial ATP synthesis in C2C12 muscle cells. *J. Biol. Chem.* 276, 15898-15904.
- Davies, K. J., Packer, L., & Brooks, G. A. (1981). Biochemical adaptation of mitochondria, muscle, and whole-animal respiration to endurance training. *Arch. Biochem. Biophys.* 209, 539-554.
- Davies, S. P., Hawley, S. A., Woods, A., Carling, D., Haystead, T. A., & Hardie, D. G. (1994b). Purification of the AMP-activated protein kinase on ATP-gamma-sepharose and analysis of its subunit structure. *Eur. J. Biochem.* 223, 351-357.
- Davies, S. P., Hawley, S. A., Woods, A., Carling, D., Haystead, T. A., & Hardie, D. G. (1994a). Purification of the AMP-activated protein kinase on ATP-gamma-sepharose and analysis of its subunit structure. *Eur. J. Biochem.* 223, 351-357.
- Dedieu, S., Mazeres, G., Cottin, P., & Brustis, J. J. (2002). Involvement of myogenic regulator factors during fusion in the cell line C2C12. *Int. J. Dev. Biol.* 46, 235-241.
- Dodds, E., Piper, T. A., Murphy, S. J., & Dickson, G. (1999). Cationic lipids and polymers are able to enhance adenoviral infection of cultured mouse myotubes. *J. Neurochem.* 2105-2112.
- Donsmark, M., Langfort, J., Holm, C., Ploug, T., & Galbo, H. (2004). Contractions induce phosphorylation of the AMPK site Ser565 in hormone-sensitive lipase in muscle. *Biochem. Biophys. Res. Commun.* 316, 867-871.
- Durante, P. E., Mustard, K. J., Park, S. H., Winder, W. W., & Hardie, D. G. (2002). Effects of endurance training on activity and expression of AMP-activated protein kinase isoforms in rat muscles. *Am. J. Physiol. Endocrinol. Metab.* 283, E178-E186.

- El-mir, M., Nogueira, V., Fontaine, E., Averetm N., Rigoulet, M., & Leverve, X. (2000). Dimethylbiguanide inhibits cell respiration via an indirect effect targeted on the respiratory chain complex I. *J. Biol. Chem.* 275, 223-228.
- Evans, M. J. & Scarpulla, R. C. (1989). Interaction of nuclear factors with multiple sites in the somatic cytochrome c promoter. Characterization of upstream NRF-1, ATF, and intron Sp1 recognition sequences. *J. Biol. Chem.* 264, 14361-14368.
- Fasbender, A., Zabner, J., Chillon, M., Moninger, T. O., Puga, A. P., Davidson, B. L., & Welsh, M. J. (1997). Complexes of adenovirus with polycationic polymers and cationic lipids increase the efficiency of gene transfer in vitro and in vivo. *J. Biol. Chem.* 272, 6479-6489.
- Flotow, H. & Roach, P. J. (1989). Synergistic phosphorylation of rabbit muscle glycogen synthase by cyclic AMP-dependent protein kinase and casein kinase I. Implications for hormonal regulation of glycogen synthase. *J. Biol. Chem.* 264, 9126-9128.
- Freysenet, D., Irrcher, I., Connor, M. K., Di Carlo, M., & Hood, D. A. (2004). Calcium-regulated changes in mitochondrial phenotype in skeletal muscle cells. *Am. J. Physiol. Cell Physiol.* 286, C1053-1061.
- Frosig, C., Jorgensen, S. B., Hardie, D. G., Richter, E. A., & Wojtaszewski, J. F. (2004). 5'-AMP-activated protein kinase activity and protein expression are regulated by endurance training in human skeletal muscle. *Am. J. Physiol. Endocrinol. Metab.* 286, E411-E417.
- Fryer, L. G., Fougelle, F., Barnes, K., Baldwin, S. A., Woods, A., & Carling, D. (2002a). Characterization of the role of the AMP-activated protein kinase in the stimulation of glucose transport in skeletal muscle cells. *Biochem. J.* 363, 167-174.
- Fryer, L. G., Parbu-Patel, A., & Carling, D. (2002b). The Anti-diabetic drugs rosiglitazone and metformin stimulate AMP-activated protein kinase through distinct signaling pathways. *J. Biol. Chem.* 277, 25226-25232.
- Galuska, D., Zierath, J., Thorne, A., Sonnenfeld, T., & Wallberg-Henriksson, H. (1991). Metformin increases insulin-stimulated glucose transport in insulin-resistant human skeletal muscle. *Diabete Metab.* 17, 159-163.

- Gilde, A. J. & Van Bilsen, M. (2003). Peroxisome proliferator-activated receptors (PPARS): regulators of gene expression in heart and skeletal muscle. *Acta Physiol. Scand.* 178, 425-434.
- Gollnick, P. D. & King, D. W. (1969). Effect of exercise and training on mitochondria of rat skeletal muscle. *Am. J. Physiol.* 216, 1502-1509.
- Gray, J. J. (1999). Assays for Virus Infection. In *Virus Culture: A Practical Approach*, ed. Cann, A. J., pp. 81-108. Oxford University Press, New York.
- Hamai, N., Nakamura, M., & Asano, A. (1997). Inhibition of mitochondrial protein synthesis impaired C2C12 myoblast differentiation. *Cell Struct. Funct.* 22, 421-431.
- Hardie, D.G. (2004). AMP-Activated Protein Kinase: A Key System Mediating Metabolic Responses to Exercise. *Med. Sci. Sports & Exerc.* 36, 28-34.
- Hawley, J. A. (2002). Adaptations of skeletal muscle to prolonged, intense endurance training. *Clin. Exp. Pharmacol. Physiol.* 29, 218-222.
- Hawley, S. A., Boudeau, J., Reid, J. L., Mustard, K. J., Udd, L., Makela, T. P., Alessi, D. R., & Hardie, D. G. (2003). Complexes between the LKB1 tumor suppressor, STRADalpha/beta and MO25alpha/beta are upstream kinases in the AMP-activated protein kinase cascade. *J. Biol.* 2, 28.
- Hawley, S. A., Gadalla, A. E., Olsen, G. S., & Hardie, D. G. (2002). The antidiabetic drug metformin activates the AMP-activated protein kinase cascade via an adenine nucleotide-independent mechanism. *Diabetes* 51, 2420-2425.
- Hayashi, T., Hirshman, M. F., Kurth, E. J., Winder, W. W., & Goodyear, L. J. (1998). Evidence for 5' AMP-activated protein kinase mediation of the effect of muscle contraction on glucose transport. *Diabetes* 47, 1369-1373.
- He, T. C., Zhou, S., da Costa, L. T., Yu, J., Kinzler, K. W., & Vogelstein, B. (1998). A simplified system for generating recombinant adenoviruses. *Proc. Natl. Acad. Sci. U.S.A* 95, 2509-2514.

- Henin, N., Vincent, M. F., & Van den, B. G. (1996). Stimulation of rat liver AMP-activated protein kinase by AMP analogues. *Biochim. Biophys. Acta* 1290, 197-203.
- Holloszy, J. O. & Coyle, E. F. (1984). Adaptations of skeletal muscle to endurance exercise and their metabolic consequences. *J. Appl. Physiol.* 56(4), 831-838.
- Holmes, B. F., Kurth-Kraczek, E. J., & Winder, W. W. (1999). Chronic activation of 5'-AMP-activated protein kinase increases GLUT-4, hexokinase, and glycogen in muscle. *J. Appl. Physiol.* 87, 1990-1995.
- Holtzer, H. & Abbott, J. (1958). Contraction of glycerinated embryonic myoblasts. *Anat. Rec.* 131, 417-428.
- Hood, D. A. (2001). Invited Review: contractile activity-induced mitochondrial biogenesis in skeletal muscle. *J. Appl. Physiol.* 90, 1137-1157.
- Horman, S., Browne, G., Krause, U., Patel, J., Vertommen, D., Bertrand, L., Lavoine, A., Hue, L., Proud, C., & Rider, M. (2002). Activation of AMP-activated protein kinase leads to the phosphorylation of elongation factor 2 and an inhibition of protein synthesis. *Curr. Biol.* 12, 1419-1423.
- Hudson, E. R., Pan, D. A., James, J., Lucocq, J. M., Hawley, S. A., Green, K. A., Baba, O., Terashima, T., & Hardie, D. G. (2003). A novel domain in AMP-activated protein kinase causes glycogen storage bodies similar to those seen in hereditary cardiac arrhythmias. *Curr. Biol.* 13, 861-866.
- Irrcher, I., Adhietty, P. J., Sheehan, T., Joseph, A. M., & Hood, D. A. (2003). PPARgamma coactivator-1alpha expression during thyroid hormone- and contractile activity-induced mitochondrial adaptations. *Am. J. Physiol. Cell Physiol.* 284, C1669-C1677.
- Jenne, D. E., Reimann, H., Nezu, J., Friedel, W., Loff, S., Jeschke, R., Muller, O., Back, W., & Zimmer, M. (1998). Peutz-Jeghers syndrome is caused by mutations in a novel serine threonine kinase. *Nat. Genet.* 18, 38-43.
- Jhun, B. S., Jin, Q., Oh, Y. T., Kim, S. S., Kong, Y., Cho, Y. H., Ha, J., Baik, H. H., & Kang, I. (2004). 5-Aminoimidazole-4-carboxamide riboside suppresses lipopolysaccharide-induced TNF-alpha production through inhibition of

phosphatidylinositol 3-kinase/Akt activation in RAW 264.7 murine macrophages. *Biochem. Biophys. Res. Commun.* 318, 372-380.

Johnson, L. N., Noble, M. E., & Owen, D. J. (1996). Active and inactive protein kinases: structural basis for regulation. *Cell* 85, 149-158.

Jorgensen, S.B., Viollet, B., Andreelli, F., Frosig, C., Birk, J.B., Scherling, P., Vaulont, S., Richter, E.A., Wojtaszewski, J.F. (2004). Knockout of the alpha2 but not alpha1 5'-AMP-activated protein kinase isoform abolishes 5-aminoimidazole-4-carboxamide-1-beta-4-ribofuranoside but not contraction-induced glucose uptake in skeletal muscle. *J. Biol. Chem.* 279, 1070-1079.

Kalderon, N. & Gilula, N. B. (1979). Membrane events involved in myoblast fusion. *J. Cell Biol.* 81, 411-425.

Kaner, R. J., Worgall, S., Leopold, P. L., Stolze, E., Milano, E., Hidaka, C., Ramalingam, R., Hackett, N. R., Singh, R., Bergelson, J., Finberg, R., Falck-Pedersen, E., & Crystal, R. G. (1999). Modification of the genetic program of human alveolar macrophages by adenovirus vectors in vitro is feasible but inefficient, limited in part by the low level of expression of the coxsackie/adenovirus receptor. *Am. J. Respir. Cell Mol. Biol.* 20, 361-370.

Kemp, B. E., Mitchelhill, K. I., Stapleton, D., Michell, B. J., Chen, Z. P., & Witters, L. A. (1999). Dealing with energy demand: the AMP-activated protein kinase. *Trends Biochem. Sci.* 24, 22-25.

Kimura, E., Maeda, Y., Arima, T., Nishida, Y., Yamashita, S., Hara, A., Uyama, E., Mita, S., & Uchino, M. (2001). Efficient repetitive gene delivery to skeletal muscle using recombinant adenovirus vector containing the Coxsackievirus and adenovirus receptor cDNA. *Gene Ther.* 8, 20-27.

Kirkwood, S. P., Munn, E. A., & Brooks, G. A. (1986). Mitochondrial reticulum in limb skeletal muscle. *Am. J. Physiol. Cell Physiol.* 251, C395-C402.

Kirkwood, S. P., Packer, L., & Brooks, G. A. (1987). Effects of endurance training on a mitochondrial reticulum in limb skeletal muscle. *Arch. Biochem. Biophys.* 255, 80-88.

- Kurth-Kraczek, E. J., Hirshman, M. F., Goodyear, L. J., & Winder, W. W. (1999). 5' AMP-activated protein kinase activation causes GLUT4 translocation in skeletal muscle. *Diabetes* 48, 1667-1671.
- Langfort, J., Ploug, T., Ihlemann, J., Saldo, M., Holm, C., & Galbo, H. (1999). Expression of hormone-sensitive lipase and its regulation by adrenaline in skeletal muscle. *Biochem. J.* 340, 459-465.
- Leary, S. C., Battersby, B. J., Hansford, R. G., & Moyes, C. D. (1998). Interactions between bioenergetics and mitochondrial biogenesis. *Biochim. Biophys. Acta* 1365, 522-530.
- Leff, T. (2003). AMP-activated protein kinase regulates gene expression by direct phosphorylation of nuclear proteins. *Biochem. Soc. Trans.* 31, 224-227.
- Lenka, N., Vijayasathy, C., Mullick, J., & Avadhani, N. G. (1998). Structural organization and transcription regulation of nuclear genes encoding the mammalian cytochrome c oxidase complex. *Prog. Nucleic Acid Res. Mol. Biol.* 61:309-44., 309-344.
- Lin, J., Wu, H., Tarr, P. T., Zhang, C. Y., Wu, Z., Boss, O., Michael, L. F., Puigserver, P., Isotani, E., Olson, E. N., Lowell, B. B., Bassel-Duby, R., & Spiegelman, B. M. (2002). Transcriptional co-activator PGC-1 alpha drives the formation of slow-twitch muscle fibres. *Nature* 418, 797-801.
- Livak, K. J. & Schmittgen, T. D. (2001). Analysis of relative gene expression data using real-time quantitative PCR and the 2(-Delta Delta C(T)) Method. *Methods* 25, 402-408.
- McGee, S. L., Howlett, K. F., Starkie, R. L., Cameron-Smith, D., Kemp, B. E., & Hargreaves, M. (2003). Exercise Increases Nuclear AMPK alpha(2) in Human Skeletal Muscle. *Diabetes* 52, 926-928.
- McKinsey, T. A., Zhang, C. L., & Olson, E. N. (2001). Control of muscle development by dueling HATs and HDACs. *Curr. Opin. Genet. Dev.* 11, 497-504.
- Mehnert, H. (2001). Metformin, the rebirth of a biguanide: mechanism of action and place in the prevention and treatment of insulin resistance. *Exp. Clin. Endocrinol. Diabetes* 109 Suppl 2:S259-64.

- Merrill, G. F., Kurth, E. J., Hardie, D. G., & Winder, W. W. (1997). AICA riboside increases AMP-activated protein kinase, fatty acid oxidation, and glucose uptake in rat muscle. *Am. J. Physiol. Endocrinol. Metab.* 273, E1107-E1112.
- Michael, L. F., Wu, Z., Cheatham, R. B., Puigserver, P., Adelmant, G., Lehman, J. J., Kelly, D. P., & Spiegelman, B. M. (2001). Restoration of insulin-sensitive glucose transporter (GLUT4) gene expression in muscle cells by the transcriptional coactivator PGC-1. *Proc. Natl. Acad. Sci. U.S.A* 98, 3820-3825.
- Minor, P. D. (1999). Concentration and Purification of Viruses. In *Virus Culture: A Practical Approach*, ed. Cann, A. J., pp. 61-80. Oxford University Press, New York.
- Mitchelhill, K. I., Michell, B. J., House, C. M., Stapleton, D., Dyck, J., Gamble, J., Ullrich, C., Witters, L. A., & Kemp, B. E. (1997). Posttranslational modifications of the 5'-AMP-activated protein kinase beta1 subunit. *J. Biol. Chem.* 272, 24475-24479.
- Molkentin, J. D. & Olson, E. N. (1996). Defining the regulatory networks for muscle development. *Curr. Opin. Genet. Dev.* 6, 445-453.
- Moyes, C. D., Mathieu-Costello, O. A., Tsuchiya, N., Filburn, C., & Hansford, R. G. (1997). Mitochondrial biogenesis during cellular differentiation. *Am. J. Physiol. Cell Physiol.* 272, C1345-C1351.
- Mu, J., Brozinick, J. T., Jr., Valladares, O., Bucan, M., & Birnbaum, M. J. (2001). A role for AMP-activated protein kinase in contraction- and hypoxia-regulated glucose transport in skeletal muscle. *Mol. Cell* 7, 1085-1094.
- Murphy, R. M., Watt, K. K., Cameron-Smith, D., Gibbons, C. J., & Snow, R. J. (2003). Effects of creatine supplementation on housekeeping genes in human skeletal muscle using real-time RT-PCR. *Physiol. Genomics* 12, 163-174.
- Nalbantoglu, J., Pari, G., Karpati, G., & Holland, P. C. (1999). Expression of the primary coxsackie and adenovirus receptor is downregulated during skeletal muscle maturation and limits the efficacy of adenovirus-mediated gene delivery to muscle cells. *Hum. Gene Ther.* 10, 1009-1019.

- Nelson, B. D., Luciakova, K., Li, R., & Betina, S. (1995). The role of thyroid hormone and promoter diversity in the regulation of nuclear encoded mitochondrial proteins. *Biochim. Biophys. Acta* 1271, 85-91.
- Ness, G. W., Gardiner, P. F., Secord, D. C., & Taylor, A. W. (1975). The effects of swimming and running regimens on skeletal muscle glycogen in the rat. *Rev. Can. Biol.* 34, 45-50.
- Nielsen, J. N., Mustard, K. J., Graham, D. A., Yu, H., MacDonald, C. S., Pilegaard, H., Goodyear, L. J., Hardie, D. G., Richter, E. A., & Wojtaszewski, J. F. (2003). 5'-AMP-activated protein kinase activity and subunit expression in exercise-trained human skeletal muscle. *J. Appl. Physiol* 94, 631-641.
- Ojuka, E. O., Nolte, L. A., & Holloszy, J. O. (2000). Increased expression of GLUT-4 and hexokinase in rat epitrochlearis muscles exposed to AICAR in vitro. *J. Appl. Physiol.* 88, 1072-1075.
- Orlicky, D. J., DeGregori, J., & Schaack, J. (2001). Construction of stable coxsackievirus and adenovirus receptor-expressing 3T3-L1 cells. *J. Lipid Res.* 42, 910-915.
- Pette, D. & Staron, R. S. (2000). Myosin isoforms, muscle fiber types, and transitions. *Microsc. Res. Tech.* 50, 500-509.
- Pilegaard, H., Saltin, B., & Neufer, P. D. (2003). Exercise induces transient transcriptional activation of the PGC-1alpha gene in human skeletal muscle. *J. Physiol. (Lond.)* 546, 851-858.
- Polekhina, G., Gupta, A., Michell, B. J., van Denderen, B., Murthy, S., Feil, S. C., Jennings, I. G., Campbell, D. J., Witters, L. A., Parker, M. W., Kemp, B. E., & Stapleton, D. (2003). AMPK beta subunit targets metabolic stress sensing to glycogen. *Curr. Biol.* 13, 867-871.
- Putman, C. T., Kiricsi, M., Pearcey, J., MacLean, I. M., Bamford, J. A., Murdoch, G. K., Dixon, W. T., & Pette, D. (2003). AMPK activation increases uncoupling protein-3 expression and mitochondrial enzyme activities in rat muscle without fibre type transitions. *J. Physiol. (Lond.)* 551, 169-178.
- Qiu, C., De Young, M. B., Finn, A., & Dichek, D. A. (1998). Cationic liposomes enhance adenovirus entry via a pathway independent of the fiber receptor and alpha(v)-integrins. *Hum. Gene Ther.* 9, 507-520.

- Rasmussen, B. B., Hancock, C. R., & Winder, W. W. (1998). Postexercise recovery of skeletal muscle malonyl-CoA, acetyl-CoA carboxylase, and AMP-activated protein kinase. *J Appl. Physiol.* 85, 1629-1634.
- Rasmussen, B. B. & Winder, W. W. (1997). Effect of exercise intensity on skeletal muscle malonyl-CoA and acetyl-CoA carboxylase. *J Appl. Physiol.* 83, 1104-1109.
- Reichmann, H., Hoppeler, H., Mathieu-Costello, O., von Bergen, F., & Pette, D. (1985). Biochemical and ultrastructural changes of skeletal muscle mitochondria after chronic electrical stimulation in rabbits. *Pflügers Arch.* 404, 1-9.
- Rondinelli, R. H., Epner, D. E., & Tricoli, J. V. (1997). Increased glyceraldehyde-3-phosphate dehydrogenase gene expression in late pathological stage human prostate cancer. *Prostate Cancer Prostatic Dis.* 1, 66-72.
- Ruderman, N. B., Park, H., Kaushik, V. K., Dean, D., Constant, S., Prentki, M., & Saha, A. K. (2003a). AMPK as a metabolic switch in rat muscle, liver and adipose tissue after exercise. *Acta Physiol. Scand.* 178, 435-442.
- Ruderman, N. B., Saha, A. K., & Kraegen, E. W. (2003b). Minireview: malonyl CoA, AMP-activated protein kinase, and adiposity. *Endocrinol.* 144, 5166-5171.
- Salt, I., Celler, J. W., Hawley, S. A., Prescott, A., Woods, A., & Carling, D. (1998). AMP-activated protein kinase: greater dependence, and preferential nuclear localization, of complexes containing the alpha-2 isoform. *Biochem. J.* 334, 177-187.
- Saranchuk, R. Activity and Isoform Specific Distribution of AMP-Activated Protein Kinase in Rat Skeletal Muscle of Different Fibre-Types. (2004). M.Sc. Thesis, University of Alberta.
- Shen, X., Collier, J. M., Hlaing, M., Zhang, L., Delshad, E. H., Bristow, J., & Bernstein, H. S. (2003). Genome-wide examination of myoblast cell cycle withdrawal during differentiation. *Dev. Dyn.* 226, 128-138.
- Shimokawa, T., Kato, M., Ezaki, O., & Hashimoto, S. (1998). Transcriptional regulation of muscle-specific genes during myoblast differentiation. *Biochem. Biophys. Res. Commun.* 246, 287-292.

- Shoubridge, E. A., Challiss, R. A., Hayes, D. J., & Radda, G. K. (1985). Biochemical adaptation in the skeletal muscle of rats depleted of creatine with the substrate analogue beta-guanidinopropionic acid. *Biochem. J.* 232, 125-131.
- Sim, A. T. & Hardie, D. G. (1988). The low activity of acetyl-CoA carboxylase in basal and glucagon-stimulated hepatocytes is due to phosphorylation by the AMP-activated protein kinase and not cyclic AMP-dependent protein kinase. *FEBS Lett.* 233, 294-298.
- Stapleton, D., Mitchelhill, K. I., Gao, G., Widmer, J., Michell, B. J., Teh, T., House, C. M., Fernandez, C. S., Cox, T., Witters, L. A., & Kemp, B. E. (1996). Mammalian AMP-activated protein kinase subfamily. *J. Biol. Chem.* 271, 611-614.
- Stapleton, D., Woollatt, E., Mitchelhill, K. I., Nicholl, J. K., Fernandez, C. S., Michell, B. J., Witters, L. A., Power, D. A., Sutherland, G. R., & Kemp, B. E. (1997). AMP-activated protein kinase isoenzyme family: subunit structure and chromosomal location. *FEBS Lett.* 409, 452-456.
- Tamiya, S., Dean, W. L., Paterson, C. A., & Delamere, N. A. (2003). Regional distribution of Na,K-ATPase activity in porcine lens epithelium. *Invest. Ophthalmol. Vis. Sci.* 44, 4395-4399.
- Terada, S., Goto, M., Kato, M., Kawanaka, K., Shimokawa, T., & Tabata, I. (2002). Effects of low-intensity prolonged exercise on PGC-1 mRNA expression in rat epitrochlearis muscle. *Biochem. Biophys. Res. Commun.* 296, 350-354.
- Terjung, R. L. (1979). The turnover of cytochrome c in different skeletal-muscle fibre types of the rat. *Biochem. J.* 178, 569-574.
- Tokunaga, C., Yoshino, K., & Yonezawa, K. (2004). mTOR integrates amino acid- and energy-sensing pathways. *Biochem. Biophys. Res. Commun.* 313, 443-446.
- Tomko, R. P., Xu, R., & Philipson, L. (1997). HCAR and MCAR: the human and mouse cellular receptors for subgroup C adenoviruses and group B coxsackieviruses. *Proc. Natl. Acad. Sci. U.S.A.* 94, 3352-3356.
- Toyoda, T., Hayashi, T., Miyamoto, L., Yonemitsu, S., Nakano, M., Tanaka, S., Ebihara, K., Masuzaki, H., Hosoda, K., Inoue, G., Otaka, A., Sato, K., Fushiki, T., & Nakao, K. (2004). Possible involvement of the alpha1 isoform of 5'AMP-

activated protein kinase in oxidative stress-stimulated glucose transport in skeletal muscle. *Am. J. Physiol. Endocrinol. Metab.* 287, E166-E173.

- Vincent, M. F., Marangos, P. J., Gruber, H. E., & Van den, B. G. (1991). Inhibition by AICA riboside of gluconeogenesis in isolated rat hepatocytes. *Diabetes* 40, 1259-1266.
- Viollet, B., Andreelli, F., Jorgensen, S.B., Perrin, C., Flamez, D., Mu, J., Wojtaszewski, J.F.P., Schuit, F.C., Birnbaum, M., Richter, E., Burcelin, R., Vaulont, S. (2003). Physiological role of AMP-activated protein kinase (AMPK): insights from knockout mouse models. *Biochem. Soc. Trans.*, 31, 216-219.
- Virbasius, J. V. & Scarpulla, R. C. (1994). Activation of the human mitochondrial transcription factor A gene by nuclear respiratory factors: a potential regulatory link between nuclear and mitochondrial gene expression in organelle biogenesis. *Proc. Natl. Acad. Sci. U.S.A* 91, 1309-1313.
- Wang, K., Guan, T., Cheresch, D. A., & Nemerow, G. R. (2000). Regulation of adenovirus membrane penetration by the cytoplasmic tail of integrin beta5. *J. Virol.* 74, 2731-2739.
- Wickham, T. J., Mathias, P., Cheresch, D. A., & Nemerow, G. R. (1993). Integrins alpha v beta 3 and alpha v beta 5 promote adenovirus internalization but not virus attachment. *Cell* 73, 309-319.
- Wilhelm, J. & Pingoud, A. (2003). Real-time polymerase chain reaction. *Chembiochem.* 4, 1120-1128.
- Williams, R. S. (1986). Regulation of mitochondrial biogenesis by contractile activity in skeletal muscle: recent advances and directions for future research. In *Biochemical Aspects of Physical Exercise*, eds. Benzi, G., Packer, L., & Siliprandi, N., pp. 171-180. Elsevier, New York.
- Williams, R. S., Salmons, S., Newsholme, E. A., Kaufman, R. E., & Mellor, J. (1986). Regulation of nuclear and mitochondrial gene expression by contractile activity in skeletal muscle. *J. Biol. Chem.* 261, 376-380.
- Winder, W. W. & Hardie, D. G. (1996). Inactivation of acetylCoA carboxylase and activation of AMP-activated protein kinase in muscle during exercise. *Am. J. Physiol. Endocrinol. Metab.* 270, E299-E304.

- Winder, W. W., Holmes, B. F., Rubink, D. S., Jensen, E. B., Chen, M., & Holloszy, J. O. (2000). Activation of AMP-activated protein kinase increases mitochondrial enzymes in skeletal muscle. *J. Appl. Physiol.* 88, 2219-2226.
- Wojtaszewski, J. F., Nielsen, P., Hansen, B. F., Richter, E. A., & Kiens, B. (2000). Isoform-specific and exercise intensity-dependent activation of 5'-AMP-activated protein kinase in human skeletal muscle. *J. Physiol (Lond.)* 528, 221-226.
- Wu, H., Kanatous, S. B., Thurmond, F. A., Gallardo, T., Isotani, E., Bassel-Duby, R., & Williams, R. S. (2002). Regulation of mitochondrial biogenesis in skeletal muscle by CaMK. *Science* 296, 349-352.
- Wu, Z., Puigserver, P., Andersson, U., Zhang, C., Adelmant, G., Mootha, V., Troy, A., Cinti, S., Lowell, B., Scarpulla, R. C., & Spiegelman, B. M. (1999). Mechanisms controlling mitochondrial biogenesis and respiration through the thermogenic coactivator PGC-1. *Cell* 98, 115-124.
- Yaffe, D. & Saxel, O. (1977). Serial passaging and differentiation of myogenic cells isolated from dystrophic mouse muscle. *Nature* 270, 725-727.
- Yang, W., Hong, Y. H., Shen, X. Q., Frankowski, C., Camp, H. S., & Leff, T. (2001). Regulation of transcription by AMP-activated protein kinase: phosphorylation of p300 blocks its interaction with nuclear receptors. *J. Biol. Chem.* 276, 38341-38344.
- Yu, M., Stepto, N. K., Chibalin, A. V., Fryer, L. G., Carling, D., Krook, A., Hawley, J. A., & Zierath, J. R. (2003). Metabolic and mitogenic signal transduction in human skeletal muscle after intense cycling exercise. *J. Physiol. (Lond.)* 546, 327-335.
- Yun, K. & Wold, B. (1996). Skeletal muscle determination and differentiation: story of a core regulatory network and its context. *Curr. Opin. Cell Biol.* 8, 877-889.
- Zhou, G., Myers, R., Li, Y., Chen, Y., Shen, X., Fenyk-Melody, J., Wu, M., Ventre, J., Doebber, T., Fujii, N., Musi, N., Hirshman, M. F., Goodyear, L. J., & Moller, D. E. (2001). Role of AMP-activated protein kinase in mechanism of metformin action. *J. Clin. Invest.* 108, 1167-1174.
- Zou, M.H., Kirkpatrick, S.S., Davis, B.J., Nelson, J.S., Wiles IV, W.G., Schlettner, U., Neumann, D., Brownlee, M., Freeman, M.B., Goldman, M.H. (2004). Activation

of the AMP-activated protein kinase by the anti-diabetic drug metformin in vivo:
Role of mitochondrial reactive nitrogen species. *J. Biol. Chem.* (Epub), 2004.

CHAPTER II: MATERIALS AND METHODS

2.1 Experimental Model

2.1.1 In Vitro System

C2C12 myoblasts were obtained from American Type Culture Collection (ATCC CRL-1772, Manassas, VA, USA). Cells were passaged in Dulbecco's modified Eagle's media (DMEM) containing 10% fetal calf serum (Gibco; Burlington, ON, Canada), 4 mM L-glutamine (Sigma-Aldrich, Oakville, ON, Canada) and 1X penicillin-streptomycin antibiotics (Sigma-Aldrich). Cells were plated onto 60 mm polyethylene plates (Falcon, Bedford, MA, USA) coated with Cultrex Basement Membrane Extract (Trevigen™, Gaithersburg, MD, USA) in growth medium at a density of 7.5×10^5 cells/well. Cultures were maintained at 37°C in a 90% air and 10% CO₂ humidified atmosphere according to product instructions. The plating density was such that cells reached 80-90% confluency following one day of growth, at which point they were switched to differentiation media containing DMEM, 4 mM glutamine, and 2% horse serum (Sigma-Aldrich), and media was changed every two days thereafter until cells were treated.

2.1.2 Testing of Differentiation State

Cells were harvested for Western blotting over a time-course immediately prior to and every two days following serum reduction up to day 10. Extracts were blotted for myoD and myogenin as markers of differentiation, and based on these results along with the general health and appearance of the cells, day 6 post-differentiation was chosen as an optimal time for treatment with adenovirus constructs and/or pharmacological agents. Following treatment, samples were also blotted for the same two markers to ensure that various treatments did not alter the differentiated state of the cells.

2.1.3 Pharmacological Treatment

AMPK was activated within the C2C12 cells via two different pharmacological treatments. AICAR and metformin were administered to cells at doses ranging from 0.1 mM – 5 mM. Once the optimal doses of 0.2 mM and 0.5 mM, respectively, were determined, both agents were administered to separate plates during each media change beginning on day 6 and every two days thereafter until cessation of the experiment.

2.1.4 Viral Infection

Following 6 days of exposure to differentiation media, cells were infected with an adenovirus vector containing either the green-fluorescent protein (GFP) gene alone, which served as a control, or GFP plus a dominant negative construct of α_2 AMPK, both kindly supplied by Dr. Jason Dyck of the University of Alberta. Viruses had been previously prepared by subcloning cDNA sequences into a pAdTrack-CMV shuttle vector, linearizing the plasmid DNA with the restriction endonuclease *PME1*, and inserting it into the adenovirus genome using the pAdEasy-1 system followed by homologous recombination in *E. coli* (He *et al.*, 1998). Infection efficiency was assessed primarily by GFP fluorescence, and follow-up analysis was conducted using immunostaining for the myc-tag and Western blotting for markers of AMPK activity. Two different approaches were used to attempt to increase the efficiency of infection, as mentioned in Chapter I.

2.1.4.1 Retroviral Infection and CAR Overexpression

To overexpress the adenoviral receptor within our cell line, C2C12 host cells were infected with a retrovirus designed to overexpress CAR using methods described previously (Miller *et al.*, 1993). Two retrovirus-packaging cell lines (RPCLs) that overexpressed the CAR receptor were kindly donated by Dr. Paul Holland of McGill University. RPCLs were plated into 75cm² flasks at 2×10^6 cells/flask while host cells were plated onto 60 mm dishes at 5×10^5 cells/dish. Upon reaching confluency, flasks

containing RPCLs were sealed with parafilm to prevent gas exchange and incubated at 30°C overnight. The following day, media from each flask was centrifuged twice at 3000 RPM for 10 minutes, and the supernatant was saved following each spin. Media was aspirated from the 60 mm dishes containing host cells, and 2.5 ml antibiotic-free growth media containing 16 µg/ml sterile hexadimethrine bromide (polybrene; Sigma-Aldrich), an infection agent, was added in its place. An additional 2.5 ml of media extracted from the RPCLs was added to each dish. Flasks were then incubated at 37°C, and the procedure was repeated again every 2 hours for a total of 4 times with the final infection left overnight. The following day, cells were trypsinized and centrifuged at 2000 RPM for 5 minutes. Cells were resuspended in selection media consisting of growth media with 0.8 mg/ml G418 (Gibco), diluted 1:20, and plated onto 90 mm plates. Plates were incubated for 1 week to allow colonies to grow, and specific clones were then selected with cloning rings and grown further until $\sim 1 \times 10^7$ cells were available for freezing in growth media containing 5% dimethylsulfoxide (DMSO; Fisher Scientific, Nepean, ON, Canada). Following clone selection, 0.02 mg/ml of G418 was retained in the growth media to preserve selection pressure on the colonies. Two 60 mm plates of each clone were also grown prior to freezing and extracted for Western blotting using the procedure described below. Clones were blotted and probed for the CAR receptor, and those clones expressing relatively higher levels of the receptor were grown in 12-well plates and infected with various doses of the adenovirus constructs (20, 50, and 100 PFU/cell) to test their practical use.

2.1.4.2 Polycationic Lipid Infection Aid

Various doses of Lipofectamine (10 and 20 µg) (Invitrogen, Burlington, ON, Canada) and virus (20, 50 and 100 PFU/cell) were administered to C2C12 cells grown and differentiated in 12-well plates. Infection efficiency was assessed by GFP fluorescence, with the optimal dose determined to be 10 µg/well. For 60 mm plates, doses of both virus and lipofectamine were not proportional to the increase in surface area from the 12-well plates (3.8 cm² vs. 28 cm²), and the lipofectamine dose was re-optimized to 18 µg/well. Virus concentration was optimized to approximately 150

PFU/cell, and the number of cells was estimated based on a doubling time of 16 hours during exposure to growth media (Dodds *et al.*, 1999). Lipofectamine was incubated with the virus in serum-free media for 45 minutes prior to infection. Cells were serum-starved during and for 6-8 hours following the infection, at which point horse serum was added to the media to a final concentration of 2%. Cultures were exposed to virus-containing media for 15-20 hours before differentiation media was changed, and media was subsequently changed every two days for the duration of the experiment. In some cases, the media changes included treatment with 0.2 mM AICAR.

Although CAR overexpression appeared somewhat successful, the Lipofectamine addition to normal C2C12 cells proved to be more effective in eliciting a strong infection. Therefore, Lipofectamine was chosen as the method of infection for all remaining experiments.

2.2 Protein Expression Analysis

2.2.1 Harvesting: Whole Cell Lysate

Cells were rinsed twice with cold phosphate buffered saline (PBS, pH 7.4) before a lysis buffer was applied. The buffer consisted of 20 mM Tris/HCl, pH 7.4 at 4°C (Bio-Rad Laboratories; Mississauga, ON, Canada), 50 mM sodium chloride (Fisher Scientific), 50 mM sodium fluoride (Fisher Scientific), 5 mM sodium pyrophosphate (Anachemia, Edmonton, AB, Canada), 5 mM sucrose (ACP, Toronto, ON, Canada), 1% Triton-X 100 (Sigma-Aldrich), 1 mM DTT (ICN Biomedicals, Irvine, CA, USA), 5 mg/ml protease inhibitor cocktail (Roche, Laval, PQ, Canada), and 1% phosphatase inhibitor cocktail (Sigma-Aldrich). Approximately 400 µl of cold buffer was applied to each plate on ice and subsequently rocked over the cells for ~60 seconds prior to scraping. The homogenate was incubated on ice for 15 minutes followed by centrifugation at 1,000 x g for 5 minutes at 4°C. Following this, the supernatant was isolated, frozen in liquid nitrogen and stored at -70°C. Prior to the Western blot, protein levels were measured using the Bradford total protein assay (Bio-Rad Laboratories); all samples were subsequently diluted in lysis buffer to a final concentration of 2.2 mg/ml.

2.2.2 *Harvesting: Nuclear Extract Enhancement*

To obtain lysate enhanced with nuclear proteins, cells were disrupted with hypotonic lysis followed by a high-salt extraction of nuclear proteins (Andrews & Faller, 1991). Initially, cells were scraped into cold PBS buffer, with two plates pooled in a total of 1.5 ml PBS. Cells were spun at 2,000 x g for 30 seconds, and the pellet was gently resuspended in 400 µl cold Buffer A, consisting of 10 mM HEPES-KOH (Fisher Scientific), pH 7.9 at 4°C, 1.5 mM magnesium chloride (BDH, Toronto, ON, Canada), 10 mM potassium chloride (ACP), 0.5 mM DTT (ICN Biomedicals), 0.2 mM EDTA (Sigma-Aldrich), and protease inhibitor cocktail diluted 1:1000 (Sigma-Aldrich). Cells were then permitted to swell on ice for 10 minutes, followed by a 10-second vortex to complete the lysis procedure. Solid material was again pelleted at 2,000 x g for 30 seconds to spin down the nuclei, the supernatant was discarded once again and the pellet was resuspended in 30 µl of cold Buffer B, consisting of 20 mM HEPES-KOH (Fisher Scientific), pH 7.9 at 4°C, 25% glycerol (Invitrogen), 420 mM sodium chloride (Fisher Scientific), 1.5 mM magnesium chloride (BDH), 0.2 mM EDTA (Sigma-Aldrich), 0.5 mM DTT (ICN Biomedicals), and protease inhibitor cocktail diluted 1:1000 (Sigma-Aldrich). This was followed by a 20-minute on-ice incubation serving as the high-salt extraction. Finally, cells were centrifuged at 2,000 x g for 2 minutes at 4°C, and the supernatant fraction was isolated and stored at -70°C. Prior to the Western blot, protein levels were measured by a Bradford total protein assay, and samples were diluted in Buffer B to a final concentration of 2.2 mg/ml.

2.2.3 *SDS-PAGE and Western Blotting*

Cell extracts were combined with a sample buffer consisting of 40 mM Tris-HCl (Fisher Scientific), pH 6.8, 2% sodium dodecyl sulfate (SDS; Bio Rad Laboratories), 10% glycerol (Invitrogen), 5 mg/ml protease inhibitor cocktail (Roche) and 1% β-mercaptoethanol (Bio Shop, Gaithersburg, MD, USA), and 22 micrograms of protein per lane were run on a polyacrylamide gel. The concentration of acrylamide and running voltage depended on the proteins being isolated; see Table 2.1 for further details.

Table 2.1: Western blotting conditions for various antibodies.

| Antibody | Running Conditions | Blocking Solution | Dilution |
|---|--------------------|-------------------|----------|
| Phospho-ACC (Upstate Biotech, Waltham, MA, USA) | 7.5% gel, 16 mA | 5% milk, TBS-T | 1:1000 |
| ACC (Upstate Biotech) | 7.5% gel, 16 mA | 5% milk/1%BSA | 1:500 |
| Phospho-AMPK (Cell Signalling Technology, Beverly, USA) | 10% gel, 110 V | 5% BSA, TBS-T | 1:500 |
| AMPK pan α (Upstate Biotech) | 10% gel, 110 V | 3% milk, TBS-T | 1:500 |
| Citrate Synthase (Dr. B. Robinson, University of Toronto) | 10% gel, 110 V | 5% milk, TBS-T | 1:2000 |
| GAPDH (Novus Biologicals, Littleton, CO, USA) | 10% gel, 110 V | 5% milk, TBS-T | 1:2000 |
| PGC-1 α (Calbiochem, Mississauga, ON, Canada) | 10% gel, 110 V | 5% milk, TBS-T | 1:500 |
| β -actin (Abcam, Cambridge, MA, USA) | 10% gel, 110 V | 5% milk, TBS-T | 1:2000 |
| MyoD (Santa Cruz Biotechnology, Santa Cruz, CA, USA) | 12% gel, 110 V | 5% milk, TBS-T | 1:500 |
| Myogenin (Santa Cruz Biotechnology) | 12% gel, 110 V | 5% milk, TBS-T | 1:500 |
| CAR (Santa Cruz Biotechnology) | 10% gel, 110 V | 5% milk, TBS-T | 1:500 |
| Peroxidase-labelled streptavidin (Kirkegaard & Perry) | | 5% milk, TBS-T | 1:500 |
| Biotinylated goat-anti-rabbit IgG (Vector Laboratories, Burlington, ON, Canada) | | 5% milk, TBS-T | 1:2000 |
| Peroxidase-labelled goat-anti-rabbit IgG (Vector Laboratories) | | 5% milk, TBS-T | 1:2000 |

Proteins were then blotted onto a nitrocellulose membrane, blocked in their appropriate solution of fat-free milk powder and/or bovine serum albumin (BSA) dissolved in Tris-buffered saline, pH 7.6, with 0.1 % Tween 20 detergent (Caledon; Georgetown, ON, Canada) (TBS-T) (Table 2.1), and incubated with the appropriate primary antibody overnight at 4°C. All primary antibodies were polyclonal and had been produced in rabbit. The following day, the membrane was washed in TBS-T and incubated with the appropriate horseradish peroxidase conjugated secondary anti-rabbit antibody, made in goat (1:2000) for 1 hour at room temperature in the appropriate blocking solution (Table 2.1). Weaker primary antibodies were instead hybridized with a biotinylated secondary antibody, washed thoroughly in TBS-T, and incubated for one hour with peroxidase-labelled streptavidin (Kirkegaard and Perry, Gaithersburg, MD, USA). Following either

peroxidase-labelled secondary or streptavidin incubation, membrane-bound antibodies were washed extensively in both TBS-T and TBS, and visualized with enhanced chemiluminescence (Amersham Biosciences, Piscataway, NJ, USA) using the Syngene ChemiGenius apparatus and GeneSnap software. Densitometry of the protein bands was analyzed using GeneTools software (Syngene, Frederick, MD, USA). Membranes were stripped in buffer containing 62.5 mM Tris-HCl (Fisher Scientific), pH 6.7, 2% SDS (Bio Rad Laboratories), and 100 mM β -mercaptoethanol (Bio Shop), and re-probed to a maximum of four additional times for other proteins. β -actin was used as a loading control for all membranes except for those probed for phosphorylated proteins, in which case the total protein (i.e. both phosphorylated and dephosphorylated) was used as a loading reference.

The ratio between the protein of interest and β -actin on the same membrane was obtained, and results were expressed as a fold-difference relative to the control condition. Certain membranes were also stained with Ponceau S (Sigma-Aldrich) for 15 minutes and destained in distilled water and TBS-T prior to blocking to ensure equal loading. Unless otherwise indicated, Western blotting results reflect a sample size of $n=8$.

2.3 Real-Time RT-PCR

2.3.1 RNA Isolation and Preparation

C2C12 cells were lysed in cold Trizol Reagent (Invitrogen) at 1 ml/ 60mm plate and homogenized via several passages through a syringe. Following homogenization, solid material was removed from samples using centrifugation at 12,000 x g for 10 minutes at 4°C. Phase separation was performed using 0.2 ml chloroform (Fisher Scientific) followed by incubations at 4°C for 15 minutes, room temperature for another 15 minutes, and finally centrifugation at 12,000 x g for 15 minutes at 4°C. The aqueous upper phase was isolated (~0.5 ml), combined with an additional 0.5 ml of cold isopropanol (Fisher Scientific), and RNA was allowed to precipitate overnight at -20°C. The following day, samples were spun at 12,000 x g for 60 minutes at 4°C, the

supernatant discarded and pellet washed with cold 75% ethanol. After a final spin at 12,000 x g for 10 minutes at 4°C, the supernatant was again discarded and the RNA pellet resuspended in 10 µl diethyl pyrocarbonate-treated water (DEPC H₂O, BIO 101 Systems, Carlsbad, CA, USA).

RNA was quantified by assessing the absorbance and purity of diluted RNA at 260 nm and 280 nm with a spectrophotometer (Okamoto and Okabe, 2000). RNA was diluted to 1 µg/µl in DEPC H₂O and stored at -70°C.

2.3.2 Reverse Transcription of RNA to cDNA

cDNA synthesis was performed using 1 µg total RNA per reaction, forming a total volume of 7.5 µl. The reaction mixture also consisted of 20 units RNase OUT, 1X First Strand Buffer diluted from 5X stock (250 mM Tris-HCl pH 8.3, 375 mM potassium chloride, 15mM magnesium chloride), 1 mM dNTP mixture, 10 mM DTT, 0.5 µg oligo (dT)₁₂₋₁₈, 150 units Moloney Murine Leukemia Virus reverse transcriptase, and 1µl DEPC H₂O (BIO 101 Systems). All reagents used were obtained from Invitrogen unless otherwise indicated. Reverse transcription was conducted at 37°C for 60 minutes in a thermal cycler (Techne Genius, Burlington, NJ, USA), and the cDNA product was stored at 4°C.

2.3.3 Synthesis of Primers and Probes

Oligonucleotide sequences for citrate synthase, ALA synthase, PGC-1, p300 and cyclophilin were derived from DNA sequences published on the National Center for Biotechnology Information GenBank website¹. Primers and fluorescent-labelled probes were synthesized by ABI PRISM Assay-by-Design (Applied Biosystems, Streetsville, ON, Canada). Cyclophilin was labelled with a 5'-VIC fluorescent probe, while the remaining primers were labelled with 5'-FAM. Primer sequences can be found in Table 2.2.

¹<http://www.ncbi.nlm.nih.gov/Genbank/index.html>

2.3.4 Real-Time Polymerase Chain Reaction

Reactions were carried out in standard 96-well optical plates (Applied Biosystems). In each well, 2 µl of reverse transcript was combined with 1X TaqMan Universal PCR Master Mix diluted from 2X stock (AmpliTaq Gold® DNA Polymerase, dNTPs with dUTP, Passive Reference 1, and optimized buffer components; Applied Biosystems/Roche), 1X primer/probe mix diluted from 20X stock (Applied Biosystems), and DEPC H₂O (BIO 101 Systems) to a final volume of 25 µl/well.

The PCR reaction was analyzed in real-time using the ABI Prism 7700 Sequence Detector thermal cycler (Perkin Elmer, Woodbridge, ON, Canada) and ABI Prism Sequence Detection Systems v.1.7a software (Applied Biosystems). Thermal cycler

Table 2.2: DNA sequences for real-time RT-PCR primers and probes.

| Gene | Accession ID | Primer | Sequence |
|-------------|--------------|---------|-----------------------------------|
| CS | NT 081856 | Forward | CCT GCC TCG TCC TTG CT |
| | | Reverse | CTG CTC CTT AGG TAT CAG ATT GCT |
| | | Probe | FAM-CTT CTT CCA CGA ATT TGA |
| ALAS | NT 039477 | Forward | CTC GAA CCC TGT CCA CAT CAG |
| | | Reverse | CCT TGG CAG TTT TCT CTT TCT CAT T |
| | | Probe | FAM-CAG GGT CAA AGA AAC CC |
| PGC-1 | NT 039340 | Forward | GCA GCC AAG ACT CTG TAT GGA |
| | | Reverse | TTC AGG AAG ATC TGG GCA AAG AG |
| | | Probe | FAM-CAG AGC AGC ACA CTC TA |
| p300 | NT 081922 | Forward | CAT CTC CGG CCC TCT CG |
| | | Reverse | TCA TGT TCC AGG TCA AAC AGT GAA |
| | | Probe | FAM-ATG GCA CAG ATT TTG G |
| Cyclophilin | NT 039515 | Forward | TCT CCT TCG AGC TGT TTG CA |
| | | Reverse | CAG TGC TCA GAG CTC GAA AGT TT |
| | | Probe | VIC-ACA AAG TTC CAA AGA CAG CAG |

conditions were as follows: 50.0°C for 2:00 minutes, 95.0°C for 10:00 min, followed by a cycle of 95.0°C for 0:15 min and 60.0°C for 1:00 min for 40 repetitions. Each sample was run in duplicate for both the gene of interest and cyclophilin, which served as the housekeeping gene. The $\Delta\Delta C_T$ value, described above, was calculated for each sample at each time point of harvest, with n=6.

2.4 Statistical Analysis

All values are expressed as mean \pm standard error. Analysis was run using Statistica software, and comparisons of various conditions were conducted at individual time points using a one-way ANOVA with planned comparisons between groups. The presence of an effect in the housekeeping gene or loading control was tested by regression analysis. Outliers were assessed as any data points beyond two standard deviations of the mean, and such results were discarded. Results were considered significant at $p < 0.05$.

2.5 References

- Andrews, N. C. & Faller, D. V. (1991). A rapid micropreparation technique for extraction of DNA-binding proteins from limiting numbers of mammalian cells. *Nucleic Acids Res.* 19, 2499.
- Dodds, E., Piper, T. A., Murphy, S. J., & Dickson, G. (1999). Cationic lipids and polymers are able to enhance adenoviral infection of cultured mouse myotubes. *J. Neurochem.* 2105-2112.
- Miller, D., Miller, D., Garcia, V., & Lynch, C. M. (1993). Use of Retroviral Vectors for Gene Transfer and Expression. In *Methods in Enzymology* pp. 581-599. Academic Press Inc., New York.
- Okamoto, T., & Okabe, S. (2000). Ultraviolet absorbance at 260 and 280 nm in RNA measurement is dependent on measurement solution. *Int. J. Mol. Med.* 5, 657-659.

CHAPTER III: RESULTS

3.1 Model Efficiency

3.1.1 In Vitro System

Within 24 hours of plating, cells attached to the ECM as a monolayer and divided until nearly confluent while developing longitudinal extensions characteristic of myoblasts (Figure 3.1). After differentiation was induced by serum withdrawal, cells began to migrate and fuse end-to-end into elongated myotubes as expected. Fusion was evident by day 2 following serum withdrawal, and continued until day 6 at which point treatment was administered (Figure 3.1).

During the differentiation period, a small sample of cells were harvested at 2-day intervals and assayed for expression of myoD and myogenin, two key factors involved in determination of myogenic lineage and subsequent protein expression. While the sample size was too small to draw conclusions from and statistical analysis was not performed, these preliminary results were taken into account along with other evidence to determine the proper day of treatment post-differentiation. MyoD was evident in myoblasts, and its expression levels gradually increased until reaching a plateau on day 6 post-differentiation at a level approximately 4-fold higher than that of myoblasts. Myogenin, meanwhile, was present in relatively low levels in myoblasts, while its expression increased dramatically upon serum withdrawal to 5-fold higher than that of myoblasts by day 4 and decreased thereafter to near-myoblast levels once again by day 6. It should be noted that Ponceau S was used to confirm equal loading for these two membranes instead of normalizing to β -actin, as actin's expression is known to change during early stages of differentiation (Shimokawa *et al.*, 1998). Regression analysis of β -actin protein expression during differentiation produced a significant correlation of $r = -0.92$ ($p < 0.01$), confirming such previous reports. Overall, the above results combined with morphological observations and previous reports indicated that differentiation was well-established by day 6 (Leary *et al.*, 1998; Moyes *et al.*, 1997), allowing treatment with

either drugs or adenovirus to proceed without the effects of differentiation influencing subsequent results.

Preliminary tests of myoD and myogenin expression post-treatment permitted further scrutiny of the model. Cells treated with pharmacological agents were harvested 4 days post-treatment and blotted for these markers (Figures 3.2 and 3.3). MyoD expression was not significantly different in either condition at this point in time. Myogenin expression, in contrast, was significantly increased by AICAR treatment ($p < 0.01$). These findings indicate that AICAR treatment may be accelerating cell differentiation as myogenin is a marker of this process. Cells treated with virus construct \pm AICAR also displayed significant changes in myogenin expression while no changes were observable in myoD protein levels (Figures 3.4 and 3.5). Interestingly, although the $\alpha 2DN + AICAR$ condition produced a significant myogenin protein increase, the GFP + AICAR condition failed to do the same. This could indicate that AICAR's effects on cell differentiation are independent of α_2 -AMPK, as they occurred despite the inhibition of this kinase.

3.1.2 Pharmacological Treatment

Cells were treated with a variety of doses of both AICAR and metformin, and were initially judged based on their morphology as compared to controls, while their post-extraction protein concentration served as a second indicator of their viability and therefore suitability for experimentation. Optimal doses were chosen as the highest possible concentrations before marked physical effects became visible over a course of three or more days (Figures 3.6 and 3.7). Based on primarily qualitative observations and protein assay results, 0.5 mM metformin and 0.2 mM AICAR were chosen as the best doses for treatment.

Following the determination of optimal doses based on cell morphology, conditions were further tested for their ability to activate AMPK. Western blotting of samples harvested two days post-treatment was performed using phospho-specific

antibodies directed against both ACC and AMPK, as shown in Figures 3.8 and 3.9. Phosphorylation of ACC was significantly elevated approximately 1.5-fold by both metformin ($p < 0.05$) and AICAR ($p < 0.01$) treatment, while phosphorylation of AMPK was only significantly elevated in metformin-treated samples ($p < 0.05$). This may reflect the different mechanism of action of the two treatments, but nevertheless results demonstrate that AMPK is activated to some extent by both conditions.

3.1.3 Virus Treatment

3.1.3.1 Infection Enhancement

Following retroviral expression of CAR, various clones were grown on 60 mm plates, harvested upon reaching confluency and blotted for CAR expression (Figure 3.10). Based on Western blotting results, clones 2-4 and 3-1 were chosen to have their infection efficiencies tested and were treated with various doses of adenovirus in 12-well plates. In separate dishes, cells were treated with various combinations of Lipofectamine and virus. Infection efficiency of both was assessed by GFP fluorescence, which peaks on day 2 and 3 post-infection, as well as the general appearance of the cells over a course of three or more days. Comparisons between clone 3-1 and virus + Lipofectamine treated wells, both treated with 50 PFU/cell of adenovirus, can be seen in Figure 3.11. In general, fluorescence was brighter and more widespread in dishes treated with virus + Lipofectamine rather than those infected with the CAR retrovirus, and as such Lipofectamine was used for all subsequent experiments. In addition, as some reports have suggested that the extracellular matrix may impede adenoviral infection as it impairs access to portions of the cell surface (Cao *et al.*, 2002), cells plated with or without the ECM layer present were simultaneously infected and monitored together. GFP fluorescence results, shown in Figure 3.12, indicated no obvious infection differences between the two conditions.

3.1.3.2 Infection Efficiency

Once the method of infection was determined, infection efficiency was further assessed using myc expression to indicate whether or not the AMPK construct itself was being expressed alongside the GFP reporter. Fixed cells were treated with a TRITC-labelled primary antibody for the myc protein, and visualized under the appropriate wavelength of light as seen in Figure 3.13. As expected, no myc fluorescence was visible in samples treated with GFP control adenovirus, whereas adenovirus encoding myc-tagged AMPK constructs proved effective in infecting and expressing these proteins inside the C2C12 cells.

3.1.3.3 Activation and Inhibition of AMPK

Finally, the effectiveness of the experimental model was demonstrated by its ability to activate and inhibit AMPK, assessed again via Western blotting for phospho-ACC and -AMPK (Figures 3.14 and 3.15). Phosphorylation of ACC was significantly higher in samples treated with the GFP + AICAR combination as compared with control samples infected with the GFP construct and no drug ($p < 0.01$). Meanwhile, samples treated with the α_2 -dominant negative virus, either with or without AICAR treatment in addition, had approximately 50% less ACC phosphorylation than the control ($p < 0.01$). There were no significant differences between the α_2 DN conditions with or without AICAR, indicating that the α_2 DN construct was capable of blocking the AMPK-activating properties of AICAR. Similar results were seen with the phospho-AMPK antibodies, as AMPK phosphorylation of the GFP/AICAR treatment was significantly elevated above GFP/control ($p < 0.05$), whereas both α_2 DN conditions were significantly lower ($p < 0.01$) but not significantly different from each other. α_2 DN conditions were normalized to both total AMPK and β -actin to prevent skewing of the results by AMPK construct overexpression.

3.2 Experimental Results: Protein Expression

3.2.1 Metabolic Enzymes

Expression of both mitochondrial citrate synthase and cytosolic glyceraldehyde-3-phosphate dehydrogenase was assessed by Western blotting after four days of pharmacological treatment and/or five days of virus treatment. Citrate synthase expression was significantly increased nearly two-fold by both AICAR and metformin treatment ($p < 0.05$) as compared to an untreated control (Figure 3.16), however samples treated with AICAR in addition to the GFP adenovirus construct showed no such increase (Figure 3.19). Meanwhile, both α_2 DN adenovirus conditions failed to produce any effect on CS expression (Figure 3.17). It is interesting to note that while citrate synthase is theoretically composed of four identical subunits, our blotting results produced what appeared to be a doublet at the correct molecular weight (~50 kDa). The polyclonal antibody used to recognize this protein, a gift from Dr. B. Robinson, is the same as that used by Jankov *et al.* (2003). In this paper, the citrate synthase Western blot produced a very thick band that appeared to be a doublet in certain conditions, thus the densitometry of both bands in the current study was used to evaluate citrate synthase expression.

Expression of GAPDH, a glycolytic enzyme, was also significantly upregulated nearly two-fold by metformin ($p < 0.01$) and AICAR ($p < 0.05$) as compared to an untreated control (Figure 3.18). As with citrate synthase, however, the GFP + AICAR condition failed to increase GAPDH expression (Figure 3.19). Interestingly, the α_2 DN + control condition also did not affect GAPDH expression, while the α_2 DN + AICAR condition caused a small but significant upregulation of expression ($p < 0.05$). These results are highly unexpected, and may indicate that although blotting results for phospho-ACC and phospho-AMPK indicated that the α_2 DN construct was able to effectively inhibit AICAR actions, the block is perhaps not entirely complete.

3.2.2 *Transcription Factors*

PGC-1 α was the only transcription factor successfully detected by Western blotting. Initial attempts to enhance the extract with nuclear proteins using hypotonic lysis and high-salt extraction failed to improve PGC-1 α detection, as whole cell lysates produced a much stronger blotting result for this transcription factor and were used for all subsequent blotting experiments (Figure 3.20).

Blotting results of pharmacologically treated samples had large variability, yet metformin treatment was capable of significantly increasing PGC-1 α protein expression by approximately 2.5-fold ($p < 0.01$) (Figure 3.21). Conversely, however, all virus-containing conditions failed to elicit any significant increase or decrease in PGC-1 α expression (Figure 3.22).

3.3 Experimental Results: mRNA Expression

3.3.1 *Mitochondrial mRNA*

Despite significant increases in citrate synthase protein expression visible on day 4 following drug treatment, the only noteworthy changes in mRNA expression was detected with real-time RT-PCR at 6h post-metformin treatment ($p < 0.05$) (Figure 3.23). Furthermore, no changes were visible with any virus treatment, reflecting results seen at the protein level (Figure 3.24).

In addition to CS, ALA synthase mRNA expression was assayed at similar points post-treatment. ALAS mRNA was also significantly increased after 6h of metformin treatment ($p < 0.05$), while AICAR alone or in combination with the adenovirus constructs failed to cause a significant change at this or any other time point (Figures 3.25 and 3.26). Surprisingly, the α_2 DN + control condition produced a significant upregulation of ALA synthase mRNA at 6h post-treatment, which corresponds to approximately 24 hours following infection (Figure 3.26).

3.3.2 *Transcription Factor mRNA*

PGC-1 α exhibited more changes at the mRNA level following virus treatment than were visible by Western blotting as described above. At 6h, mRNA was surprisingly elevated in the α_2 DN + control condition as compared to GFP + control condition ($p < 0.01$), while α_2 DN + AICAR failed to produce a similarly significant elevation (Figure 3.28). Meanwhile, none of the pharmacological conditions alone were able to produce a significant effect at this time point (Figure 3.27). Further changes were visible at 48h, where metformin-treated cells exhibited a significant decrease in PGC-1 α mRNA expression ($p < 0.05$), while the α_2 DN + AICAR condition alone produced a significant increase ($p < 0.05$). To further complicate matters, 5d mRNA results indicated no change with drug treatment alone, however the GFP + AICAR ($p < 0.01$) and α_2 DN + control ($p < 0.05$) conditions both produced significant increases in mRNA expression (Figure 3.28).

Finally, p300 expression was also assessed at the transcriptional level. The only significant change was seen at 5d following metformin treatment, which caused a small but significant increase in mRNA expression ($p < 0.05$) (Figure 3.29), while no differences were apparent following virus treatment (Figure 3.30).

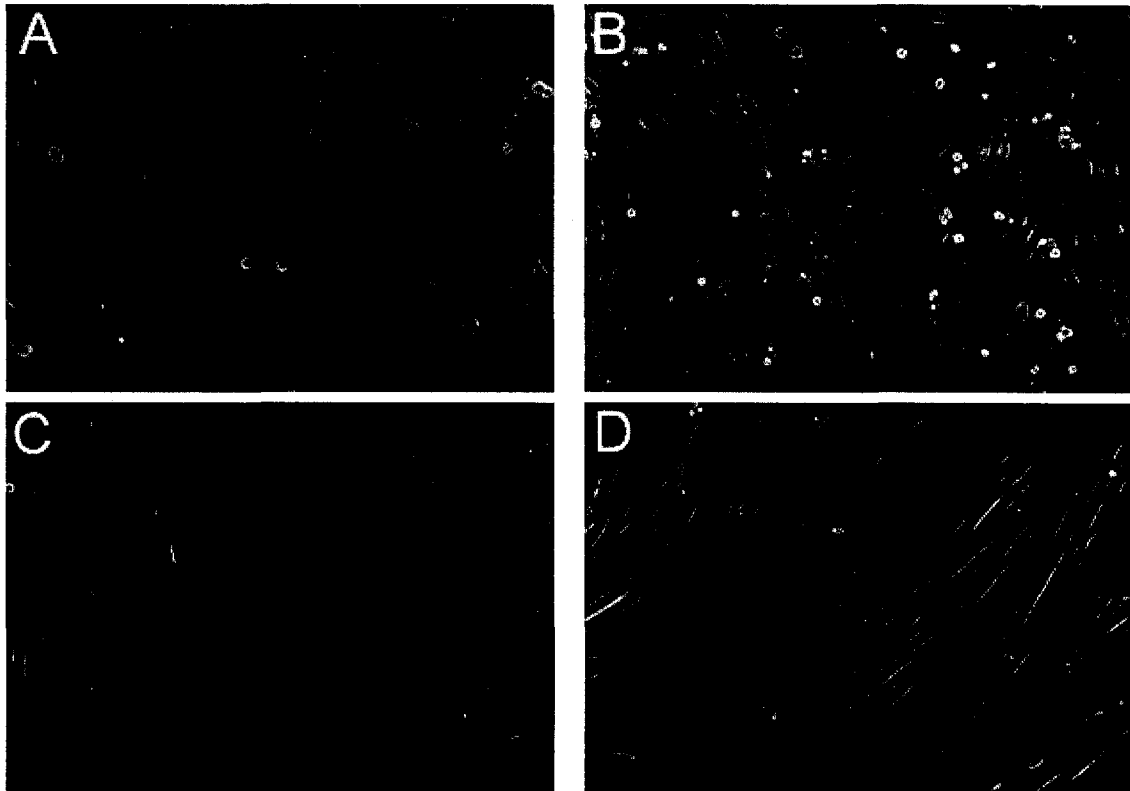


Figure 3.1: Myoblast differentiation and myotube formation on (A) day 0, (B) day 1, (C) day 4, and (D) day 6 following serum withdrawal. Cells were plated in growth media containing 10% fetal calf serum, and switching to a media containing 2% horse serum induced differentiation. As differentiation proceeded, myoblasts aligned and fused into myotubes, which are capable of contraction *in vitro*.

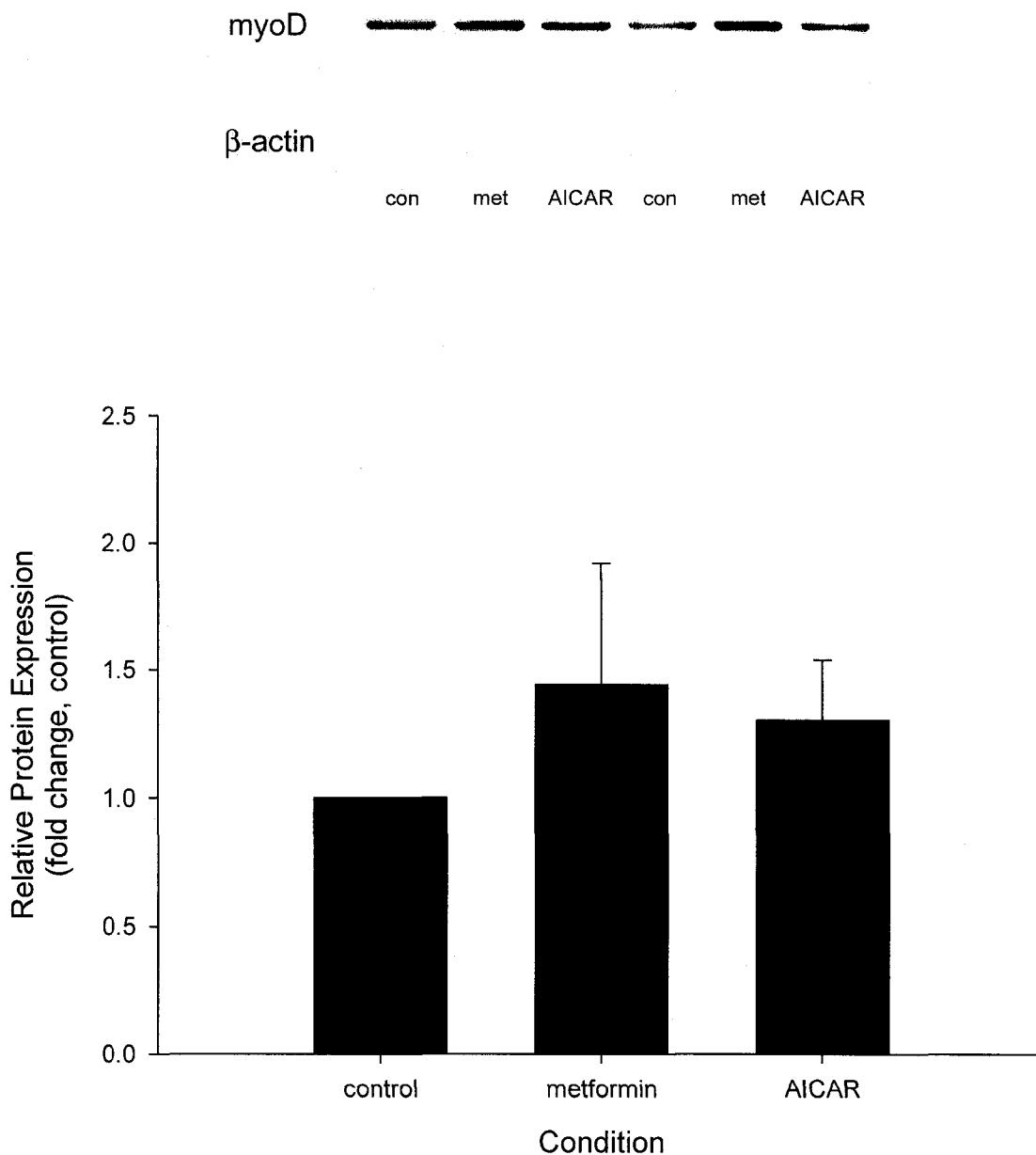


Figure 3.2: Pharmacological treatment does not affect myoD protein expression, as indicated in samples harvested on day 4 post-treatment (n=4). Whole-cell lysates were separated electrophoretically, blotted onto nitrocellulose membranes, and probed with a polyclonal myoD antibody. Membranes were subsequently stripped and reprobed with a polyclonal β -actin antibody, and the ratio of myoD to β -actin was used for statistical comparison.

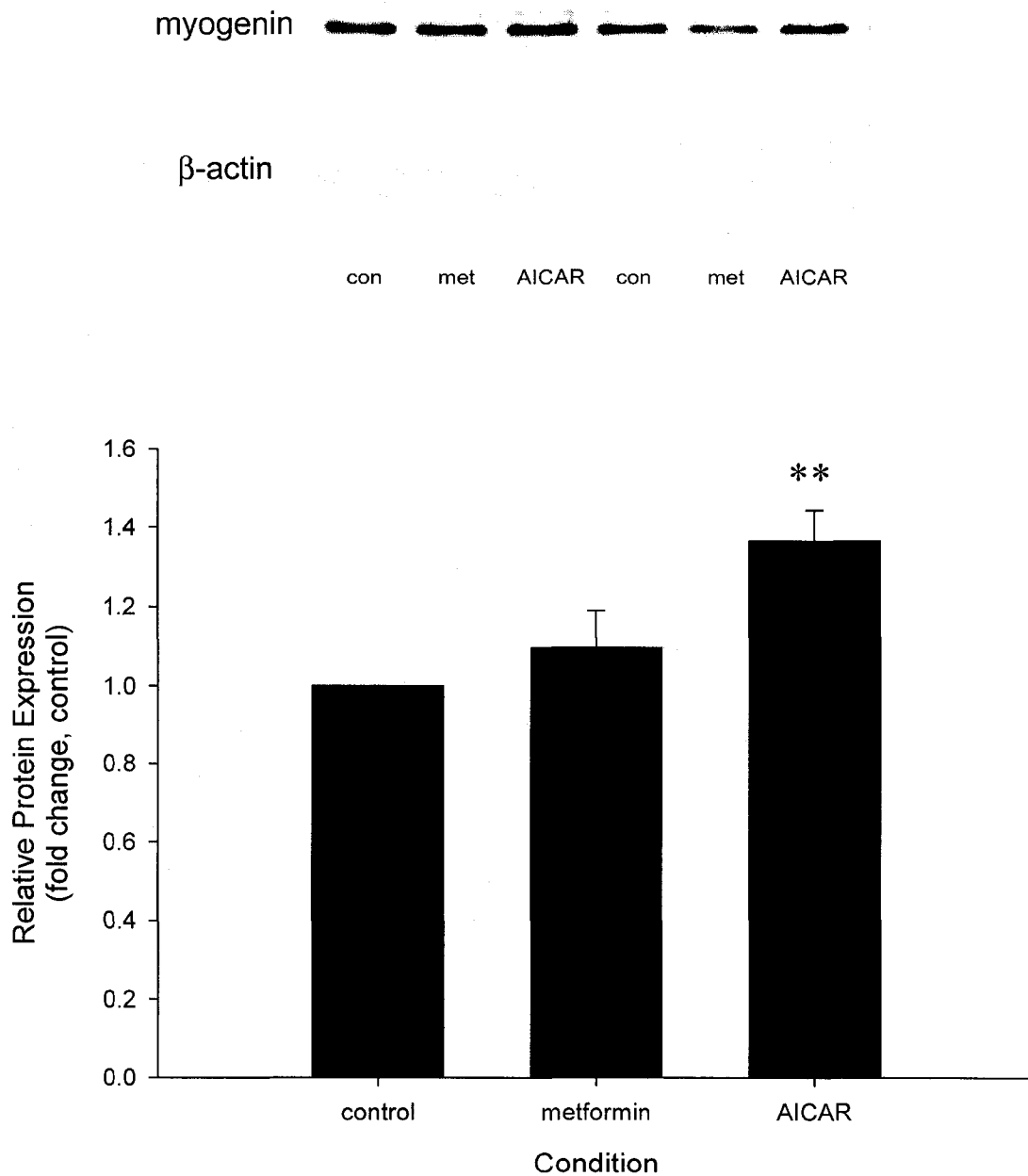


Figure 3.3: AICAR treatment, but not metformin, results in an elevation in myogenin protein expression, as indicated in samples harvested on day 4 post-treatment (n=4). Whole-cell lysates were separated electrophoretically, blotted onto nitrocellulose membranes, and probed with a polyclonal myogenin antibody. Membranes were subsequently stripped and reprobbed with a polyclonal β -actin antibody, and the ratio of myogenin to β -actin was used for statistical comparison. ** = $p < 0.01$

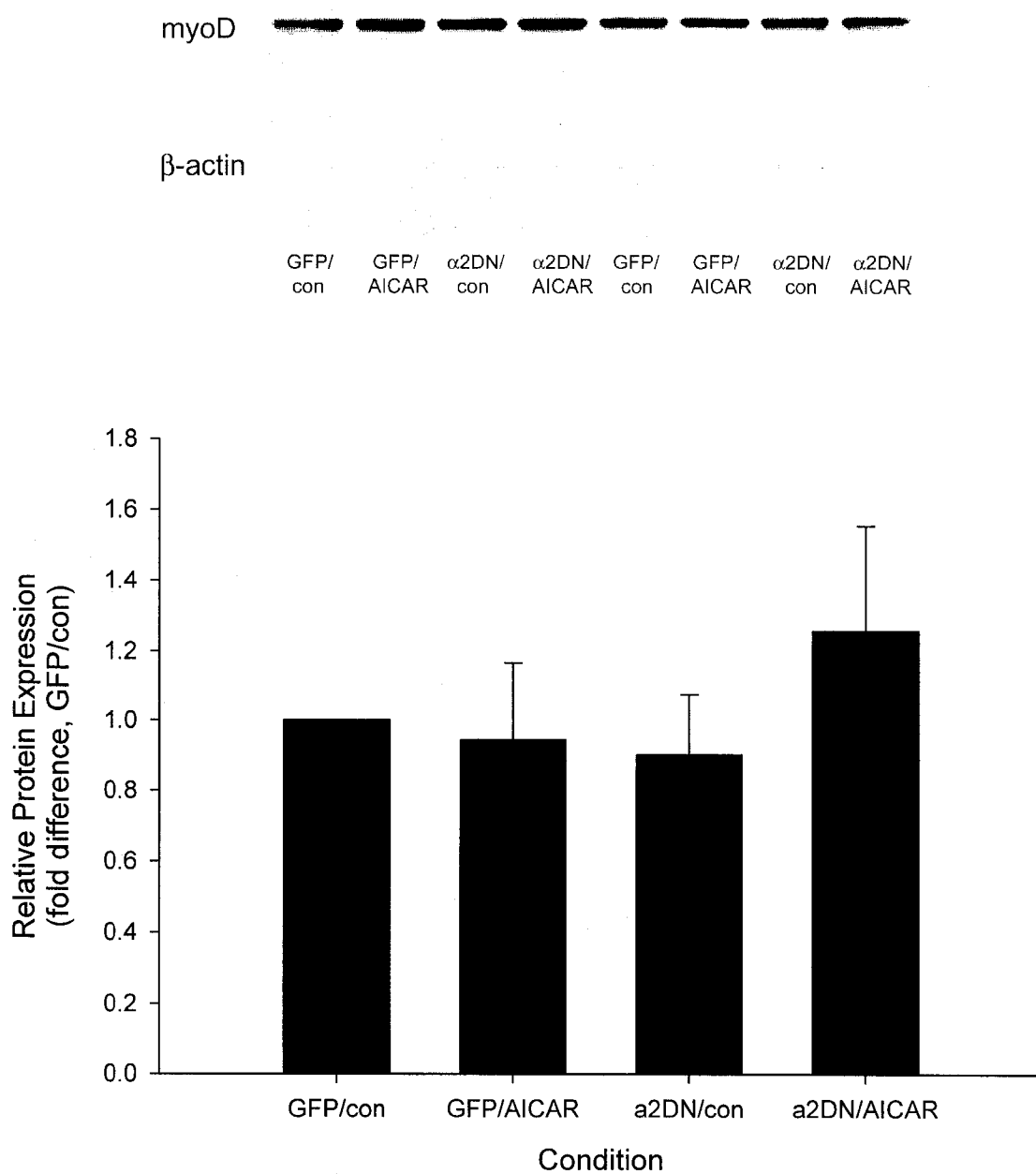


Figure 3.4: Adenovirus treatment does not affect myoD protein expression, as indicated in cells harvested 5 days following infection (n=4). Whole-cell lysates were separated electrophoretically, blotted onto nitrocellulose membranes, and probed with a polyclonal myoD antibody. Membranes were subsequently stripped and re-probed with a polyclonal β -actin antibody, and the ratio of myoD to β -actin was used for statistical comparison.

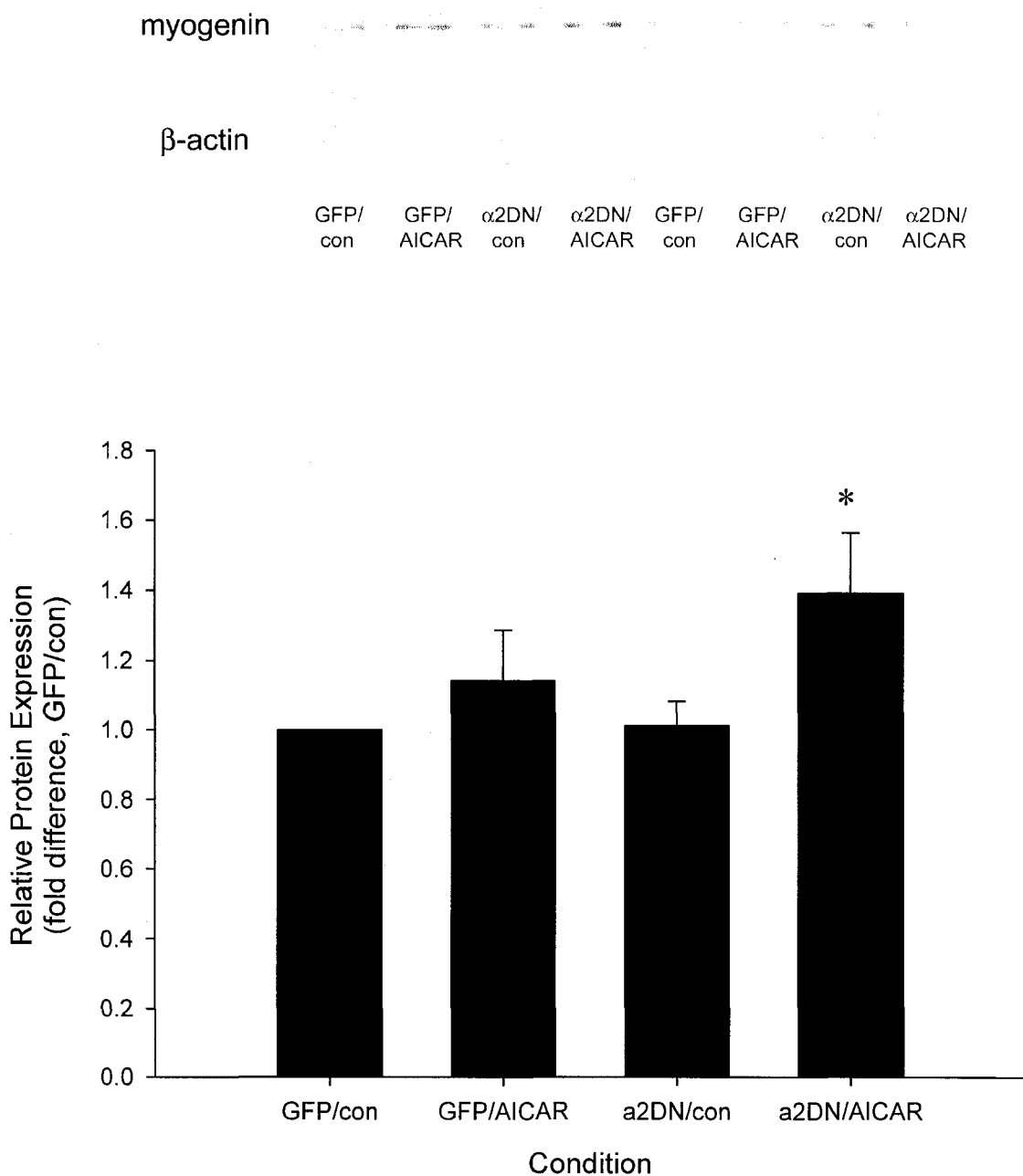


Figure 3.5: α 2DN adenovirus and AICAR, but not AICAR and the control adenovirus, result in an elevation in myogenin protein expression, as indicated in samples harvested on day 5 post-infection (n=4). Whole-cell lysates were separated electrophoretically, blotted onto nitrocellulose membranes, and probed with a polyclonal myogenin antibody. Membranes were subsequently stripped and reprobed with a polyclonal β -actin antibody, and the ratio of myogenin to β -actin was used for statistical comparison. * = p<0.05

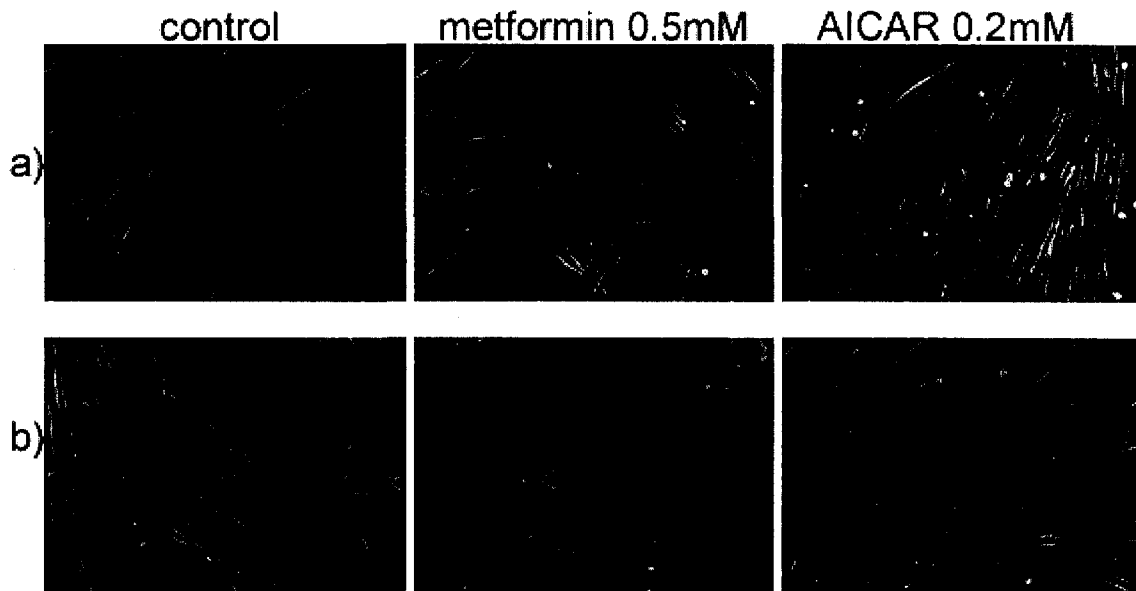


Figure 3.6: Treatment effects on cell morphology: appearance of cells following pharmacological treatment on (a) day 1 and (b) day 3 post-treatment. At optimized doses, metformin and AICAR had little effect on morphology.

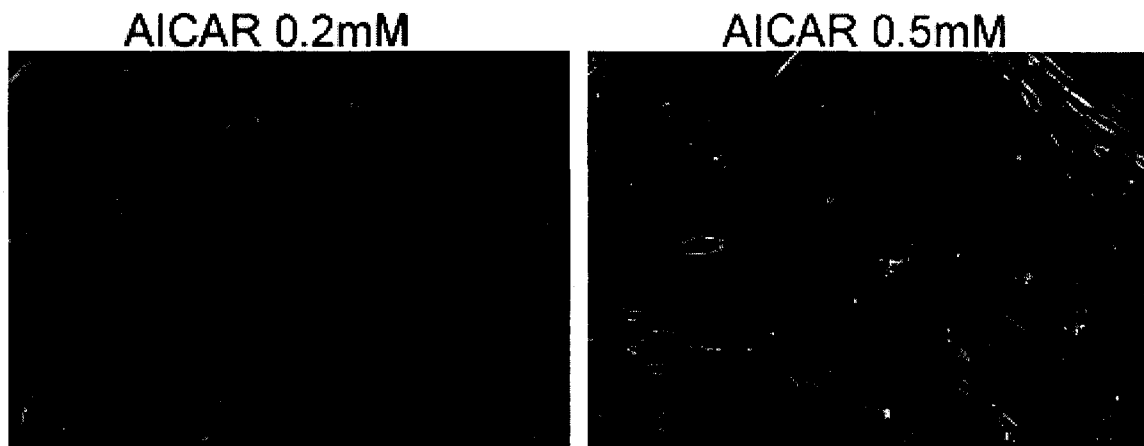


Figure 3.7: Variable cell death at different doses of AICAR. At 0.5 mM, cell death was prevalent following 2 days of treatment, while cells administered 0.2 mM were able to retain a normal appearance and morphology for the duration of treatment.

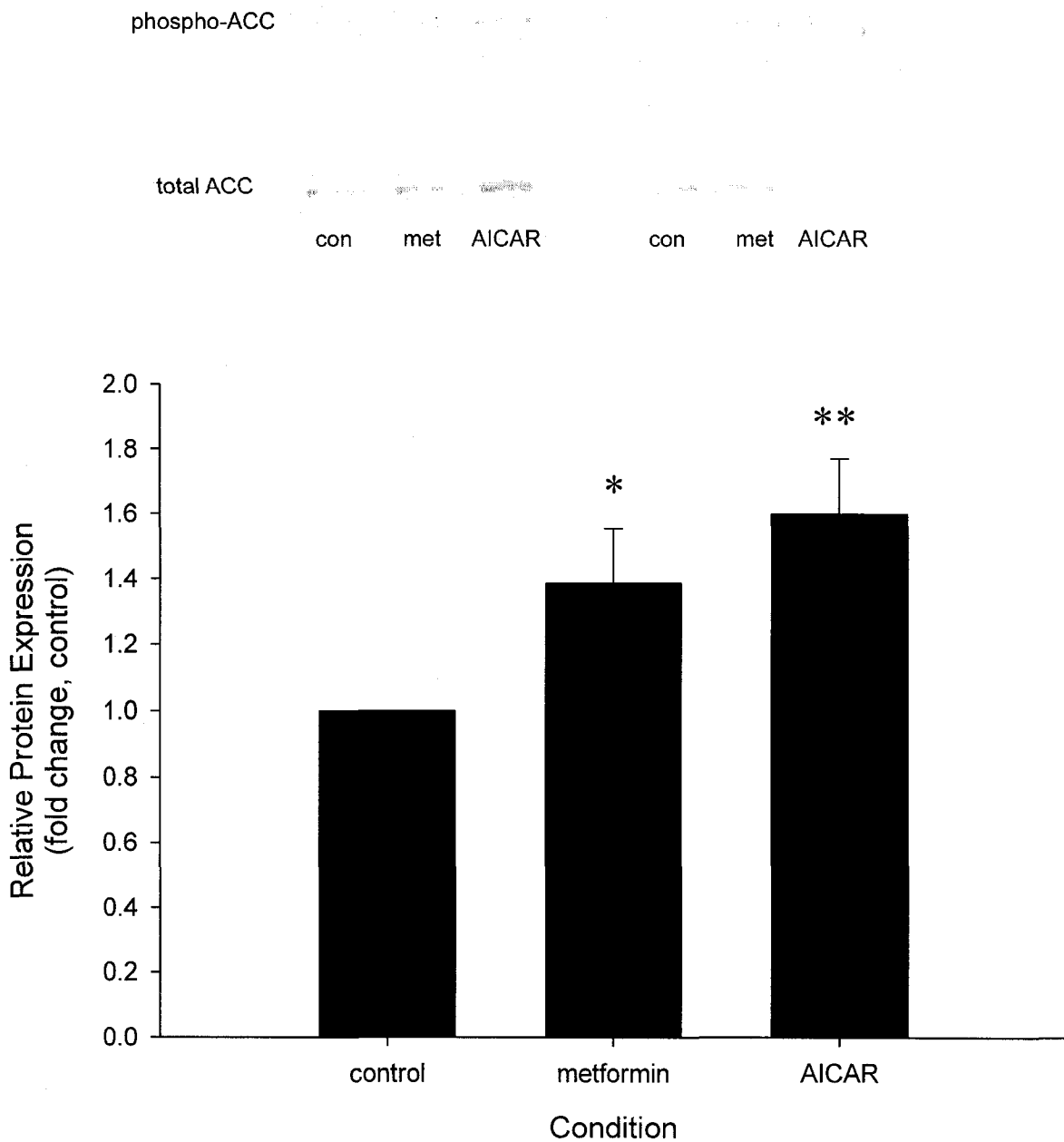


Figure 3.8: Both AICAR and metformin result in increases in ACC phosphorylation, providing evidence of increased AMPK activity in cells harvested day 4 post-treatment (n=5). Whole-cell lysates were separated electrophoretically, blotted onto nitrocellulose membranes, and probed with a polyclonal phospho-ACC antibody. Membranes were subsequently stripped and reprobbed with a polyclonal ACC antibody, and the ratio of phospho-ACC to total ACC was used for statistical comparison. * = $p < 0.05$, ** = $p < 0.01$

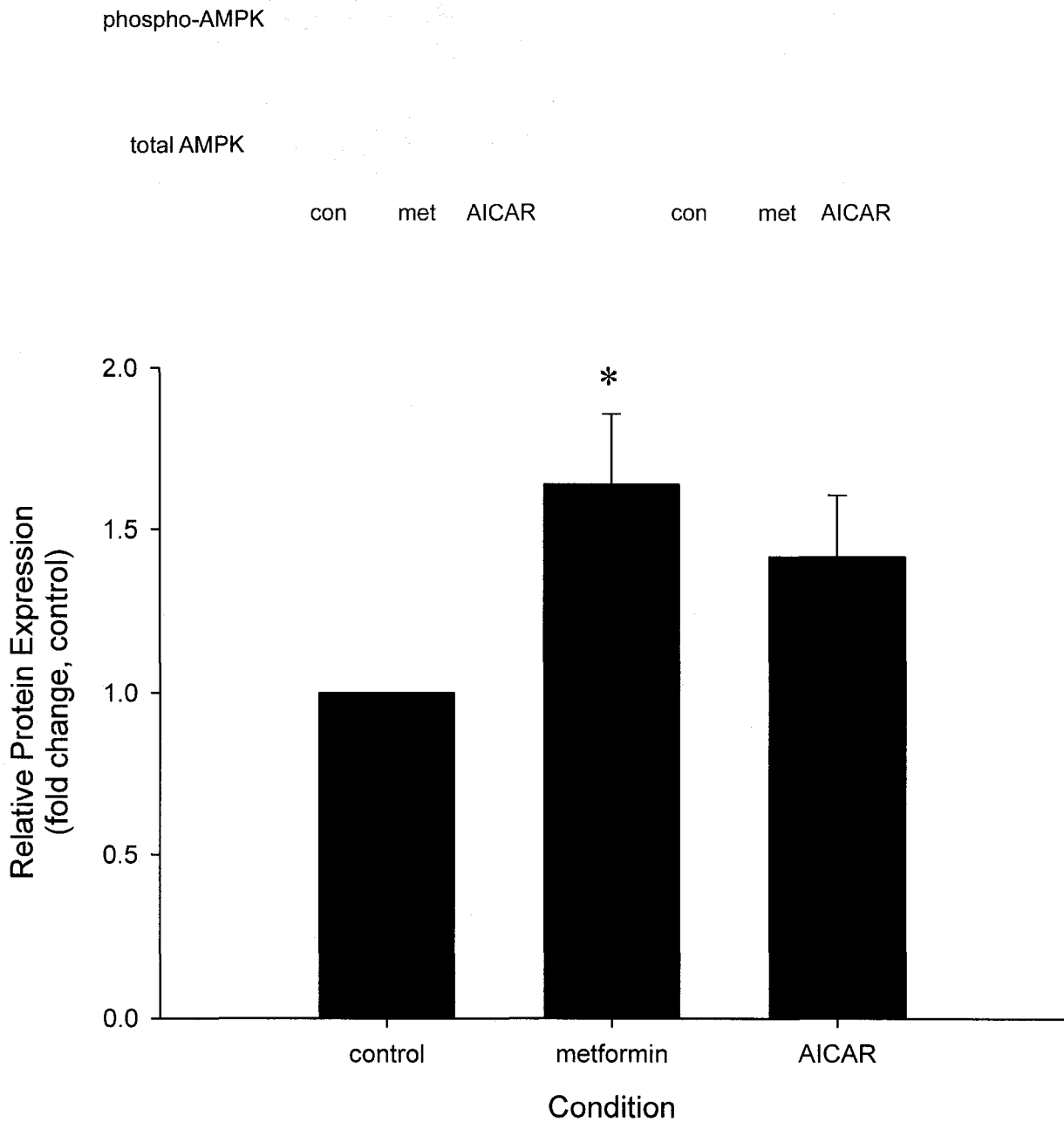


Figure 3.9: Metformin, but not AICAR, results in increases in AMPK phosphorylation, providing evidence of increased AMPK activity on day 4 post-treatment (n=5). Whole-cell lysates were separated electrophoretically, blotted onto nitrocellulose membranes, and probed with a polyclonal phospho-AMPK antibody. Membranes were subsequently stripped and reprobed with a polyclonal AMPK antibody, and the ratio of phospho-AMPK to total AMPK was used for statistical comparison.

* = p<0.05

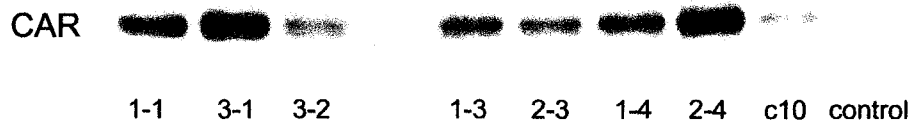


Figure 3.10: CAR protein expression in various retrovirally-infected C2C12 clones. Certain clones, such as 3-1 and 2-4, expressed large quantities of CAR as compared to both the control cells and other infected clones.

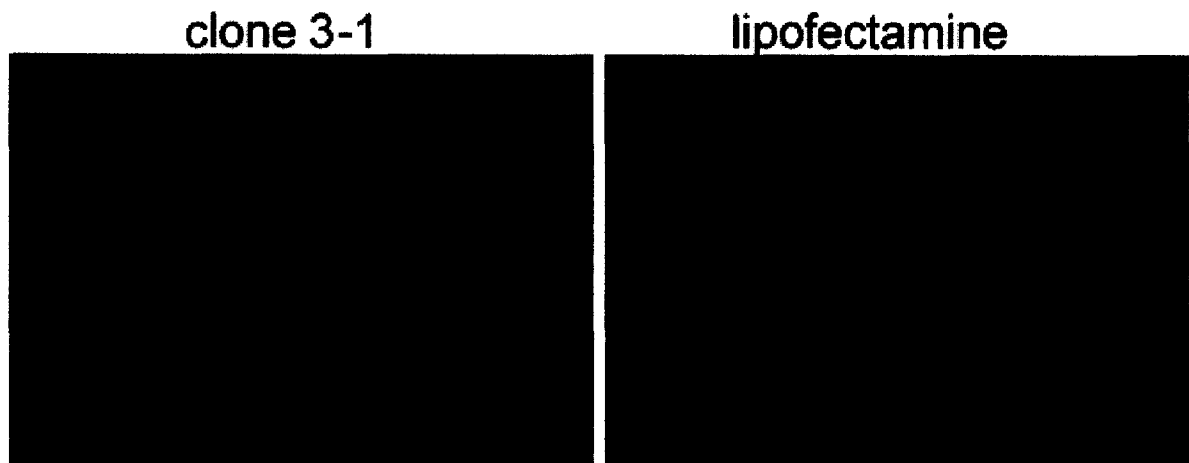


Figure 3.11: Lipofectamine treatment produced a more efficient infection than the CAR-overexpressing clones, as assessed by GFP expression. Both conditions were infected at 50 PFU/cell.

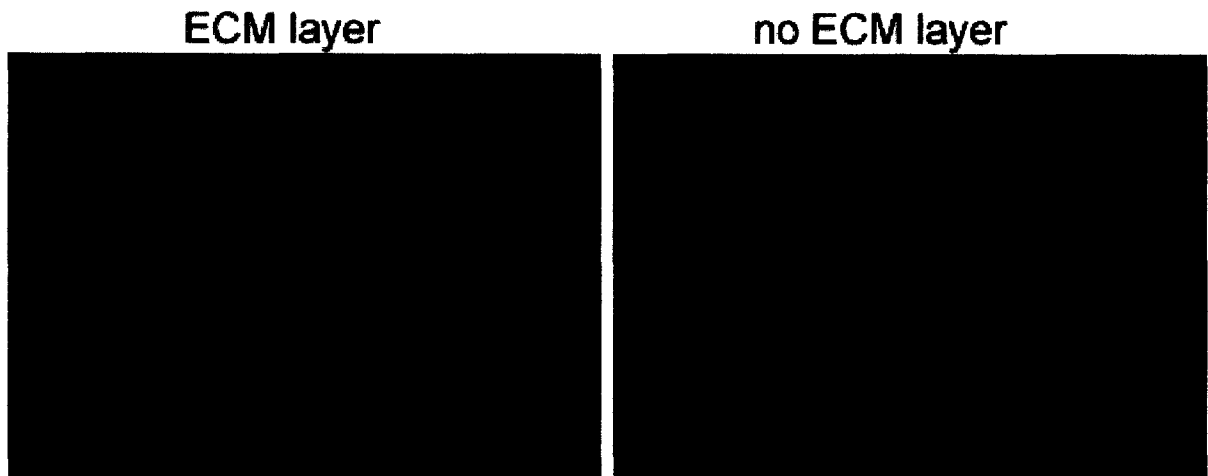


Figure 3.12: The presence of an extracellular matrix gel *in vitro* does not appear to affect infection efficiency.

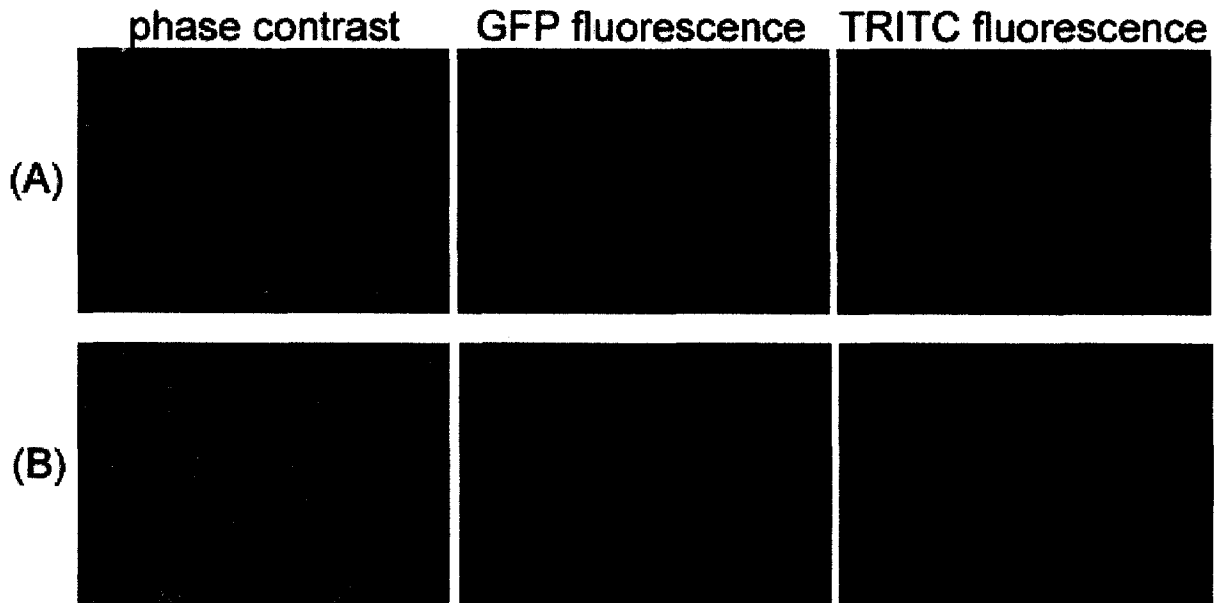


Figure 3.13: Further evidence of efficient infection. Expression of (A) GFP-encoding and (B) AMPK-encoding adenoviral constructs in cells fixed and treated with a TRITC-labelled myc-tag antibody and visualized for GFP fluorescence.

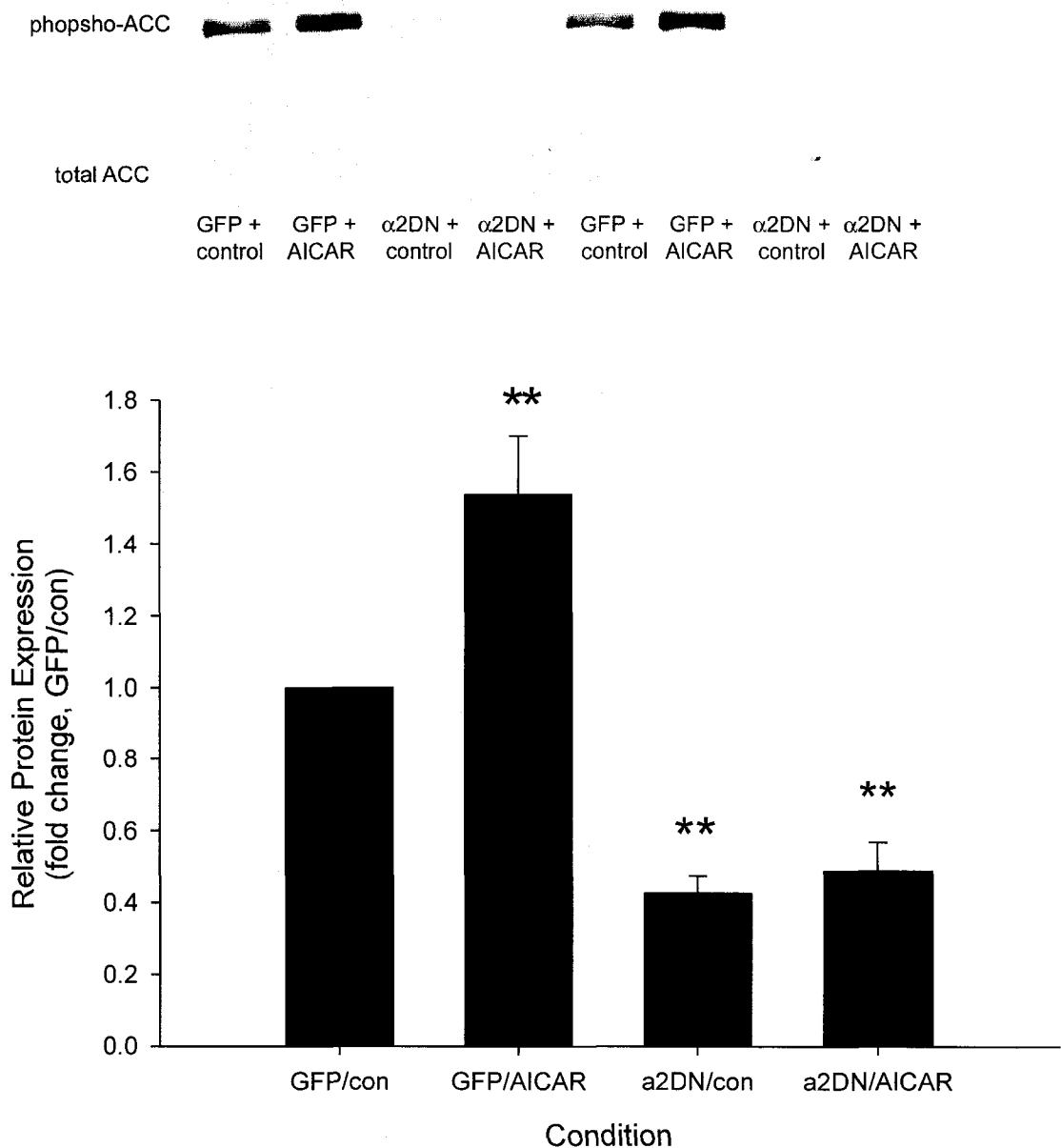


Figure 3.14: ACC phosphorylation following AICAR treatment is not inhibited in the presence of a control adenovirus, however phosphorylation with or without AICAR treatment is inhibited by the presence of an $\alpha 2$ -dominant negative AMPK construct in cells harvested day 5 post-infection (n=5). Whole-cell lysates were separated electrophoretically, blotted onto nitrocellulose membranes, and probed with a polyclonal phospho-ACC antibody. Membranes were subsequently stripped and reprobed with a polyclonal ACC antibody, and the ratio of phospho-ACC to total ACC was used for statistical comparison. ** = p<0.01

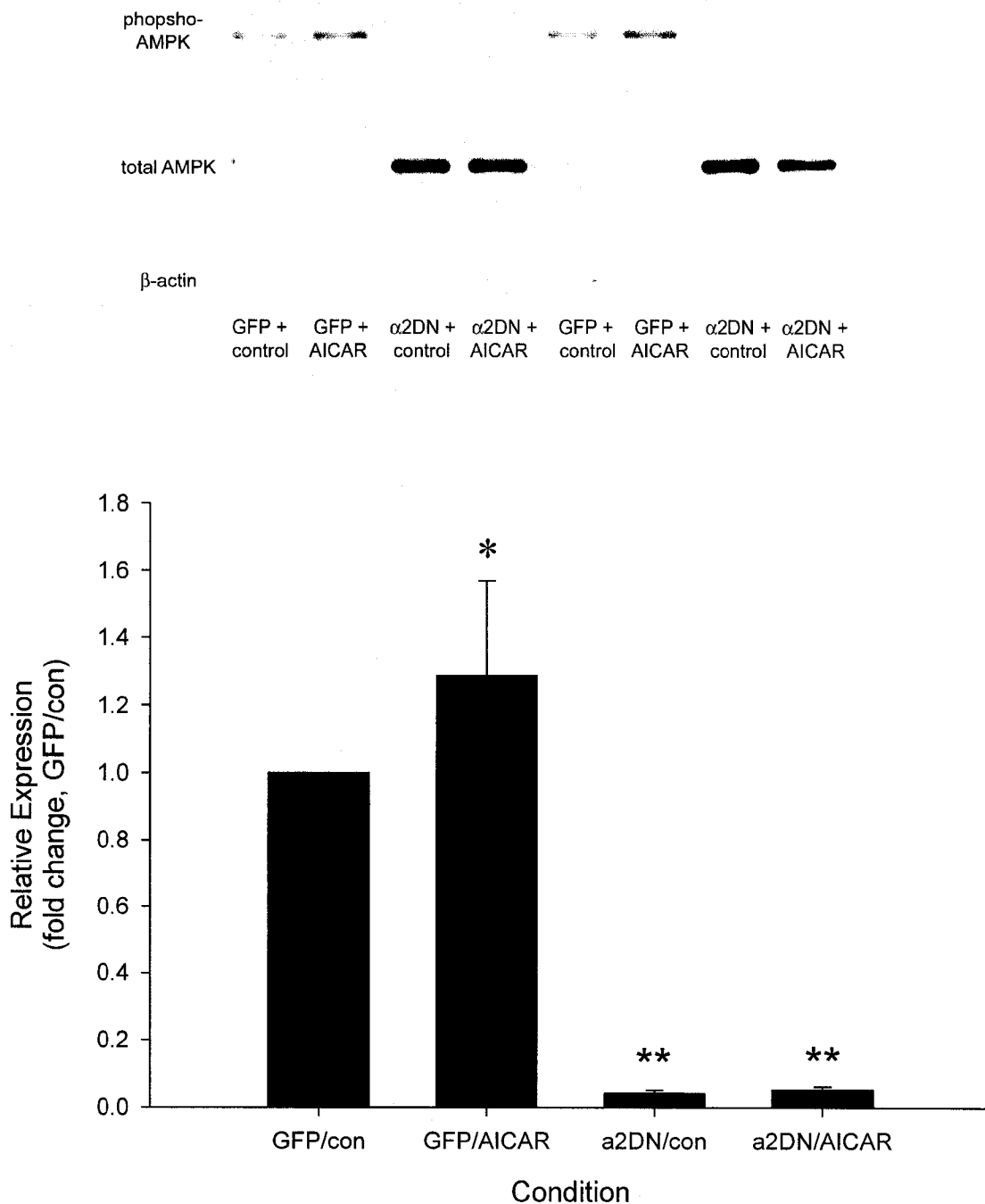


Figure 3.15: AMPK phosphorylation following AICAR treatment is not inhibited in the presence of a control adenovirus, however phosphorylation with or without AICAR treatment is inhibited by the presence of an α 2-dominant negative AMPK construct in cells harvested day 5 post-infection (n=5). Whole-cell lysates were separated electrophoretically, blotted onto nitrocellulose membranes, and probed with a polyclonal phospho-ACC antibody. Membranes were subsequently stripped and reprobed with a polyclonal AMPK antibody, and the ratio of phospho-AMPK to total AMPK was used for statistical comparison. Membranes were also stripped and reprobed for β -actin as another loading control. * = $p < 0.05$, ** = $p < 0.01$

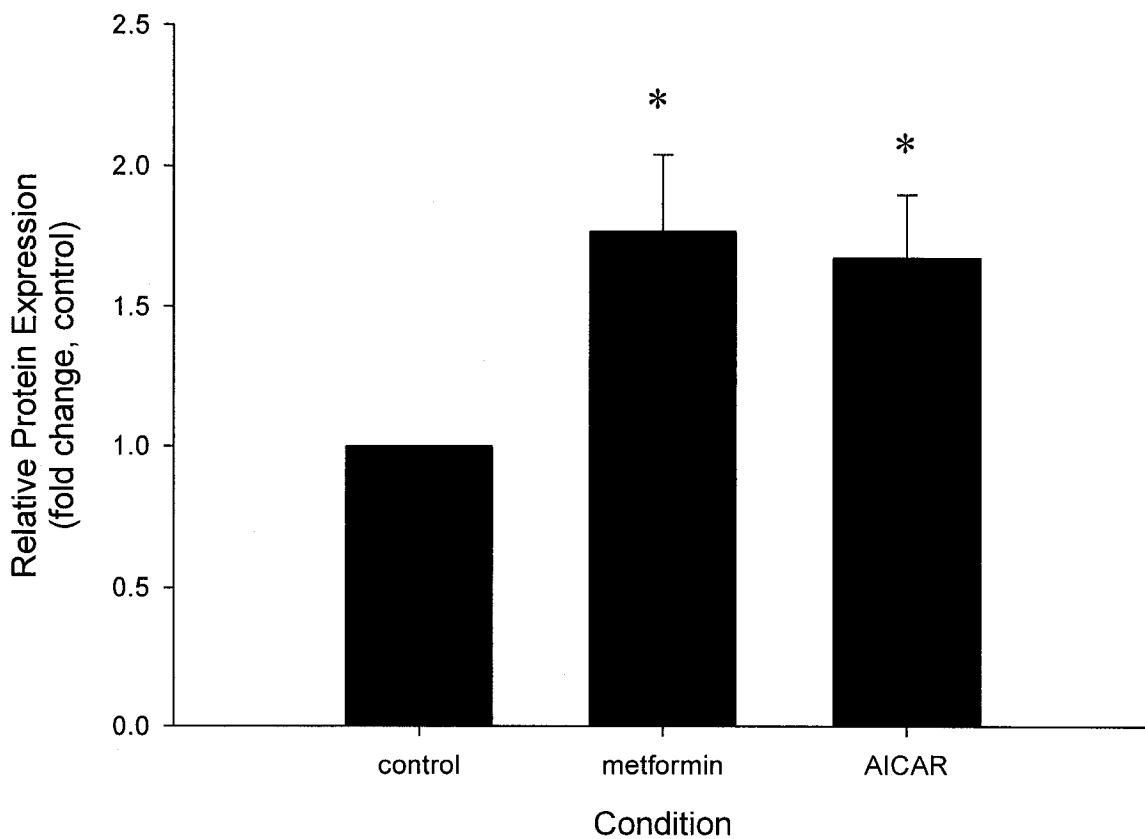
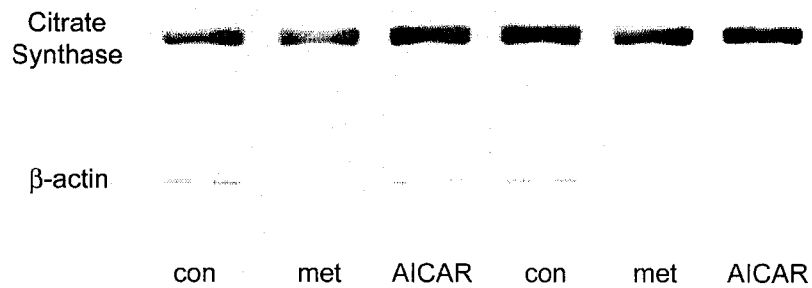


Figure 3.16: Both AICAR and metformin treatment result in increases in citrate synthase expression, providing evidence of mitochondrial biogenesis on day 4 post-treatment (n=8). Whole-cell lysates were separated electrophoretically, blotted onto nitrocellulose membranes, and probed with a polyclonal citrate synthase antibody. Membranes were subsequently stripped and reprobed with a polyclonal β -actin antibody, and the ratio of citrate synthase to β -actin was used for statistical comparison. * = $p < 0.05$

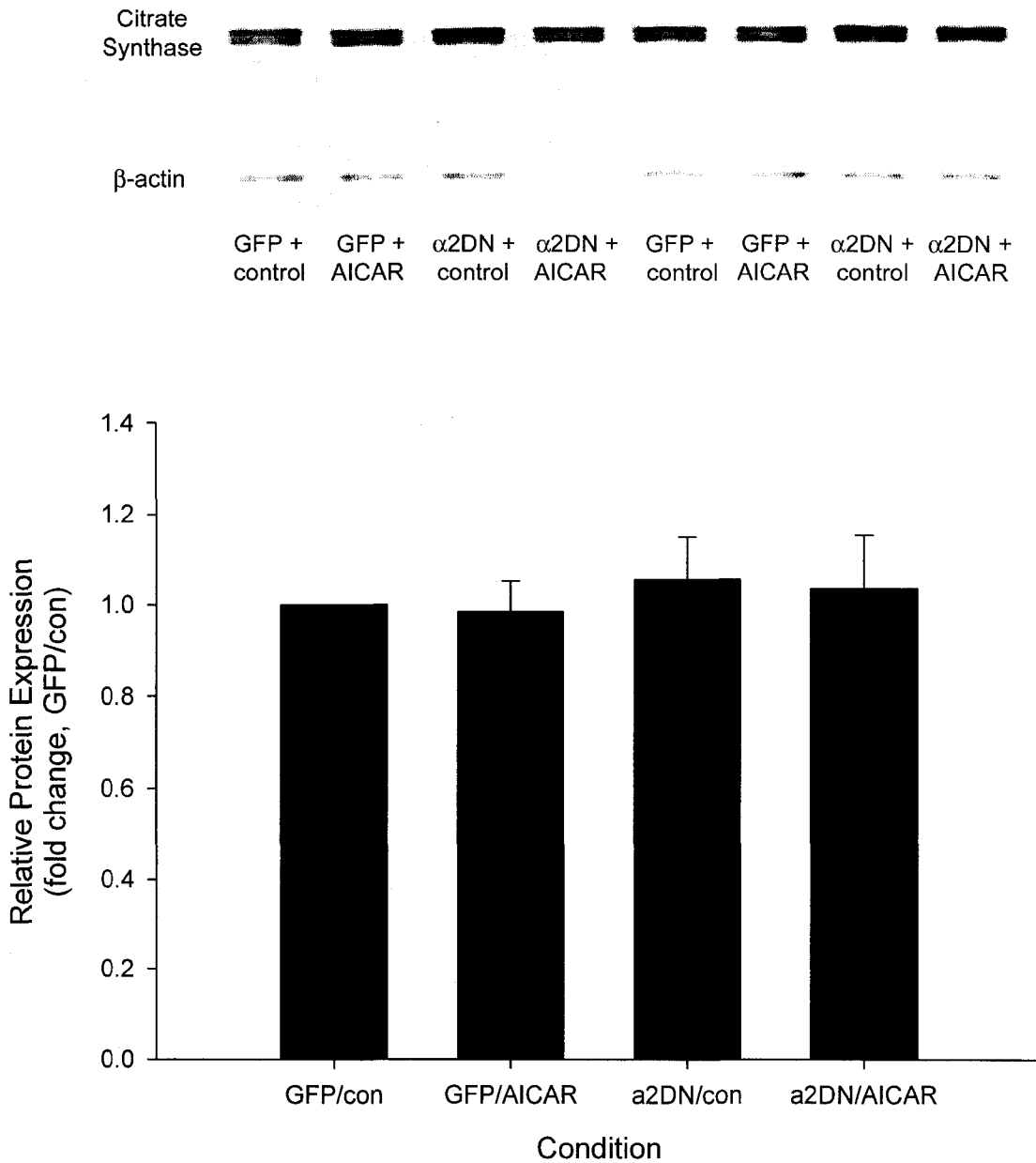


Figure 3.17: No changes in citrate synthase expression were visible for any adenovirus-treated condition, providing no evidence of mitochondrial biogenesis on day 5 post-infection (n=8). Whole-cell lysates were separated electrophoretically, blotted onto nitrocellulose membranes, and probed with a polyclonal citrate synthase antibody. Membranes were subsequently stripped and re-probed with a polyclonal β -actin antibody, and the ratio of citrate synthase to β -actin was used for statistical comparison.

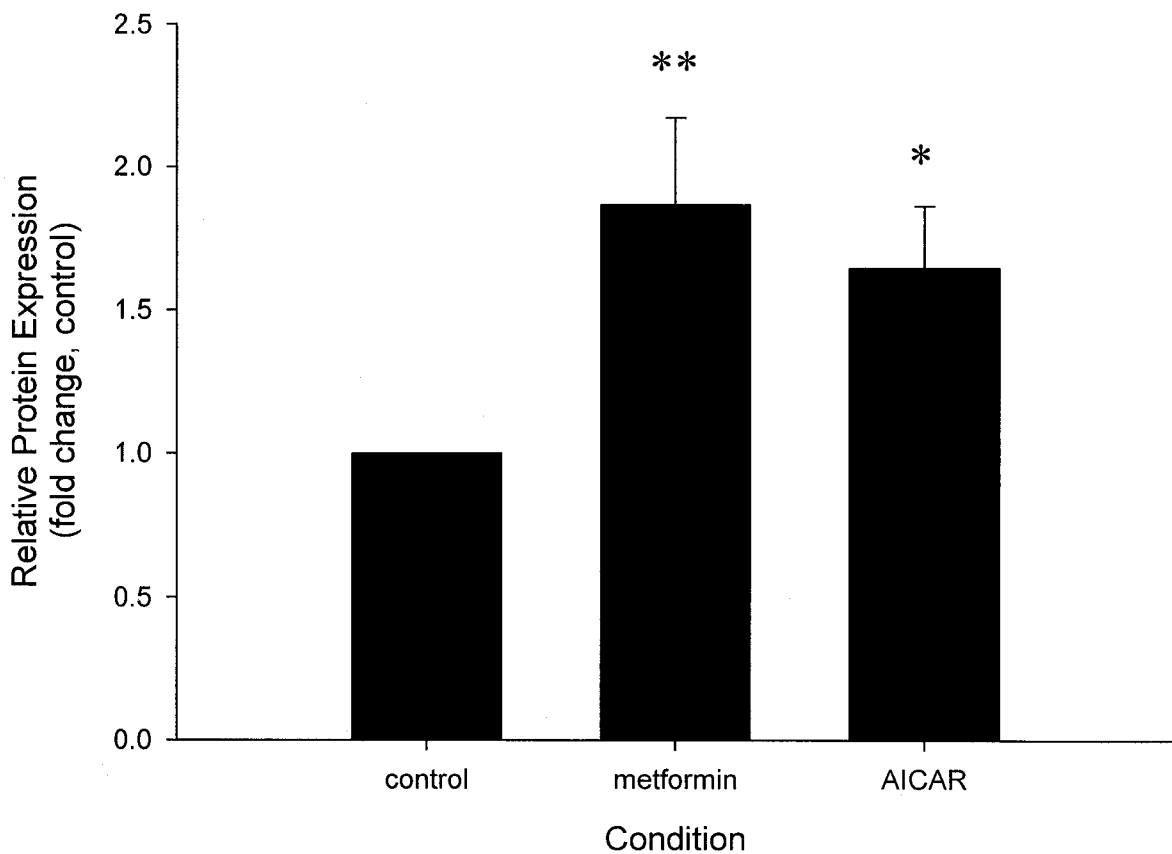
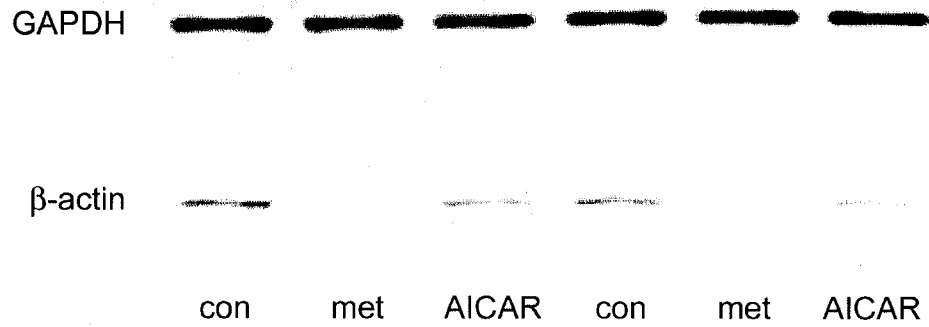


Figure 3.18: Both AICAR and metformin treatment result in increases in GAPDH expression, providing evidence of increased glycolytic flux on day 4 post-treatment (n=8). Whole-cell lysates were separated electrophoretically, blotted onto nitrocellulose membranes, and probed with a polyclonal GAPDH antibody. Membranes were subsequently stripped and reprobbed with a polyclonal β -actin antibody, and the ratio of citrate synthase to β -actin was used for statistical comparison. * = $p < 0.05$, ** = $p < 0.01$

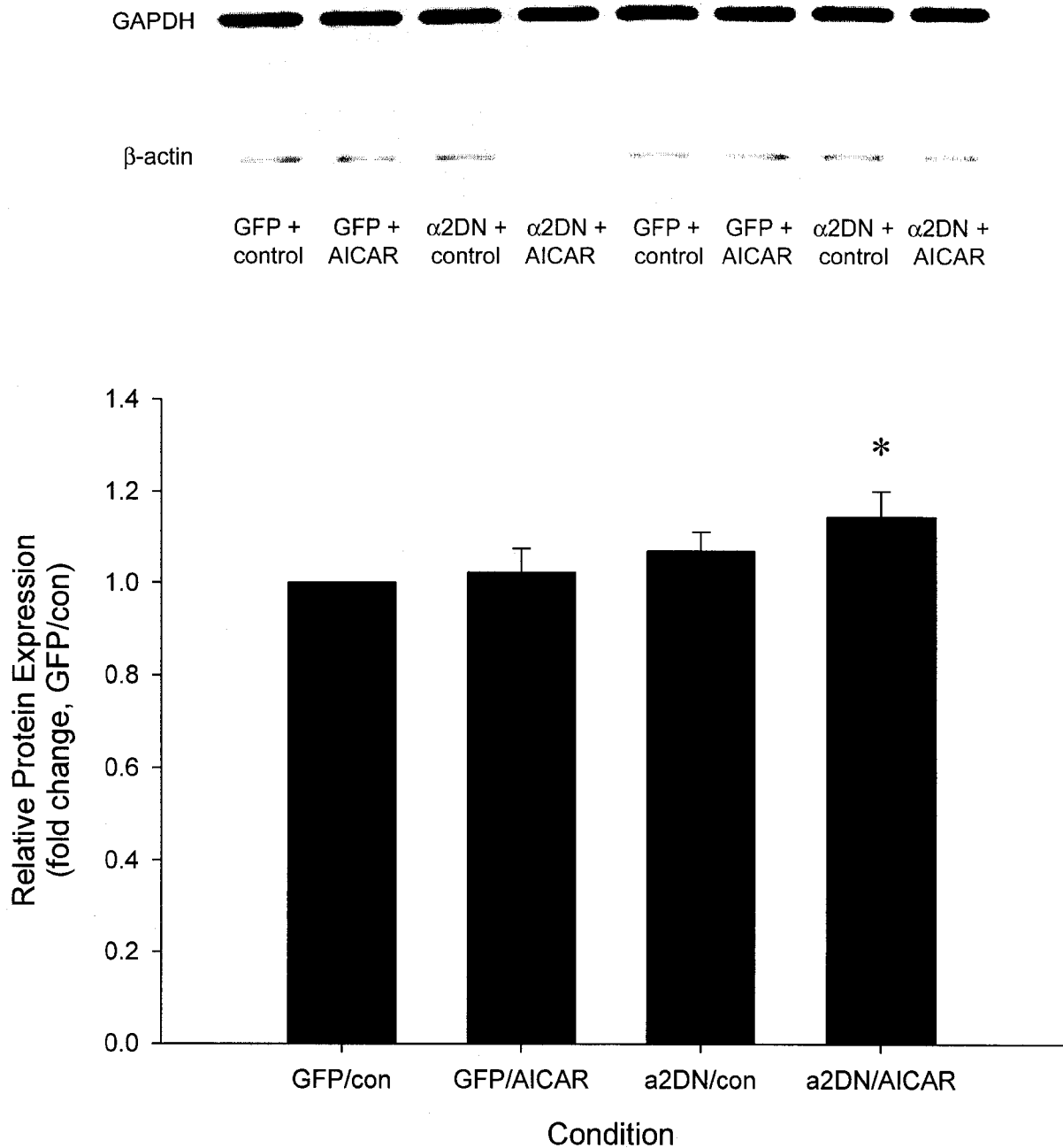


Figure 3.19: α 2DN + AICAR results in a small but significant increase in GAPDH expression, indicating an increase in glycolytic flux on day 5 post-infection (n=8). Whole-cell lysates were separated electrophoretically, blotted onto nitrocellulose membranes, and probed with a polyclonal GAPDH antibody. Membranes were subsequently stripped and re probed with a polyclonal β -actin antibody, and the ratio of citrate synthase to β -actin was used for statistical comparison. * = $p < 0.05$

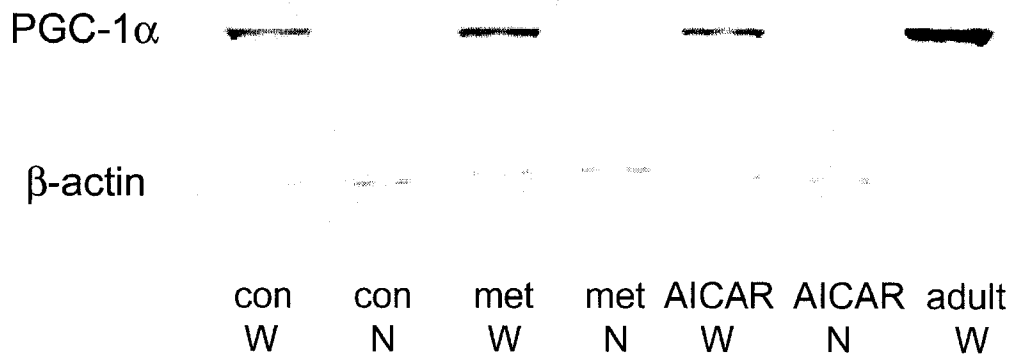


Figure 3.20: Whole-cell (W) and nuclear-enhanced extracts (N) treated with various pharmacological conditions, blotted for PGC-1α. PGC-1α expression was much stronger for whole-cell lysates and adult tissue than the nuclear-enhanced extracts.

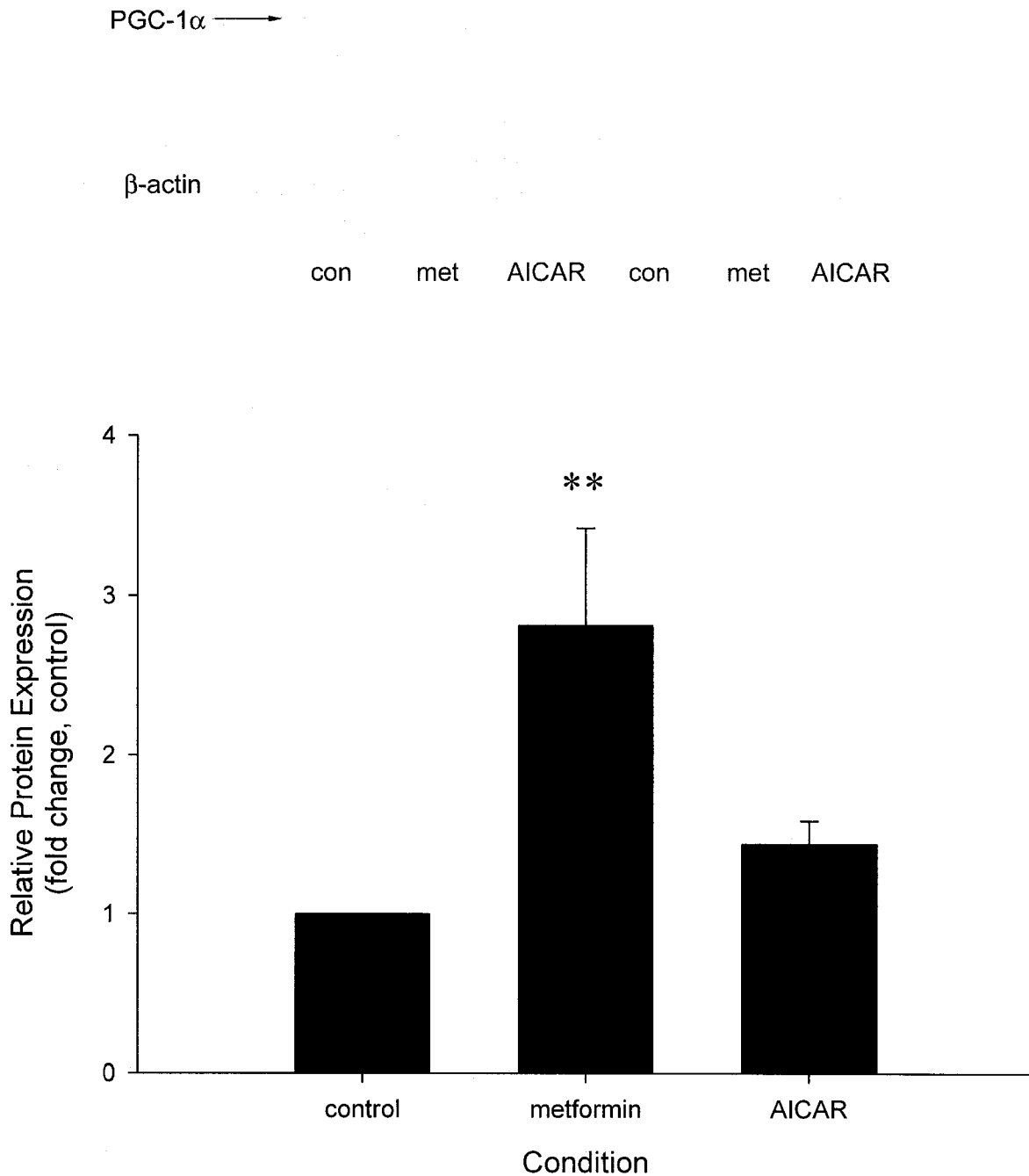


Figure 3.21: Metformin treatment, but not AICAR, results in nearly a 3-fold increase in PGC-1 α expression, providing evidence of PGC-1 α signalling during mitochondrial biogenesis on day 4 post-treatment (n=8). Whole-cell lysates were separated electrophoretically, blotted onto nitrocellulose membranes, and probed with a polyclonal PGC-1 α antibody. Membranes were subsequently stripped and re-probed with a polyclonal β -actin antibody, and the ratio of PGC-1 α to β -actin was used for statistical comparison. ** = p<0.01

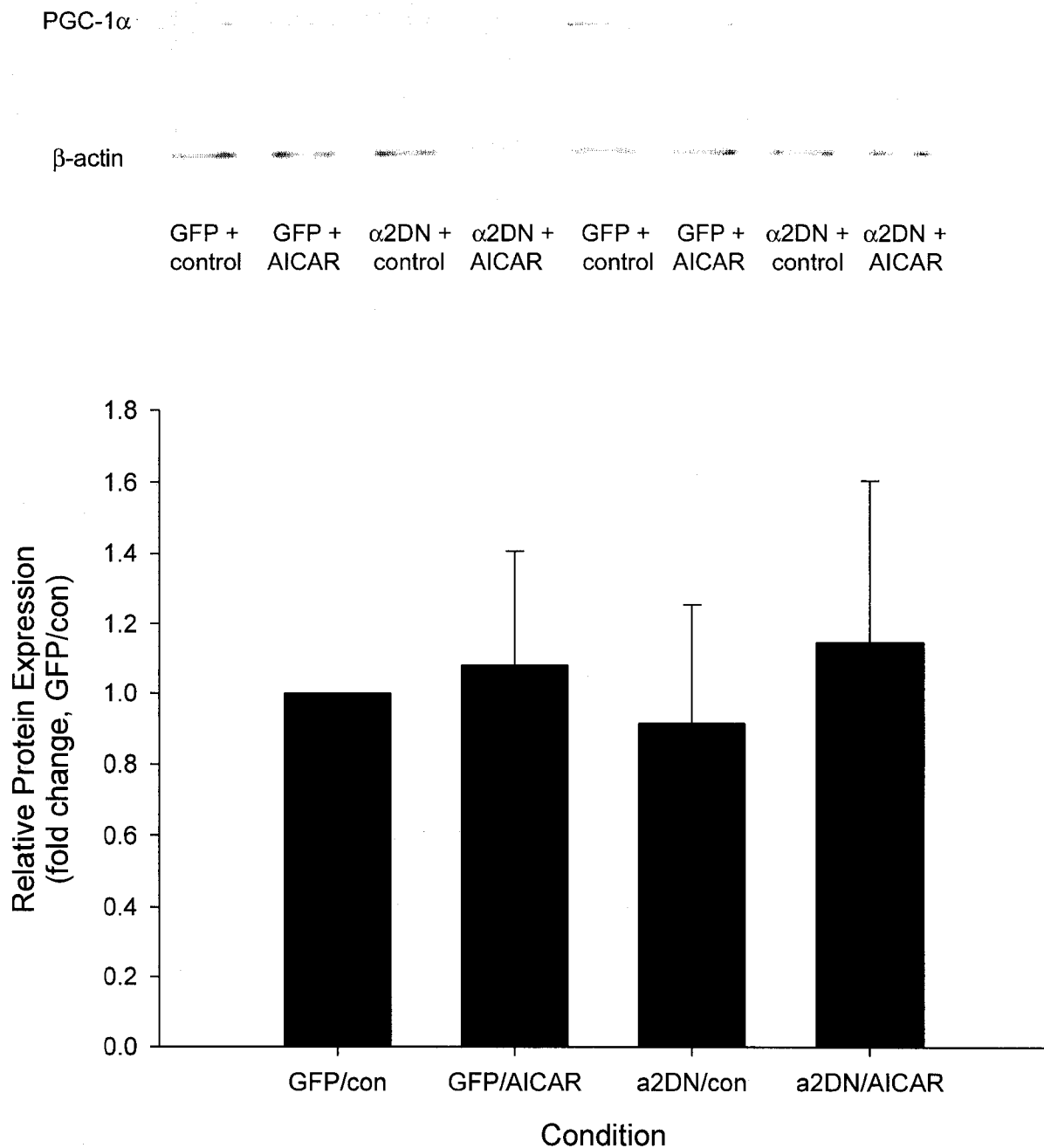


Figure 3.22: No changes in PGC-1 α expression visible for any adenovirus-treated condition, providing no evidence of PGC-1 α signalling during mitochondrial biogenesis on day 5 post-infection (n=8). Whole-cell lysates were separated electrophoretically, blotted onto nitrocellulose membranes, and probed with a polyclonal PGC-1 α antibody. Membranes were subsequently stripped and re-probed with a polyclonal β -actin antibody, and the ratio of PGC-1 α to β -actin was used for statistical comparison.

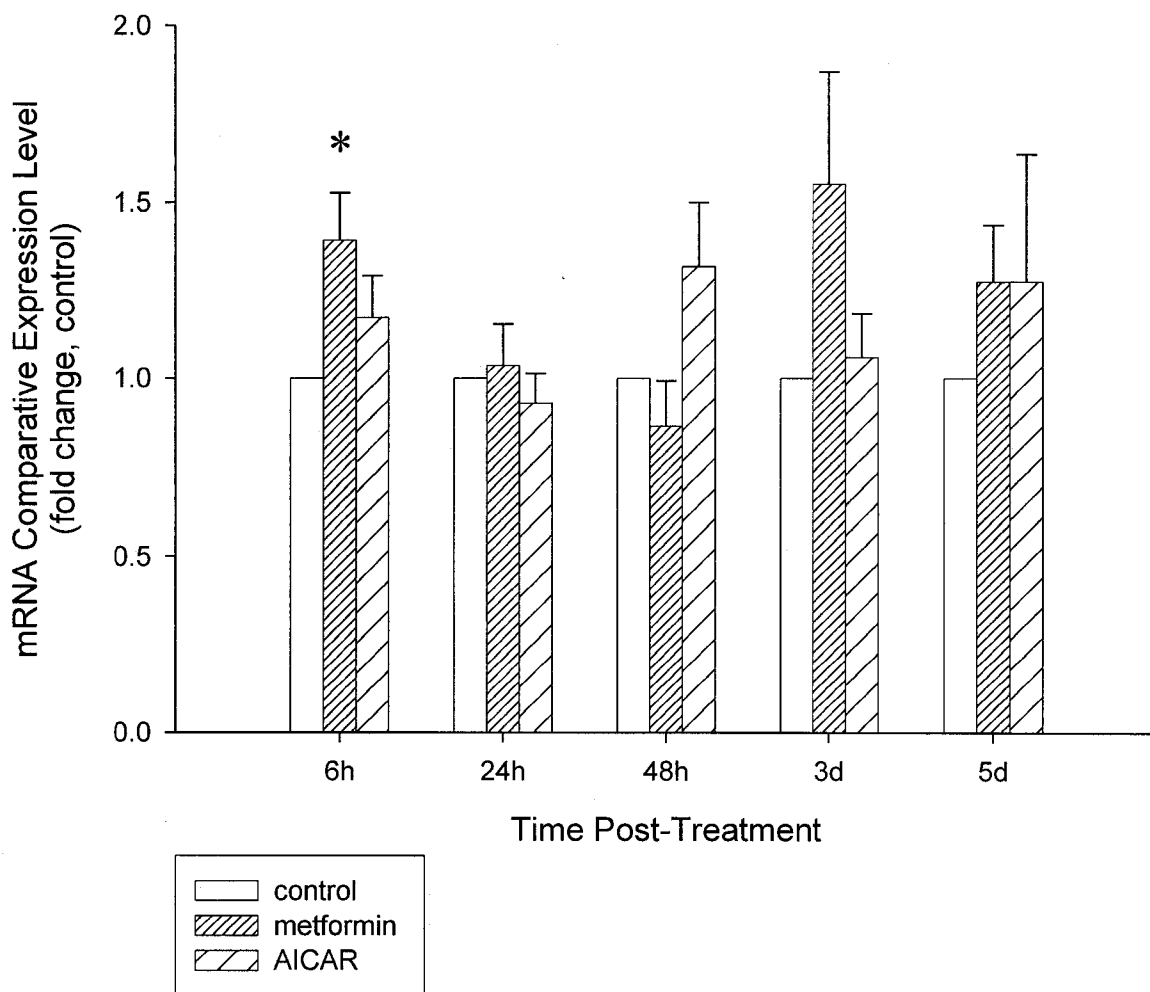


Figure 3.23: Citrate synthase mRNA expression at various time points following pharmacological treatment (n=6). The early 6h increase in citrate synthase transcription following metformin treatment provides evidence of mitochondrial biogenesis. mRNA was extracted from cells, reverse-transcribed into cDNA, and assayed using real-time PCR for gene expression relative to the control condition. Cyclophilin was used as a housekeeping gene. * = $p < 0.05$

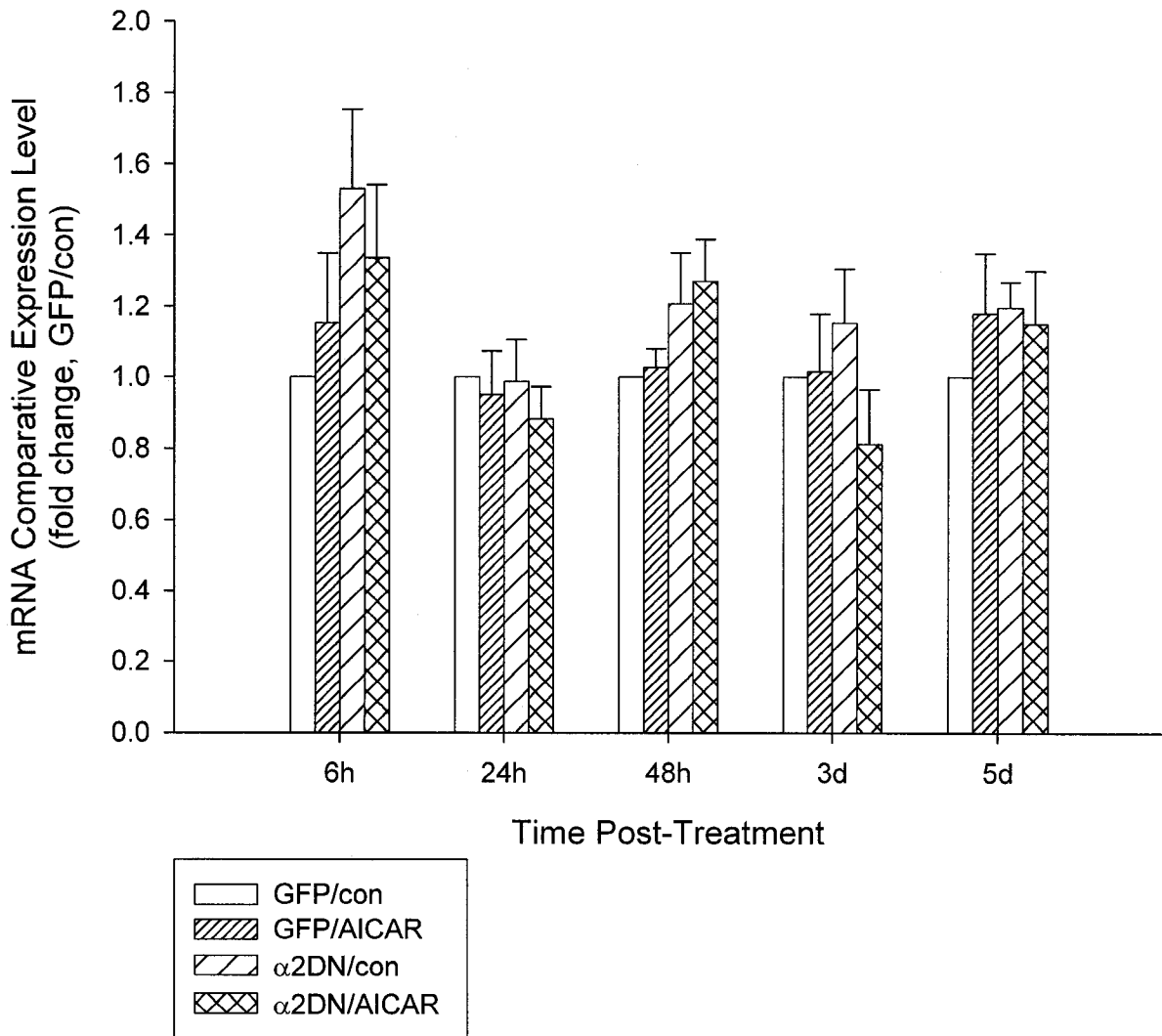


Figure 3.24: Citrate synthase mRNA expression at various time points following adenovirus infection (n=6). No evidence of changes in citrate synthase mRNA expression was apparent. mRNA was extracted from cells, reverse-transcribed into cDNA, and assayed using real-time PCR for gene expression relative to the GFP/control condition. Cyclophilin was used as a housekeeping gene.

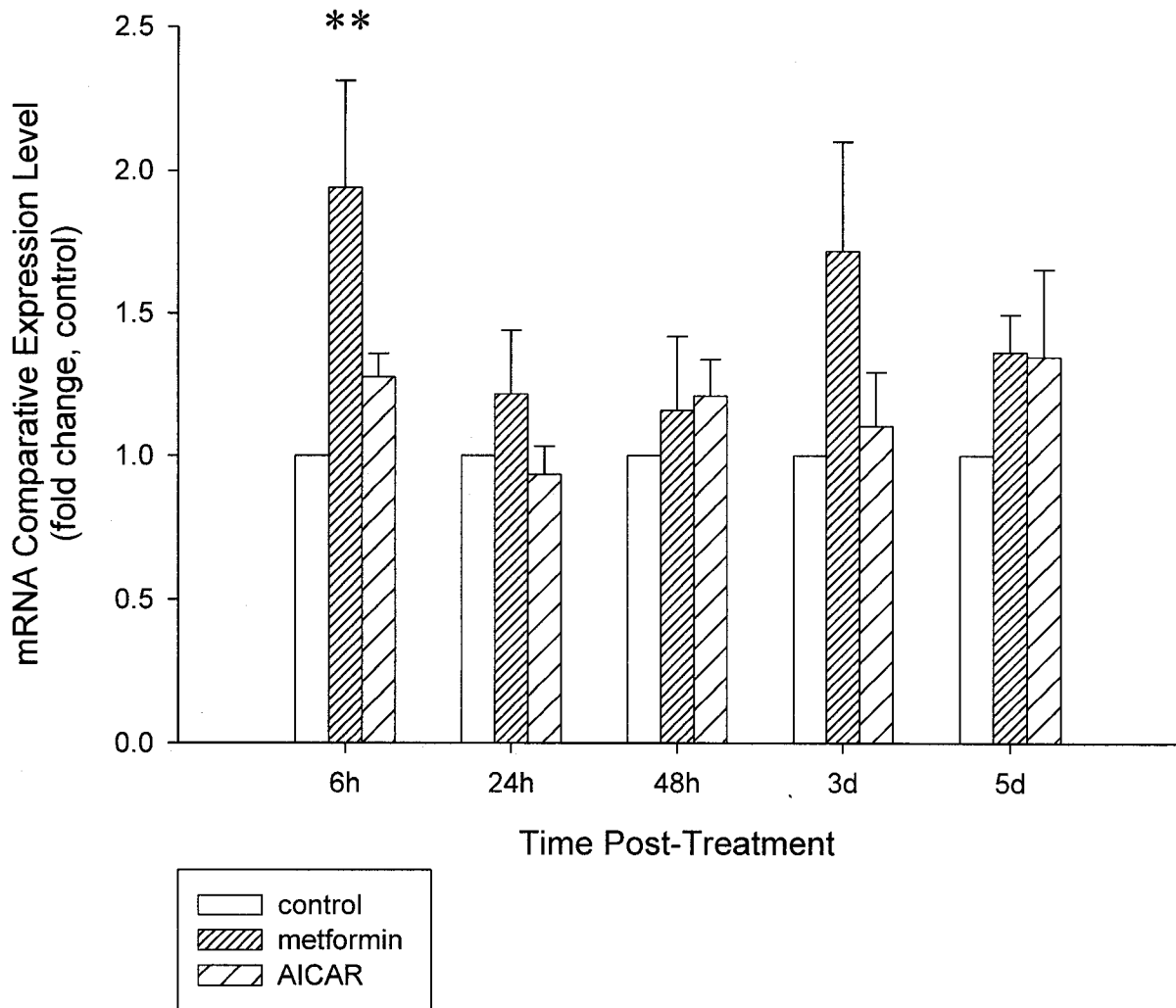


Figure 3.25: ALA synthase mRNA expression at various time points following pharmacological treatment (n=6). The early 6h increase in ALA synthase transcription following metformin treatment provides evidence of mitochondrial biogenesis. mRNA was extracted from cells, reverse-transcribed into cDNA, and assayed using real-time PCR for gene expression relative to the control condition. Cyclophilin was used as a housekeeping gene. ** = p<0.01

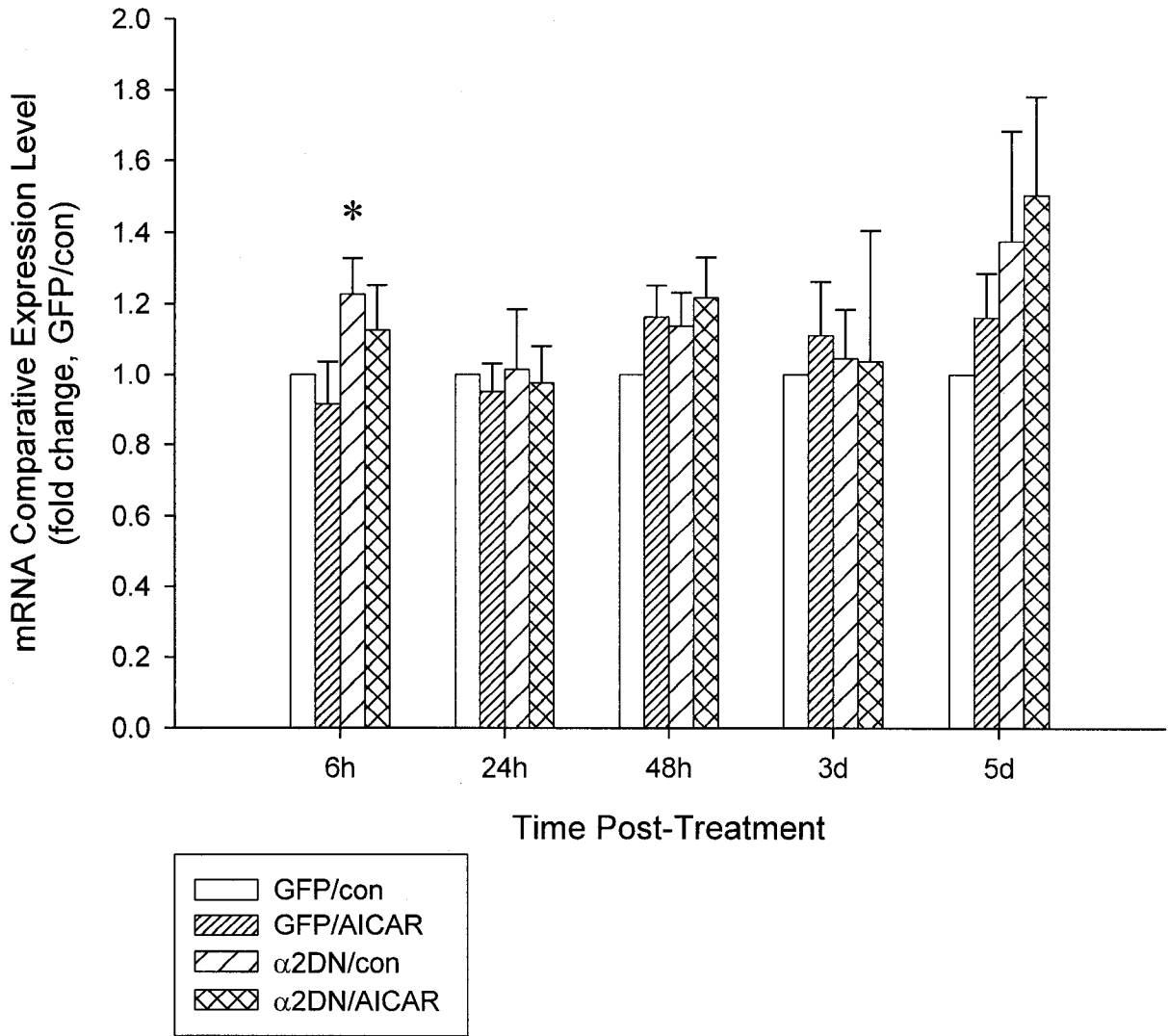


Figure 3.26: ALA synthase mRNA expression at various time points following adenovirus infection (n=6). Early increase in ALA synthase transcription following α_2 DN adenovirus treatment provides evidence of mitochondrial biogenesis. mRNA was extracted from cells, reverse-transcribed into cDNA, and assayed using real-time PCR for gene expression relative to the control condition. Cyclophilin was used as a housekeeping gene. * = p<0.05

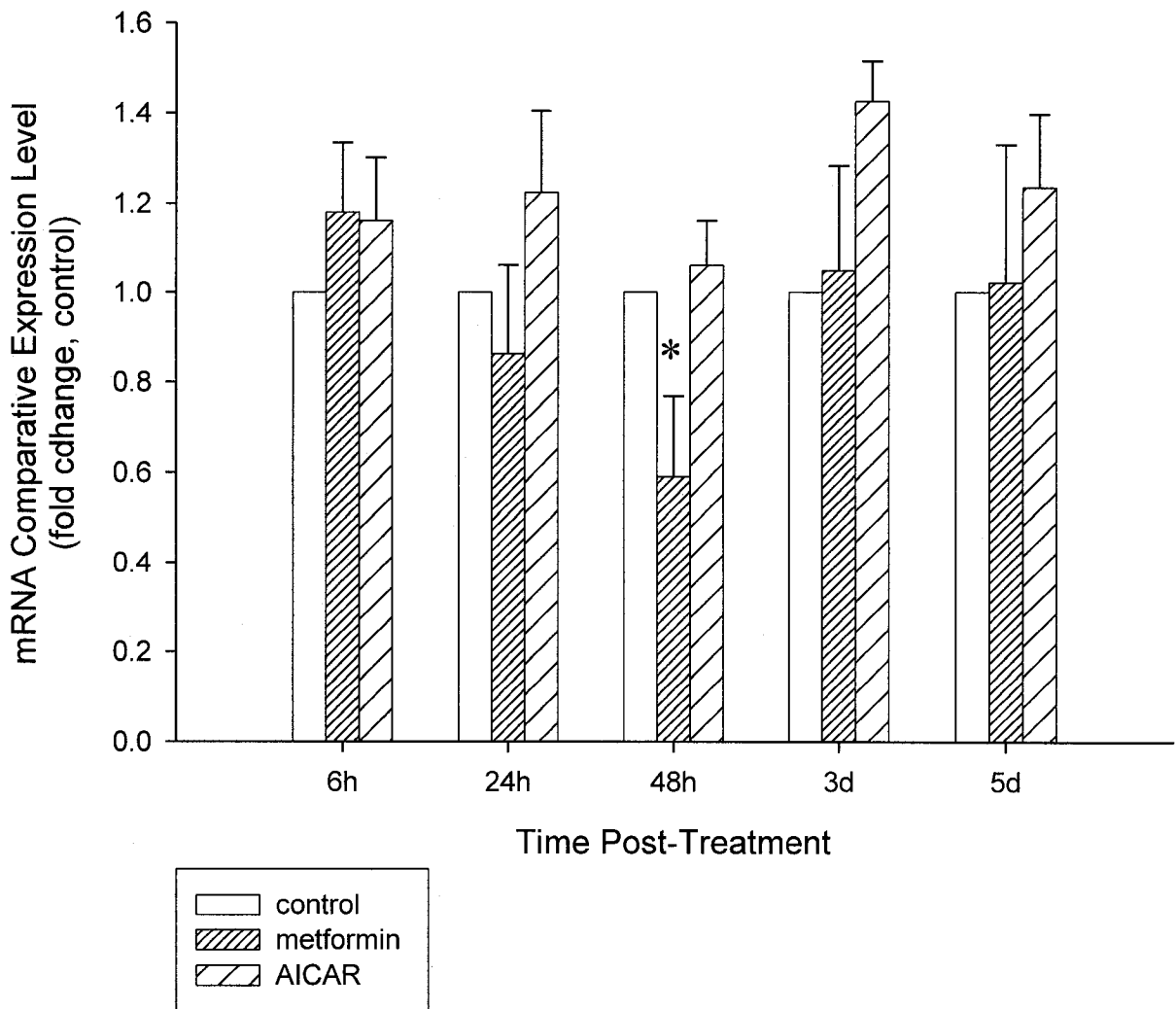


Figure 3.27: PGC-1 α mRNA expression at various time points following pharmacological treatment (n=6). Decreases in PGC-1 α transcription 48 hours following metformin treatment fails to explain the large increase in protein expression visible on day 4 (Figure 3.21). mRNA was extracted from cells, reverse-transcribed into cDNA, and assayed using real-time PCR for gene expression relative to the control condition. Cyclophilin was used as a housekeeping gene. * = p<0.05

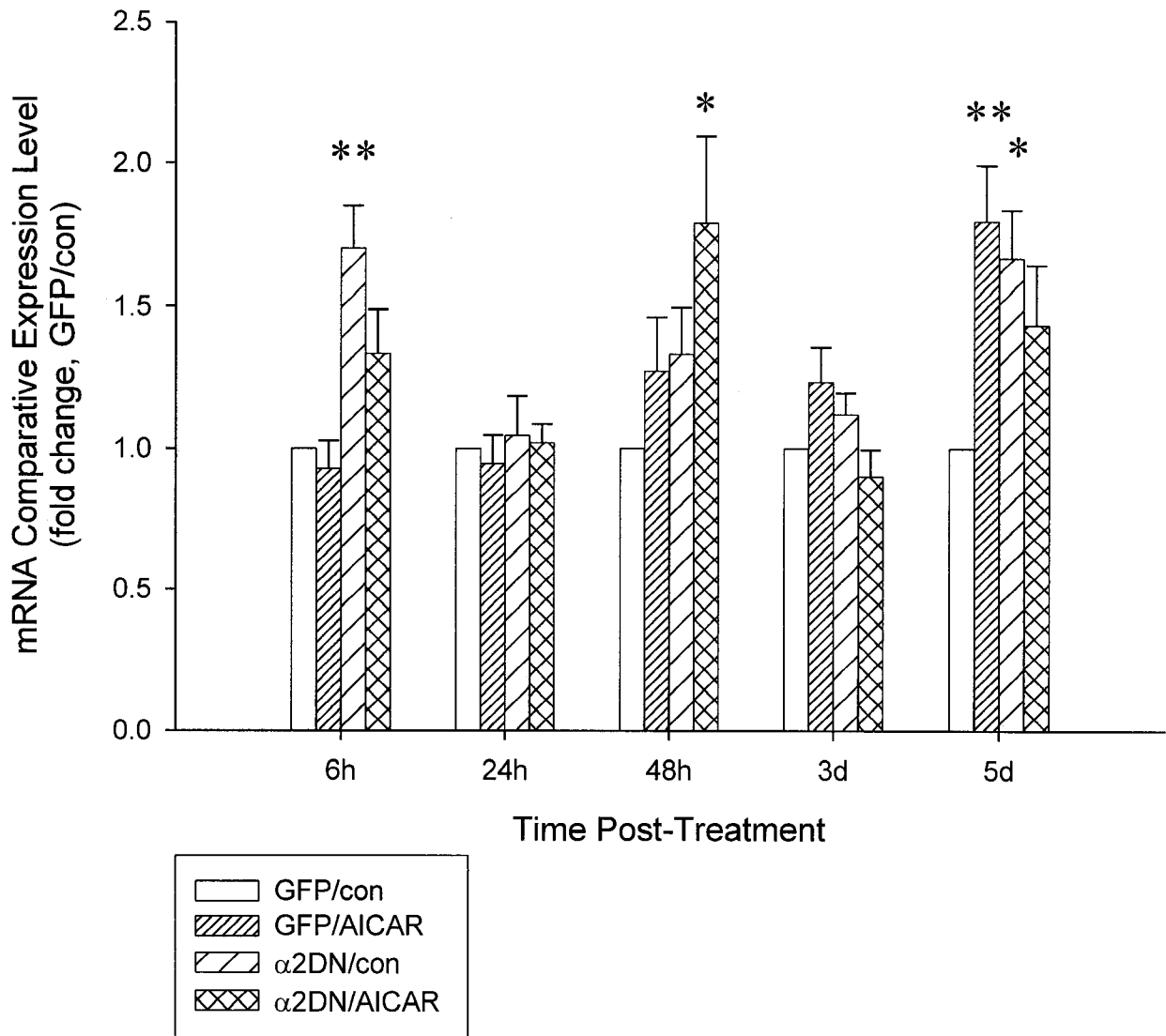


Figure 3.28: PGC-1 α mRNA expression at various time points following adenovirus infection (n=6). Increases in PGC-1 α transcription following α_2 DN adenovirus treatment at 6 hours, 48 hours and 5 days post-treatment refute the hypothesis of PGC-1 α downregulation in response to AMPK inhibition. The increase in PGC-1 α mRNA following 5d of AICAR treatment does support the hypothesis of PGC-1 α upregulation in response to AMPK activation. mRNA was extracted from cells, reverse-transcribed into cDNA, and assayed using real-time PCR for gene expression relative to the control condition. Cyclophilin was used as a housekeeping gene. * = p<0.05, ** = p<0.01

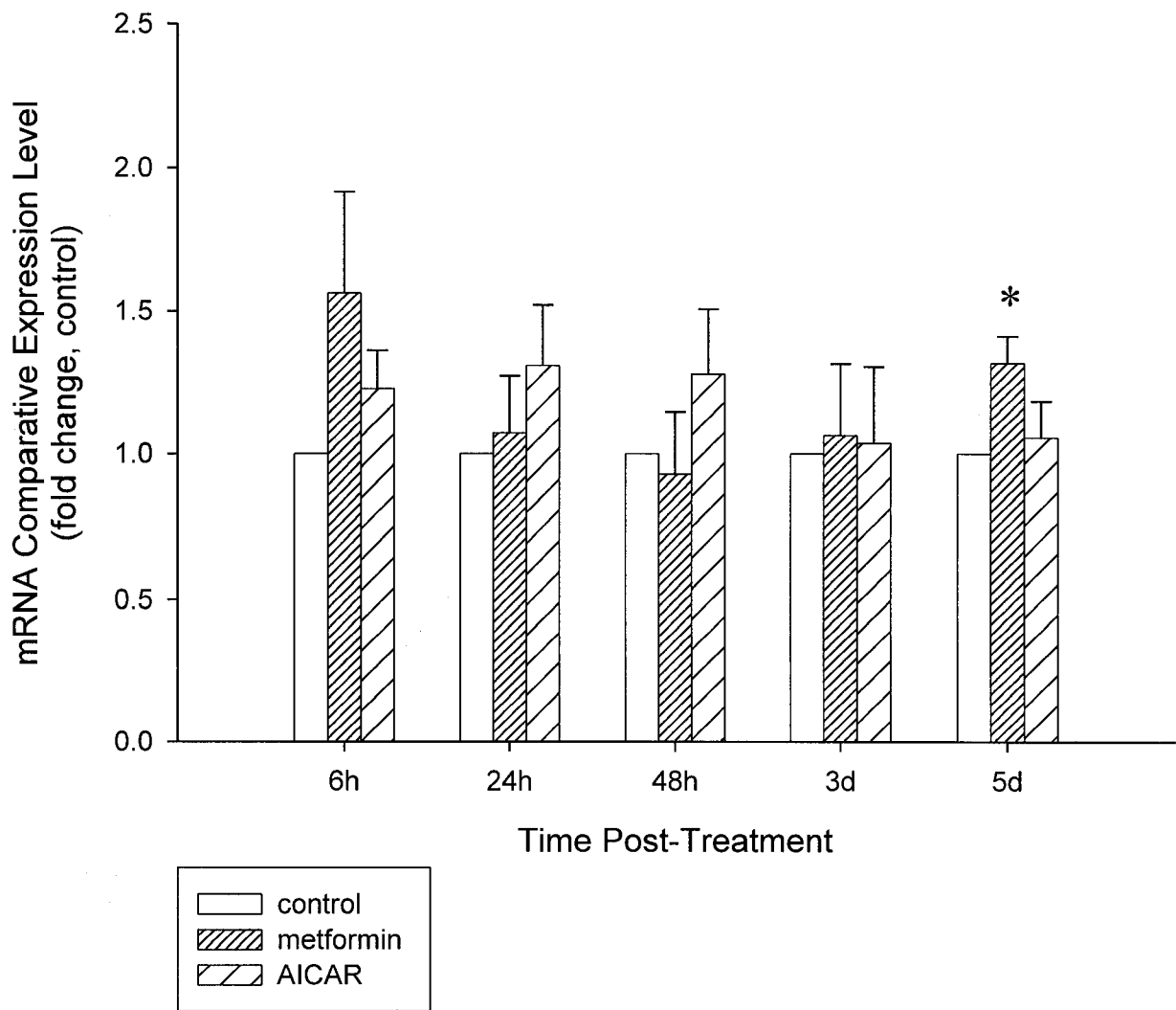


Figure 3.29: p300 mRNA expression at various time points following pharmacological treatment (n=6). Increase in p300 transcription 5 days following metformin indicates potential long-term transcriptional regulation of p300 expression by AMPK. mRNA was extracted from cells, reverse-transcribed into cDNA, and assayed using real-time PCR for gene expression relative to the control condition. Cyclophilin was used as a housekeeping gene. * = p<0.05

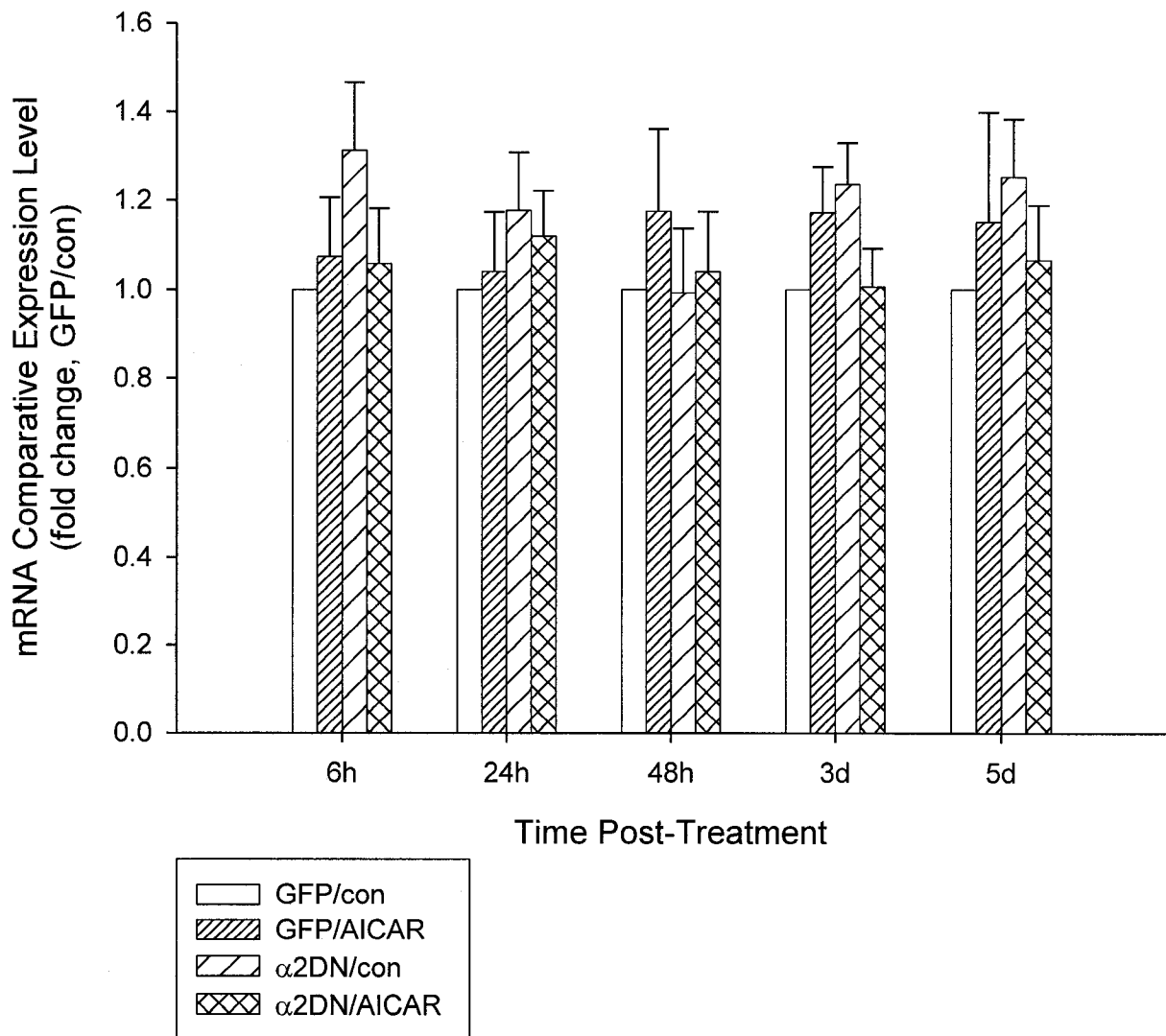


Figure 3.30: p300 mRNA expression at various time points following adenovirus infection (n=6). No evidence of changes in p300 mRNA expression were present, supporting the experimental hypothesis. mRNA was extracted from cells, reverse-transcribed into cDNA, and assayed using real-time PCR for gene expression relative to the GFP/control condition. Cyclophilin was used as a housekeeping gene.

3.4 References

- Cao, B., Mytinger, J. R., & Huard, J. (2002). Adenovirus mediated gene transfer to skeletal muscle. *Microsc. Res. Tech.* 58, 45-51.
- Jankov, R.P., Johnstone, L., Luo, X., Robinson, B.H., Tanswell, A.K. (2003). Macrophages as a major source of oxygen radicals in the hyperoxic newborn rat lung. *Free Radic. Biol. Med.* 35, 200-209.
- Leary, S. C., Battersby, B. J., Hansford, R. G., & Moyes, C. D. (1998). Interactions between bioenergetics and mitochondrial biogenesis. *Biochim. Biophys. Acta* 1365, 522-530.
- Moyes, C. D., Mathieu-Costello, O. A., Tsuchiya, N., Filburn, C., & Hansford, R. G. (1997). Mitochondrial biogenesis during cellular differentiation. *Am. J. Physiol Cell Physiol.* 272, C1345-C1351.
- Shimokawa, T., Kato, M., Ezaki, O., & Hashimoto, S. (1998). Transcriptional regulation of muscle-specific genes during myoblast differentiation. *Biochem. Biophys. Res. Commun.* 246, 287-292.

CHAPTER IV: DISCUSSION

4.1 Evaluation of Experimental Model

4.1.1 Differentiation of Cells

Appropriate cellular differentiation is important for studies of mitochondrial biogenesis, as previous work has indicated that undifferentiated C2C12 myoblasts rely primarily on glycolysis for their energy production, yet slowly shift towards oxidative metabolism as they differentiate into myotubes (Moyes *et al.*, 1997). Researchers have assayed numerous glycolytic and mitochondrial enzymes over a time course following C2C12 cell differentiation, finding that mitochondrial matrix enzyme activity increased almost linearly over a 16-day period following serum withdrawal and achieving a four-fold increase overall (Moyes *et al.*, 1997). Metabolic studies in the same cells have indicated that while myoblasts derive ~30% of their energy production from oxidative phosphorylation, this fraction reaches ~60% following 12 days of differentiation with concomitant decreases in glycolytic metabolism (Leary *et al.*, 1998). Based on observations from preliminary experiments in which cells were infected only one day post-differentiation, untreated cells often appeared to reach a more advanced state in their differentiation program than infected cells. Therefore, one can speculate that the combined treatment of adenovirus and Lipofectamine, which can disrupt various cellular membranes, could potentially inhibit differentiation. As a result, cells are somewhat suspended at an early state of development before the majority of endogenous mitochondrial biogenesis has taken place, while control cells that receive no treatment are able to differentiate normally. Conclusions from preliminary experiments indicated that cells should be permitted to differentiate for a longer period of time prior to infection, allowing them to become more naturally oxidative before manipulating their aerobic capacity via AMPK.

One means used to verify the extent of differentiation within our cells was protein expression of myoD, a marker of myogenic induction, and myogenin, a marker of

differentiation, over a time course of differentiation. As mentioned above, these results were drawn from a very small sample size and therefore definitive conclusions could not be made, however they were able to provide some evidence of the appropriate period required for cell differentiation. As earlier studies have indicated that myoD expression remains fairly constant both at the protein and mRNA level throughout C2C12 differentiation (Dedieu *et al.*, 2002; Shen *et al.*, 2003; Shimokawa *et al.*, 1998), our results demonstrating a small increase and plateau at day 6 were somewhat surprising. This may be explained in part by the varying differentiation rates of different cells in culture. For example, by day 12 post-differentiation, there are many large and branched myotubes resulting from fusion of numerous cells, yet several myoblasts remain present as well. Indeed, Dedieu and coworkers (Dedieu *et al.*, 2002) found that C2C12 fusion plateaued on day 8, at which point 60% of cell nuclei were in myotubes and therefore 40% remained as unfused myoblasts. Regardless of this potential variability, the myoD plateau achieved by day 6 indicated this was a suitable time in which to treat cells as the stability of myoD expression demonstrated the minimal contribution of differentiation processes on subsequent results. Myogenin expression behaved as expected (Dedieu *et al.*, 2002; Shimokawa *et al.*, 1998), providing further evidence that the majority of differentiation was complete by day 6 following serum withdrawal.

Following treatment, myoD and myogenin protein expression was again assessed to indicate if the experimental conditions affected C2C12 differentiation, and if such effects may be influencing the results. Unfortunately, results did highlight one of the inherent weaknesses of the model. More specifically, there were changes evident in myogenic marker expression resulting from treatment, as AICAR led to an increase in myogenin protein levels when used alone or in combination with the α_2 DN AMPK construct. This indicated that AICAR was accelerating the cellular differentiation state through a means independent of α_2 -AMPK; either via α_1 -AMPK or a different pathway altogether. Regardless of the mechanism, results indicated that the treatments involving AICAR might still be affecting differentiation even after allowing six days for development following serum withdrawal, which may have influenced expression of mitochondrial proteins independent of AMPK-induced biogenesis.

4.1.2 Efficiency of AMPK Activation and Inhibition

Treatment with metformin and AICAR alone produced an average 1.5-fold increase in phospho-ACC expression, while a similar significant increase in AMPK phosphorylation was produced following metformin treatment only. This may be in part due to the different mechanisms of action of the two treatments, as AICAR is known to convert into an allosteric activator of AMPK while metformin does not directly bind the kinase (Zhou *et al.*, 2001). Metformin, as mentioned earlier, has been suggested to promote AMPK phosphorylation via upstream kinases, explaining the significant increase in phospho-AMPK expression. AICAR, or its active form ZMP, may not have as great of an effect on upstream kinases as was previously hypothesized (Hardie & Carling, 1997), and perhaps a higher dose is required before such actions can occur.

All cells tested for AMPK activation were harvested 2 days post-treatment, as other studies have indicated that while significant increases in phospho-ACC could be seen after 6h in metformin-treated H4IIE cells, blotting results demonstrated very obvious changes after 48 hours of treatment (Hawley *et al.*, 2002). This study also found large changes in phospho-ACC were concomitant with less robust increases in phospho-AMPK, indicating that perhaps only small changes in AMPK activity are required to produce large downstream effects (Hawley *et al.*, 2002). This may also, however, result from differences in substrate affinity of the two different phospho-specific antibodies. Meanwhile, the optimized pharmacological doses were fairly similar to other *in vitro* studies using various types of cells (Hawley *et al.*, 2002; Leclerc *et al.*, 2004; Zhou *et al.*, 2001), and in experiments in which much larger doses were used, the incubation time was usually less than 24 hours (Fryer *et al.*, 2002; Hawley *et al.*, 2002). While C2C12 cells were able to withstand larger doses of treatment for 24-48 hours, such high concentrations proved unsuitable for 4-day incubations and impeded normal cell morphology.

In the case of the combined virus and drug conditions, the model appeared to work very well. Significant increases in both phospho-ACC and phospho-AMPK

expression in samples treated with GFP + AICAR, as compared to GFP + control, indicated the virus treatment did not inhibit the ability of AICAR to activate AMPK. In addition, cells treated with the α_2 DN virus with or without AICAR both showed significantly reduced phospho-ACC and phospho-AMPK expression as compared to the GFP control. Not only does this indicate that the dominant-negative virus is an effective AMPK inhibitor, but also shows that the actions of AICAR are indeed mediated through AMPK as the addition of AICAR failed to produce a significant increase in activity for α_2 DN-treated cells.

For virus-treated conditions, cells were assayed for AMPK activity markers on day 3 post-infection, which was therefore day 2 post-AICAR treatment for the particular cells treated with this drug. The added day allowed adequate time for the infection to occur and the appropriate proteins to be translated, all of which must occur prior to any downstream effects taking place on AMPK and its subsequent effectors. As a further indicator, GFP fluorescence reached its peak expression days 2 and 3 post-infection, showing again that the virus constructs require an approximate 1-day lag prior to achieving their full activity. Furthermore, harvesting 2 days post-AICAR or -no drug treatment maintained consistency between these conditions and the metformin- and AICAR-treated conditions discussed above.

Compared to other *in vitro* models, the dose of 150 PFU/cell used in this study was high. This is due in part to the low expression of CAR, which was overcome somewhat by the addition of Lipofectamine but nevertheless required a generous dose of adenovirus in order to work effectively. In other work dealing with C2C12 cells, an efficient infection was achieved using an MOI of 250 with virus alone, but could be improved to 50 when aided by a polycationic lipid (Dodds *et al.*, 1999). Preliminary experiments were able to produce an efficient infection at a similar virus dose in myoblasts (Figure 3.11), however myotubes proved even more resistant to infection and as a result the dose was tripled. This could be due to the more mature state of myotubes compared with myoblasts, as skeletal muscle mRNA expression of CAR *in vivo* rapidly diminishes between postnatal days 3 and 10 in mice and is completely undetectable in the

adult (Nalbantoglu *et al.*, 1999). In addition, myotube fusion would logically lead to a decrease in the surface area to volume ratio of the muscle cells, which may decrease the proportion of CAR available for a similar volume of intracellular space.

4.1.3 Limitations of the Experimental Model

The most obvious problem with this particular model is its inability to sustain itself for a long duration of time. The study of mitochondrial biogenesis, and other long-term effects of AMPK activation/inhibition for that matter, may require more longevity built into the design in order to obtain consistent and accurate results. As mentioned earlier, mitochondrial biogenesis is apparent *in vivo* after approximately six weeks of training, although some mitochondrial proteins have a half-life of 7 days (Hood, 2001). Fortunately, other proteins such as ALA synthase do turn over much faster (Baar *et al.*, 2002), allowing some utility for this model but still preventing one from obtaining a complete understanding of all events that transpire. In addition, indications that the cell differentiation may still be somewhat affected by the pharmacological treatments, as indicated by changes in myogenin expression, caused further compromises to be made regarding length of treatment. This model is ideal for examining very short-term changes, thus is more ideally designed to assay changes in mRNA expression rather than protein expression and activity.

Another difficulty experienced during the development of this system was the low tolerance of the cells to pharmacological treatment over a period of 3 days or more. While higher doses of either AICAR or metformin sufficed for 24-48 hours, the appearance of thin, ragged myotubes and accompanying cell death ensued beyond this time. Media changes were made more often, which did circumvent the problem somewhat, but eventually doses were lowered to a more acceptable level. After 48 hours of treatment, cells given higher doses showed obvious increases in phospho-ACC and phospho-AMPK levels above cells given the lower long-term doses. Although the lower doses did produce significant increases in expression of these phospho-proteins, changes are at best 1.5-fold higher than controls. Perhaps the lack of a robust AMPK activation

prevented more significant downstream changes from transpiring at levels detectable by our assay methods. Another potential source of error was the potential variation in drug concentration in between treatments. As it was unclear how quickly the cells metabolized either drug, treatment was administered once every 48 hours. To eliminate the potential of a short-term, pulsatile response to drug treatment, cells were harvested for mRNA expression on days 3 and 5, both only 24 hours following their last treatment.

Ironically, while drug doses may have been too low to produce a substantial effect on AMPK activity, the required doses of virus were unusually high. As well, the addition of Lipofectamine, which can be disruptive to all cellular membranes, may have contributed to the induction of other signalling systems within the cell. These may have been involved in cell cycle regulation, induction of apoptosis, and other pathways that ultimately may have influenced results. As very few significant effects were seen following virus treatment in any of the mitochondrial proteins, this may indicate adenoviral infection is not as clean acting as previously believed. In fact, upregulation of numerous signalling pathways has been shown to result from adenovirus infection, including that of Akt (Zhang *et al.*, 2004) and MAP kinase (Bhat & Fan, 2002). Both pathways have implications in skeletal muscle, as Akt activation can inhibit muscle glucose transport (Sowers, 2004) and activate glycogen synthesis (Yeaman *et al.*, 2001). Simultaneously, these two effects would decrease muscle glucose stores, thus less glucose would be available for glycolysis and subsequent oxidative phosphorylation. The MAP kinase signalling cascade is implicated in numerous transcriptional changes, and this pathway is normally upregulated in parallel with AMPK following exercise (Hawley & Zierath, 2004). This could explain that while the α_2 DN virus was able to abolish ~50% of the cellular AMPK activity, the virus failed to significantly downregulate any mitochondrial enzymes as perhaps MAP kinase signalling was counteracting such changes.

4.2 Evaluation of Mitochondrial Biogenesis

Metabolic enzymes of the glycolytic and citric acid cycle were assayed for changes in expression following AMPK activation or inhibition via the two experimental models. Interestingly, discrepancies in results produced by the two models, and between protein and mRNA expression, were quite prevalent. Citrate synthase protein expression, for example, was upregulated almost two-fold by metformin and AICAR administration as seen 4 days post-treatment. At the mRNA level, however, the only significant upregulation was seen 6h following metformin treatment, and was absent at all following time points. This implies almost a 4-day lag period exists between transcription and translation of citrate synthase to detectable levels, and although this is possible it is also somewhat unexpected. AICAR, meanwhile, failed to produce any significant effect on mRNA expression. Using the virus model, no significant changes were produced at the protein or mRNA level in any of the conditions. This again points to potential problems the virus and Lipofectamine combination may have on normal cell function, or it could indicate that the downstream effects of AMPK inhibition may not always perfectly oppose those of AMPK activation.

A similar trend was evident with regards to GAPDH expression. Protein levels were also significantly elevated, again almost two-fold, by metformin and AICAR treatment alone. However, while this was an expected response of citrate synthase as stated in the hypothesis, it was assumed GAPDH would remain unaltered by treatment. As an enzyme catalyzing the 5th reaction of glycolysis in which glyceraldehyde-3-phosphate is converted to 1,3-bisphosphoglycerate, GAPDH is not a flux-generating or rate-limiting step such as the phosphofructokinase (PFK) or hexokinase (HK) reactions. In addition, GAPDH is often used as a loading control or housekeeping gene based on its consistency, although this procedure has been somewhat questioned as of late (Rondinelli *et al.*, 1997). Particularly in studies where metabolic phenotype may be affected by experimental conditions, any step in these pathways cannot be assumed unchanged as reinforced by the findings of this study. Unfortunately, virus-treated conditions failed to produce a parallel increase in GAPDH expression following AICAR treatment of the

GFP control condition. In fact, the only significant increase following adenovirus treatment was produced by the α_2 DN + AICAR condition, but not by the α_2 DN virus alone. As these two conditions did not appear to affect AMPK activation differently, the reason for their different effects on GAPDH expression is difficult to explain. Further complicating the matter, the α_2 DN condition was expected to have the opposite effect of the AMPK-activating drug treatments and inhibit GAPDH expression. It is possible, of course, that AMPK activation may indeed be able to induce expression of citrate synthase and GAPDH, but when AMPK is inhibited other redundant pathways maintain a basal level of enzyme expression preventing an obvious change from the control condition. AICAR, meanwhile, may also affect one of these other pathways in addition to AMPK, thus causing GAPDH expression to increase enough to reach significance. If this were true, however, one would also expect the GFP virus + AICAR condition to produce a significant increase, which is clearly not the case.

Unlike citrate synthase, the mitochondrial matrix enzyme ALA synthase has a half-life of approximately 14 hours in skeletal muscle (Hood, 2001), thus changes can be detected much more quickly. Although ALA synthase is not involved in the aerobic respiration pathway, it is a mitochondrial enzyme and therefore its expression levels will reflect overall mitochondrial volume. At the mRNA level, metformin treatment led to a two-fold increase in expression 6 hours following treatment. While mRNA expression appeared elevated at other time points, this was the only significant increase using the pharmacological model. The short half-life of ALA synthase allows it to adapt quickly to changes in metabolic demand (Holloszy & Winder, 1979), therefore the early change in gene expression was not surprising. Virus treatment, on the other hand, produced unexpected mRNA results. AICAR was unable to increase ALA synthase expression when combined with the GFP control virus, however the α_2 DN virus alone did produce a small but significant increase in mRNA expression at the 6h time point. This would imply that perhaps AICAR is inhibiting ALA synthase expression through another pathway, although this inhibition was not significant when GFP control cells were treated with AICAR.

Finally, besides outright expression levels of various mitochondrial proteins, biogenesis may also be influenced by mRNA stability and mitochondrial protein import from the cytosol (Hood, 2001). Contraction has shown to elevate both mTFA mRNA levels, as well as import of the protein into the mitochondria (Hood, 2001). While it could be argued that import is governed primarily by the cytosolic concentration of various proteins, regulation at numerous stages is quite common in molecular physiology and rate of import may indeed be one level of control.

4.3 Evaluation of Transcription Factor Expression

p300 mRNA expression, as expected, was largely unaffected by the various experimental conditions. As p300 is a downstream target of AMPK, it is possible that even over the long-term this transcriptional co-activator will only fluctuate between more active and less active phosphorylation states rather than undergo overall changes in expression. Future experiments should examine changes in p300 phosphorylation and DNA binding as opposed to expression levels, as this will likely be the more telling story regarding p300's role in the AMPK pathway. It should be noted, however, that p300 mRNA levels were significantly increased on day 5 following metformin treatment. This could perhaps imply that long-term activation, or in this case inhibition, of p300 may produce enough negative feedback to result in long-term expressional changes. Again, however, further experiments will be required to determine whether or not this is the case.

Like many of the mitochondrial proteins mentioned above, the transcription factor PGC-1 α produced some very conflicting and surprising results not anticipated by the hypothesis. PGC-1 α expression was significantly increased over 2.5-fold by metformin, yet no significant changes were produced by AICAR alone or in combination with any of the virus conditions. Earlier studies in which AICAR was incubated with rat epitrochlearis muscle, however, were able to produce a 3-fold increase in PGC-1 α mRNA expression after 18 hours (Terada *et al.*, 2002). While our cell culture results did not confirm this result, it may be due to the higher AICAR dose (0.5 mM) used in the

short-term experiment, and perhaps shorter incubations with higher AICAR doses in this study would have more accurately reflected other findings in the literature. In addition, the short-term study used a more mature model as compared with our C2C12 cell line, thus basal PGC-1 α expression may have been elevated causing any changes to be much easier to detect. Meanwhile, however, more unusual results are apparent at the mRNA level. At 48h following metformin treatment, PGC-1 α mRNA is actually decreased to 60% of the control value. Although it recovers to control levels on day 3 and day 5, there is no means to explain the large increase in protein expression on day 4 revealed by Western blotting, and may indicate the influence of post-transcriptional and/or -translational processing on PGC-1 α protein levels. Meanwhile, this unexpected trend also occurs in the virus-treated samples, as conditions meant to inhibit AMPK with the α_2 DN virus led to an increase in PGC-1 α mRNA at 6h, 48h and 5d post-treatment. Strangely enough, the α_2 DN + control and α_2 DN + AICAR conditions never caused simultaneous mRNA elevation, always just one or the other. Finally, to further confuse the situation, PGC-1 α mRNA is also elevated by the GFP + AICAR condition 5 days post-treatment. While this last result is one of the few actually anticipated by the hypothesis, the others are quite difficult to explain. As mentioned earlier, adenovirus infection is thought to activate other pathways within the cell such as Akt and MAP kinase. In addition, Lipofectamine treatment has visible effects on cellular membrane integrity that are visible under a phase-contrast microscope. This has the potential to upset calcium balance within the cells, which may activate further downstream pathways involving CaM kinase IV and calcineurin. CaMKIV expression is upregulated by β -GPA treatment in mice, however transgenics that lack muscle AMPK do not experience any upregulation (Zong *et al.*, 2002). This implies that CaMKIV is activated downstream of AMPK, yet if intracellular calcium levels are elevated as a result of Lipofectamine treatment, this pathway may be activated regardless of AMPK status. CAMKIV, a protein kinase, and calcineurin, a protein phosphatase, act synergistically to mediate many of the structural and metabolic adaptations to exercise in skeletal muscle (Wu *et al.*, 2002). In addition, the PGC-1 α promoter appears to be controlled by both CAMKIV and calcineurin A (Handschin *et al.*, 2003). As the hypothesized changes in PGC-1 α mRNA expression did not manifest until day 5, the long latency period may reflect the duration

of time required for the cell membranes to recover from Lipofectamine treatment and for calcium balance to return to normal.

It should be noted that, although significant, many of the observed changes in PGC-1 α protein and mRNA expression were accompanied with relatively large standard error. If the probability of committing a type I error, α , is made more stringent to compensate and significance is only granted when $p < 0.01$, results make somewhat more sense.

4.4 Implications of Altering AMPK Activity

As AMPK's widespread role in various tissues is further revealed, it should not be surprising that very minor changes or unexpected results appear as a consequence of AMPK activation or inhibition. While skeletal muscle is a highly adaptable tissue, the mammalian system is quite homeostatic in nature. AMPK's short-term actions on fatty acid metabolism, for example, are a good illustration of the body's ability to counteract an acute energy deficit. Meanwhile, when AMPK is activated or inhibited, there are likely numerous other signalling pathways that are affected in addition which may also influence the few markers chosen to indicate downstream effects of AMPK.

For example, during muscle contraction, the increase in cytosolic calcium is sufficient to elicit signalling through the calcium-calmodulin pathway, specifically via the kinase CaMK and the phosphatase calcineurin (Wu *et al.*, 2002). Both of these second messengers have been implicated in fast-to-slow muscle fibre type transformation (Wu *et al.*, 2000), while CaMKIV has also been implicated in mitochondrial biogenesis (Wu *et al.*, 2002). In fact, CaMKIV appears capable of inducing PGC-1 α via activation of various transcription factors, including cAMP responsive element-binding protein (CREB) and myocyte-specific enhancer factor (MEF2) (Bito *et al.*, 1996; McKinsey *et al.*, 2000; Passier *et al.*, 2000). Moreover, PGC-1 α protein has shown evidence of feeding back and enhancing the transcriptional activity of MEF2C and 2D to further upregulate its own transcription (Handschin *et al.*, 2003). There is strong evidence that

the AMPK pathway may interact with that of calcium, as the upstream kinases of both CaMK and AMPK are capable of phosphorylating one another's substrates (Hawley *et al.*, 1995). Further studies have indicated that CaMKIV signalling may be downstream of AMPK, as β -GPA was capable of increasing both CaMKIV and PGC-1 α expression in mice with, but not without, functional muscle AMPK (Zong *et al.*, 2002).

Another pathway that may act alone or in conjunction with AMPK during mitochondrial biogenesis is that of MAP kinase. MAPK and intermediates in its signalling pathways are activated by acute muscle contraction, as mentioned in Chapter I (Connor *et al.*, 2001). In addition, MAPK is known to be activated by numerous consequences of muscle contraction, including increases in cytosolic calcium and mechanical stress (Hawley & Zierath, 2004). Downstream substrates of the MAP kinase pathway, such as histone H3, can alter the chromatin state of certain genes, thus influencing their transcriptional regulation (Hawley & Zierath, 2004).

Finally, as AMPK is known to have inhibitory actions on protein synthesis, this further complicates its ability to regulate expression. As mitochondrial biogenesis involves the transcription and translation of numerous proteins, the extent to which AMPK may non-specifically inhibit the production of proteins that it may be specifically inducing at the same time is unknown.

4.5 Future Directions for Research

As the extent of AMPK's actions across a broad range of tissues under numerous conditions is further elucidated, the potential for interactions and redundancy with other signalling pathways grows exponentially. While it remains likely that AMPK does exert some sort of influence over skeletal muscle mitochondrial biogenesis, the extent of its involvement, as well as its interaction with other well-defined signalling pathways, will obviously require further investigation.

While this study had many limitations, it also produced some very useful results. The elaboration of a novel *in vitro* model and discovery of the appropriate time points for changes in protein and mRNA expression will undoubtedly assist future studies in this area. Experiments examining other transcription factors, such as NRF-1 and mTFA, will likely contribute further to skeletal muscle research and help to explain the behaviour of PGC-1 α expression in this set of experiments. Future experiments could also explore interactions between AMPK and other pathways implicated in mitochondrial biogenesis, indicating the signalling hierarchy and elucidating any possible redundancies that may have compensated for AMPK downregulation in this study.

In regards to the model, the short-term duration of the *in vitro* experimental model may not be optimal to fully assess mitochondrial biogenesis-related changes in protein expression. Alterations in mitochondrial enzyme activity and expression should be reserved for *in vivo* models, which can sustain treatment for numerous weeks. In particular, the recent generation of α_1 and α_2 knockout mice may be particularly useful to further elucidate the role of AMPK in this biogenic process. The combination of knockout mice and pharmacological AMPK activators may also provide further evidence of the action mechanism of these compounds. The *in vitro* model, meanwhile, is most useful for examination of short-term changes, such as mRNA expression levels and transcription factor DNA-binding. To minimize the activation of non-specific pathways following adenovirus infection, CAR-overexpressing C2C12 clones could be used for future experiments, bypassing the need for Lipofectamine. Furthermore, combinations of the AMPK adenovirus constructs and metformin should also be tested, as this treatment activates AMPK through a different mechanism than that of AICAR and often was the only one of the two pharmacological treatments able to produce significant downstream effects on protein and mRNA expression of other substances. Unlike AICAR, metformin also failed to affect myogenin expression and thus cell differentiation to a significant degree, preventing the possibility of changes in the cell differentiation state from influencing downstream results.

4.6 References

- Baar, K., Wende, A. R., Jones, T. E., Marison, M., Nolte, L. A., Chen, M., Kelly, D. P., & Holloszy, J. O. (2002). Adaptations of skeletal muscle to exercise: rapid increase in the transcriptional coactivator PGC-1. *FASEB J.* 16, 1879-1886.
- Bhat, N. R. & Fan, F. (2002). Adenovirus infection induces microglial activation: involvement of mitogen-activated protein kinase pathways. *Brain Res.* 948, 93-101.
- Bito, H., Deisseroth, K., & Tsien, R. W. (1996). CREB phosphorylation and dephosphorylation: a Ca(2+)- and stimulus duration-dependent switch for hippocampal gene expression. *Cell* 87, 1203-1214.
- Connor, M. K., Irrcher, I., & Hood, D. A. (2001). Contractile activity-induced transcriptional activation of cytochrome C involves Sp1 and is proportional to mitochondrial ATP synthesis in C2C12 muscle cells. *J. Biol. Chem.* 276, 15898-15904.
- Dedieu, S., Mazeret, G., Cottin, P., & Brustis, J. J. (2002). Involvement of myogenic regulator factors during fusion in the cell line C2C12. *Int. J. Dev. Biol.* 46, 235-241.
- Dodds, E., Piper, T. A., Murphy, S. J., & Dickson, G. (1999). Cationic lipids and polymers are able to enhance adenoviral infection of cultured mouse myotubes. *J. Neurochem.* 2105-2112.
- Fryer, L. G., Parbu-Patel, A., & Carling, D. (2002). The Anti-diabetic drugs rosiglitazone and metformin stimulate AMP-activated protein kinase through distinct signaling pathways. *J. Biol. Chem.* 277, 25226-25232.
- Handschin, C., Rhee, J., Lin, J., Tarr, P. T., & Spiegelman, B. M. (2003). An autoregulatory loop controls peroxisome proliferator-activated receptor gamma coactivator 1alpha expression in muscle. *Proc. Natl. Acad. Sci. U.S.A* 100, 7111-7116.
- Hardie, D. G. & Carling, D. (1997). The AMP-activated protein kinase--fuel gauge of the mammalian cell? *Eur. J. Biochem.* 246, 259-273.

- Hawley, J. A. & Zierath, J. R. (2004). Integration of metabolic and mitogenic signal transduction in skeletal muscle. *Exerc. Sport Sci. Rev.* 32, 4-8.
- Hawley, S. A., Gadalla, A. E., Olsen, G. S., & Hardie, D. G. (2002). The antidiabetic drug metformin activates the AMP-activated protein kinase cascade via an adenine nucleotide-independent mechanism. *Diabetes* 51, 2420-2425.
- Hawley, S. A., Selbert, M. A., Goldstein, E. G., Edelman, A. M., Carling, D., & Hardie, D. G. (1995). 5'-AMP activates the AMP-activated protein kinase cascade, and Ca²⁺/calmodulin activates the calmodulin-dependent protein kinase I cascade, via three independent mechanisms. *J. Biol. Chem.* 270, 27186-27191.
- Holloszy, J. O. & Winder, W. W. (1979). Induction of delta-aminolevulinic acid synthetase in muscle by exercise or thyroxine. *Am. J. Physiol. Regul. Integr. Comp. Physiol.* 236, R180-R183.
- Hood, D. A. (2001). Invited Review: contractile activity-induced mitochondrial biogenesis in skeletal muscle. *J. Appl. Physiol.* 90, 1137-1157.
- Leary, S. C., Battersby, B. J., Hansford, R. G., & Moyes, C. D. (1998). Interactions between bioenergetics and mitochondrial biogenesis. *Biochim. Biophys. Acta* 1365, 522-530.
- Leclerc, I., Woltersdorf, W. W., da, S., X, Rowe, R. L., Cross, S. E., Korbitt, G. S., Rajotte, R. V., Smith, R., & Rutter, G. A. (2004). Metformin, but not leptin, regulates AMP-activated protein kinase in pancreatic islets: impact on glucose-stimulated insulin secretion. *Am. J. Physiol. Endocrinol. Metab.* 286, E1023-E1031.
- McKinsey, T. A., Zhang, C. L., Lu, J., & Olson, E. N. (2000). Signal-dependent nuclear export of a histone deacetylase regulates muscle differentiation. *Nature* 408, 106-111.
- Moyes, C. D., Mathieu-Costello, O. A., Tsuchiya, N., Filburn, C., & Hansford, R. G. (1997). Mitochondrial biogenesis during cellular differentiation. *Am. J. Physiol. Cell Physiol.* 272, C1345-C1351.
- Nalbantoglu, J., Pari, G., Karpati, G., & Holland, P. C. (1999). Expression of the primary coxsackie and adenovirus receptor is downregulated during skeletal muscle

- maturation and limits the efficacy of adenovirus-mediated gene delivery to muscle cells. *Hum. Gene Ther.* 10, 1009-1019.
- Passier, R., Zeng, H., Frey, N., Naya, F. J., Nicol, R. L., McKinsey, T. A., Overbeek, P., Richardson, J. A., Grant, S. R., & Olson, E. N. (2000). CaM kinase signaling induces cardiac hypertrophy and activates the MEF2 transcription factor in vivo. *J. Clin. Invest* 105, 1395-1406.
- Rondinelli, R. H., Epner, D. E., & Tricoli, J. V. (1997). Increased glyceraldehyde-3-phosphate dehydrogenase gene expression in late pathological stage human prostate cancer. *Prostate Cancer Prostatic. Dis.* 1, 66-72.
- Shen, X., Collier, J. M., Hlaing, M., Zhang, L., Delshad, E. H., Bristow, J., & Bernstein, H. S. (2003). Genome-wide examination of myoblast cell cycle withdrawal during differentiation. *Dev. Dyn.* 226, 128-138.
- Shimokawa, T., Kato, M., Ezaki, O., & Hashimoto, S. (1998). Transcriptional regulation of muscle-specific genes during myoblast differentiation. *Biochem. Biophys. Res. Commun.* 246, 287-292.
- Sowers, J. R. (2004). Insulin resistance and hypertension. *Am. J. Physiol Heart Circ. Physiol.* 286, H1597-H1602.
- Terada, S., Goto, M., Kato, M., Kawanaka, K., Shimokawa, T., & Tabata, I. (2002). Effects of low-intensity prolonged exercise on PGC-1 mRNA expression in rat epitrochlearis muscle. *Biochem. Biophys. Res. Commun.* 296, 350-354.
- Wu, H., Kanatous, S. B., Thurmond, F. A., Gallardo, T., Isotani, E., Bassel-Duby, R., & Williams, R. S. (2002). Regulation of mitochondrial biogenesis in skeletal muscle by CaMK. *Science* 296, 349-352.
- Wu, H., Naya, F. J., McKinsey, T. A., Mercer, B., Shelton, J. M., Chin, E. R., Simard, A. R., Michel, R. N., Bassel-Duby, R., Olson, E. N., & Williams, R. S. (2000). MEF2 responds to multiple calcium-regulated signals in the control of skeletal muscle fiber type. *EMBO J.* 19, 1963-1973.
- Yeaman, S. J., Armstrong, J. L., Bonavaud, S. M., Poinasamy, D., Pickersgill, L., & Halse, R. (2001). Regulation of glycogen synthesis in human muscle cells. *Biochem. Soc. Trans.* 29, 537-541.

- Zhang, F., Cheng, J., Hackett, N. R., Lam, G., Shido, K., Pergolizzi, R., Jin, D. K., Crystal, R. G., & Rafii, S. (2004). Adenovirus E4 gene promotes selective endothelial cell survival and angiogenesis via activation of the vascular endothelial-cadherin/Akt signaling pathway. *J. Biol. Chem.* 279, 11760-11766.
- Zhou, G., Myers, R., Li, Y., Chen, Y., Shen, X., Fenyk-Melody, J., Wu, M., Ventre, J., Doebber, T., Fujii, N., Musi, N., Hirshman, M. F., Goodyear, L. J., & Moller, D. E. (2001). Role of AMP-activated protein kinase in mechanism of metformin action. *J. Clin. Invest* 108, 1167-1174.
- Zong, H., Ren, J. M., Young, L. H., Pypaert, M., Mu, J., Birnbaum, M. J., & Shulman, G. I. (2002). AMP kinase is required for mitochondrial biogenesis in skeletal muscle in response to chronic energy deprivation. *Proc. Natl. Acad. Sci. USA* 99, 15983-15987.